# Relationships between electrical parameters and physical properties of cereal grains, oilseeds, and apples

*Péter Mészáros*

Corvinus University of Budapest
Department of Physics and Control

Budapest
2007

**PhD School/Program**

**Name:** PhD School of Food Science

**Field:** Food Science

**Head:** Prof. András Fekete
Professor
Department of Physics and Control
Faculty of Food Science
Corvinus University of Budapest

**Supervisors:** Dr. Eszter Vozáry
Associate Professor
Department of Physics and Control
Faculty of Food Science
Corvinus University of Budapest

Dr. David B. Funk
Associate Director for Methods Development,
United States Department of Agriculture—Grain Inspection Packers and Stockyards Administration

The applicant met the requirement of the PhD regulations of the Corvinus University of Budapest and the thesis is accepted for the defence process.

……. ……...
Signature of Head of School Signature of Supervisor

**According to the Doctoral Council of Life Sciences of Corvinus University of Budapest on 13th February, the following committee was designated for defence.**

**Committee:**

**Chair:**
Erika Békássy-Molnár, D.Sc.

**Members:**
András Salgó, D.Sc.
István Farkas, D.Sc.
Gyula Vatai, C.Sc.
Katalin Badak-Kerti, Ph.D.

**Referees:**
Károly Kaffka, C.Sc.
Péter Sembery, D.Sc.

**Secretary:**
Katalin Badak-Kerti, Ph.D.

# 1. CONTENTS

# 2. NOTATION

| | |
|---|---|
| Z | -Complex impedance, ohm |
| $Z_{CPE}$ | -Impedance of the Constant Phase Element, ohm |
| U | -Alternating (Potential) voltage, volt |
| I | -Current, ampere |
| X | -Imaginary part of complex impedance (Reactance), ohm |
| R | -Real part of complex impedance (Resistance), ohm |
| $R_{inf}$ | -Resistance at infinite frequency, ohm |
| $R_0$ | -Resistance at zero frequency, ohm |
| E | -Electric field intensity, volts per meter |
| D | -Vector of the dielectric displacement |
| C | -Capacitance, farad |
| $C_0$ | -Capacity of the test cell in vacuum, farad |
| Cp | -The parallel stray capacitance, farad |
| G | -Conductance, siemen |
| $R_s$ | -Residual series lead resistance, ohm |
| $L_s$ | -Residual series lead inductace, henry |
| *VG* | -Gain voltage from the AD-8302 gain/phase detector circuit, volt |
| *VP* | -Phase voltage from the AD-8302 gain/phase detector circuit, volt |
| *X* | -Dry basis moisture content, kg water per kg dry matter |
| *x* | -Wet basis moisture content, kg water per kg moist material |
| $x_{pred}$ | -Moisture value calculated from dielectric characteristics, kg water per kg moist material |
| $x_{tc}$ | -Predicted moisture content with temperature correction, kg water per kg moist material |
| $x_{adj}$ | -The reverse temperature-corrected air-oven wb moisture value, % |
| $x_{ref}$ | -Reference air-oven wb moisture content, % |
| $m_d$ | -Mass of dry matter in the product, gram |
| $m_w$ | -Mass of water in the product, gram |
| $m_t$ | -Total mass of the product, water plus dry matter, gram |
| m | -Current sample mass, gram |
| $m_0$ | -Initial sample mass, gram |
| $m_e$ | -Equilibrium sample mass, gram |
| $\rho_{target}$ | -Target density, gram per cubic centimeter |
| $\rho_{sample}$ | -Sample density, gram per cubic centimeter |
| $a_w$ | -Water activity |
| $P_w$ | -Partial pressure of water vapor at the specified conditions, pascal |
| $P_{ws}$ | -Partial pressure of water vapor at saturation and the specified temperature, pascal |
| k | -Time constant, 1 per second |
| Γ | -Complex reflection coefficient |
| $\Phi$ | -Relative humidity, percent |
| $\varepsilon_r$ | -Relative complex permittivity |
| $\varepsilon'_r$ | -Dielectric constant |
| $\varepsilon''_r$ | -Dielectric loss factor |
| j | -imaginary operator |
| $\varepsilon_0$ | -Permittivity of vacuum ($8.854 \times 10^{-12}$ Farad per meter) |
| $\varepsilon_c$ | -Density-corrected dielectric constant |
| $\varepsilon_{ec}$ | -Dielectric constant of empty test cell |
| $\varepsilon_{meas}$ | -Measured relative complex permittivity |

| | |
|---|---|
| $\varepsilon_{adj}$ | -Adjusted dielectric constant by unifying parameters |
| tgδ | -Loss tangent |
| ω | -Angular frequency, radians per second |
| f | -Measurement frequency, hertz |
| φ | -Phase angle, degree |
| τ | -Relaxation time, 1 per second |
| α | -Constant parameter |
| σ | -Conductance, siemen |
| ω | -Angular frequency, radian per second |
| SP | -Slope unifying parameter |
| OP | -Offset unifying parameter |
| TP | -Translation unifying parameter |
| Ktc | -Temperature correction coefficient |
| t | -Temperature, celsius |
| *KTC0* | -Intercept value of the moisture-dependent linear temperature function |
| *KTCS* | -Slope value of the moisture-dependent linear temperature function |
| *KTC01* | -Intercept value of linear moisture-dependent temperature correction with a quadratic temperature term |
| *KTCS1* | -Slope value of linear moisture-dependent temperature correction with a quadratic temperature term |
| *KTCQ* | -Temperature coefficient of the quadratic term |
| RF | -Radio Frequency |
| VHF | -Very High Frequency |
| CPE | -Constant Phase Element |
| EMC or Me | -Equilibrium Moisture Content |
| UGMA | -Unified Grain Moisture Algorithm |
| wb | -wet basis |
| db | -dry basis |
| TEM | -Transverse Electric-Magnetic |
| *FF* | -Filling Factor |
| AOAC | -Association of Official Analytical Chemists |
| ICC | -International Association for Cereal Science and Technology |
| ISO | -International Standards Organization |
| USDA-GIPSA | -United States Department of Agriculture - Grain Inspection, Packers and Stockyards Administration |
| USDA-ARS | -United States Department of Agriculture - Agricultural Research Service |
| FGIS | -Federal Grain Inspection Service |
| EIS | -Electrical Impedance Spectroscopy |
| BNC | -Bayonet Nut Coupling connector |
| LCR | -Inductance, Capacitance, Resistance |
| GPIB | -General Purpose Interface Bus |
| SMA | -SubMiniature coaxial connector |
| SSE | -Sum of Squares Due to Error |
| RMSE | -Root Mean Squared Error |
| R-square | -Multiple correlation coefficient or coefficient of multiple determination |
| DW test | -Durbin-Watson statistical test |
| Grain class | -Refers to different class of grain e.g. Hard Red Spring wheat, Hard Red Winter wheat |
| Grain type | -Refers to different type of grain e.g. corn, soybeans, sunflower |
| Grain group | -Different grain types or classes together in the UGMA |

# 3. INTRODUCTION

Knowledge about the electrical properties of agricultural materials becomes increasingly significant as agricultural technology becomes more sophisticated, as new uses for electric energy are developed, and as new methods, processes, and devices come into being which utilize or are influenced by the electrical nature of materials. Investigations of the dielectric properties of different agricultural products, grains, and foods stretch back more than a half-century (Burr 1950, Nelson 1973, Sembery et al. 1999).

Electrical properties of food products have generally been of interest for two reasons. One relates to the possibility of using the electrical properties as a means for determining moisture content or other quality factors (seed viability, fruit maturity, egg quality, lactose content) (Nelson 1973). The other has to do with the absorption of energy in high-frequency dielectric heating or microwave heating applications useful in the processing of food materials (Brown et al 1947, Szabó 1998, 2003).

Changes in Electrical Impedance Spectroscopy (EIS) dispersion parameters have been used for the evaluation of membrane condition during ripening and storage in fruit tissues (Harker and Maindonald 1994, László at al. 1997). Mechanically broken membrane structures were detected by changes in EIS parameters (Cox et al. 1993, Vozáry et al. 1999). EIS spectroscopy was also suitable for detecting irradiation in potatoes (*Solanum tuberosum L.*) (Felföldi et al. 1993). High frequency dielectric measurements were performed on apple tissue after different drying times (Feng et al. 2002), but no reference was found about systematic measurements (on-line, off-line) of apple tissue during drying with electrical impedance parameters.

Electrical properties of grain and seed have been utilized in devising electrical instruments that can be used for quick tests for indication of moisture content or some other quality parameters (damaged seed, protein content) (Nelson 1984). In still other possible applications, electrical properties that influence static charge behavior have been of interest in studies of electrostatic separation principles. Electrostatic charge was applied to separate grain seed from hulls and from insects (Hamond et al 1961, Matthes and Boyd 1969). Drying of grain seeds in electrostatic fields is also a possibility; thus it is also important to know grains electrical properties, how they react with the electric field, how they dissipate electric energy, how much temperature increases and how drying changes the moisture content.

Besides these areas, electrical parameters of living plants (Burr 1950, Asher 1964, Molitorisz 1966, Pullman et al. 1965), animal tissue (Schwan 1959, 1966, Nelson and Whitney 1960, Wang and Tang 2004), wood (Wittkopf and Macdonald 1949, Repo et al. 1993), paper and textile (Busker 1968, Norris 1956, Algie 1969), soil (Hilhorst 1992, Lee et al. 2004) and concrete

(Kutrubes D. L. 2000) are also determined. The number of publications in dielectric spectroscopy indicates the great interest regarding dielectric properties. Considering the different kinds of raw materials, the wide range of the measurement frequencies, and the effects of influential factors (moisture content, temperature, bulk density, oil content, protein content, etc.) the numbers of the necessary measurements are inexhaustible. It can be seen that knowing the dielectric properties of agricultural products and foods is important and offers numerous opportunities in measurement techniques and in food quality control.

Many different techniques are available for measuring the moisture content of agricultural and food materials. An extensive list of standards for moisture measurement is provided by the Association of Official Analytical Chemists (AOAC) (1990). The air oven method is the most common reference method for grain moisture determinations. There are some other more basic methods such as the phosphorous pentoxide ($P_2O_5$) (ICC Standard 1976) method and the Karl Fischer titration method (ISO Standard, ISO 760 1978). These methods provide the most accurate results for moisture content but they also require more time and various chemicals. Most air oven methods require hours or days to complete. Clearly, grain producers, handlers, and processors need much more rapid methods to assess moisture content—especially in grain trading. The available rapid indirect methods are: Near-Infrared Method, Conductivity Method, Microwave Method, and Radio-Frequency Dielectric Method. During the past fifty years, dielectric grain moisture meters have developed significantly, with many new models introduced and used world-wide (Examples include: Perten (Aquamatic 5100), Dickey-john (GAC 2100), Kett (PB-3010, Waddy PV-100, PT-2300), Seedburo (Model 1200A) and many others). Different type moisture meters have different precision in measuring grain moisture content. In grain trading there are strict rules about rapid moisture measurements in the U.S.A. and in the E.U.

In the USA it is determined by the US Department of Agriculture-Grain Inspection, Packers and Stockyards Administration (USDA-GIPSA) that official moisture content in the grain is determined only by a standardized DICKEY-john Grain Analysis Computer GAC 2100 (USDA-GIPSA Moisture Handbook 1999, U.S. Grains Council Importer Manual 1986).

In the EU, the grain quality standards are determined in intervention standards. The most recent standard is the intervention for the grain quality control and quality assurance that was developed in 2000 (824/2000 EC Comission Regulation). The definitive moisture measuring application is the air oven method. In questionable cases, only the results of the air oven method are accepted. Instruments, which apply dielectric spectroscopy or the NIR method, are also accepted for grain moisture content determination. These types of equipments have to conform to the ISO 712:1998 standard. Every two years each of these fast moisture meters has to be calibrated in an accredited laboratory. The cost of the calibration process is high—for one moisture meter it is about

50-100 euro ($70-140) per grain type. Considering this fact, it would be desirable to develop a method where the cost of calibration could be reduced.

Research collaboration between USDA-GIPSA and USDA-Agricultural Research Service (Athens, GA) over the period of 1995 to 2001 resulted in an improved RF dielectric moisture measuring method that effectively combines calibrations for many diverse grain types and classes into a single "unified calibration." This method is capable of moisture measurement accuracy that is equal to or better than what is achievable for grain-specific calibrations with current instruments. In this method, similar grain classes and types are placed in grain groups that can be measured without knowing the specific grain class. The unified calibration database has been increased year by year, with new dielectric and air-oven test results and with new calibration data. GIPSA has been supporting continuing research at Corvinus University of Budapest, Faculty of Food Science, for the purpose of developing methods for optimizing the necessary unifying parameters and developing methods that make the calibration process easier in the future, for those grain types and classes that have not yet been fit in the calibration. Some research groups in Hungary have also been interested in dielectric moisture determination. Low (1-30 MHz) and radio frequency dielectric moisture tests were also performed by Z. Gillay (2003) and B. Gillay (2002) at the Corvinus University of Budapest. For the measurement of microwave electrical properties of wheat and corn, a prototype system was developed at the Budapest University of Technology and Economics Department of Microwave and Telecommunications (Sembery and Völgyi 1989). Further Microwave measurements were performed by Sembery et al. (2001) at the Szent István University.

Another important question and problem is the temperature correction of dielectric moisture meters. Temperature has a significant effect on the dielectric parameters (Nelson 1984, Sembery 2002, Lawrence et al. 1989). Nowadays most grain dielectric moisture meter manufacturer use a linear temperature correction (percent moisture per degree Celsius) and the equipment can measure in the region of 0-45 °C, but the recommendation of the manufacturers is to use the grain moisture meter close to room temperature because the measurement is the most accurate in that region (Wallis 2006). Since some types of grain are sometimes harvested during cold weather (below 0 °C), the grains may be very cold when harvested. Storage in very cold weather (with or without prior drying) during winter may also cause the grains temperature to be very low (sometimes less than -10, -15 °C) when the grain is removed from storage for sale. In other cases, grain may be harvested at high temperatures (above 30 °C) and taken directly to market. Grain is also very warm at the output of grain dryers. Waiting for grains to equilibrate to near room temperature to obtain accurate moisture measurements causes unacceptable delays in handling. Therefore, it is very

desirable to be able to make accurate moisture measurements on grain that is very warm or very cold—even below the freezing point of water.

Electrical properties are able to follow the changes in the moisture content, and they are able to indicate the changes of inner structure of foods and agricultural products (Nelson 1973). One of the most important fruits in Hungary is apple. Apples contain about 85-89% wet-basis moisture (Mohsenin 1989, Sass and Horn 1974). Changes of this relatively high moisture content during the drying process can be followed by weighing, or since dielectric parameters are successfully used to predict moisture content in many agricultural materials, it is supposed that electrical impedance parameters are also suitable to follow a drying process (Vozáry and Horváth 1998).

The aims of this study were to examine new perspectives of measuring the electrical properties of different kinds of agricultural products. My purposes was to improve and optimize a dielectric grain moisture meter and its calibration and to measure and calculate the relationships between electrical parameters and the physical and chemical properties of cereal grains and oilseeds The other purpose was to measure the electrical impedance of apple slices during drying, determining the periods of apple drying by the electrical impedance parameters and comparing it with the traditional weighing method.

For measuring the electrical parameters of grains, oilseeds, and apples at different frequencies LCR meters (HP 4284A and HP 4285A), a HP-4291A RF Material/Impedance Analyzer and a special VHF (Very High Frequency) prototype were used. The dielectric properties of grains and oilseeds were obtained with capacitive and transmission-line test cells and the electrical impedance spectra of apples were measured by pin electrodes.

A more effective algorithm was developed for establishing "unifying parameters" for the Unified Grain Moisture Algorithm. For wheat, rapeseed, sunflower, soybeans, barley, and oats, it was found that it was possible to measure grain moisture content by the dielectric method below zero degrees Celsius if the moisture contents were below certain limits (10-20%). This suggests that there is "free" water that can be frozen in high moisture grain, but not in low-moisture grain. The temperature dependence (and the optimum correction function) for moisture predictions from dielectric constant was different at 149 MHz and at 1 to 20 MHz. The moisture limits (for dielectric moisture measurements below zero Celsius) for these grains were determined to be similar for dielectric measurements at 149 MHz and 1 to 20 MHz. Some unifying parameters, the slope coefficient and the temperature correction coefficient for dielectric grain moisture measurements at 149 MHz, were predictable from grain chemical and physical parameters. It was possible to distinguish the periods of drying of apple slices with impedance measurements. Drying apple slices identified a distinct transition in impedance characteristics at approximately 1 kg water/kg dry matter moisture content.

# 4. LITERATURE

## 4.1. Importance of drying

Drying is one of the oldest methods of preserving foods. Primitive societies practised the drying of meat and fish in the sun long before recorded history (Beke 1997). Today the drying of foods is still important as a method of preservation. Dried foods can be stored for long periods without deterioration occurring. The principal reasons for this are that the microorganisms, which cause food spoilage and decay, are unable to grow and multiply in the absence of sufficient water and many of the enzymes, which promote undesired changes in the chemical composition of the food, cannot function without water (Earle 1983).

Drying of foods implies the removal of water from the food. In most cases, drying is accomplished by vaporizing the water that is contained in the food, and to do this the latent heat of vaporization must be supplied. Drying requires intensive energy consumption because evaporation of 1 kg of water under atmospheric pressure demands about 2400 kJ of energy (Rao and Rizvi 1995).

### 4.1.1. Moisture content

No agricultural product in its natural state is completely dry; some water is always present. This could be free or bound water. The moisture is usually indicated as percent moisture content for the product. Two formulas are used to express this moisture content. These formulas are give dry basis (*X*) (Equation 1*)* and wet basis (*x*) (Equation 2*)* moisture content. (Hereafter in this dissertation dry basis and wet basis will be referred to as db and wb) In addition, the content may be expressed as a percent. The percent moisture content is found by multiplying the decimal moisture content by 100. In addition, relationships between wet-and dry-basis moisture content on a decimal basis also can be seen in Equations 1 and 2.

The general governing equations for indicating moisture content are (Wilhelm et al. 2004, Beke 1997):

$$X = \frac{m_w}{m_d} = \frac{x}{1-x} \tag{1}$$

$$x = \frac{m_w}{m_t} = \frac{m_w}{m_w + m_d} = \frac{\frac{m_w}{m_d}}{\frac{m_w}{m_d} + 1} = \frac{X}{X+1} \tag{2}$$

where:

$m_d$ = mass of dry matter in the product, g
$m_w$ = mass of water in the product, g
$m_t$ = total mass of the product, water plus dry matter, g

Use of the wet basis measurement is common in the grain industry where moisture content is typically expressed as percent wet basis. (Wilhelm et al. 2004) However, use of the wet basis has one clear disadvantage—the total mass changes as moisture is removed. Since the total mass is the reference base for the moisture content, the reference condition is changing as the moisture content changes. On the other hand, the amount of dry matter does not change. Thus, the reference condition for dry basis measurements does not change as moisture is removed. For a given product, the dry basis moisture content is always higher than the wet basis moisture content. This is obvious from a comparison of Equations 1 and 2. The difference between the two basis is small at low moisture levels, but it increases rapidly at higher moisture levels. Fruit and vegetables have moisture contents near 0.90 (or 90%) (wb). On a dry basis, this would be 900% if expressed as a percentage (Wilhelm et al. 2004). For products of this type, moisture is often given as mass of water per unit mass of dry product.

### 4.1.2. Equilibrium moisture content

A material held for a long time at a fixed temperature and relative humidity will eventually reach a moisture content that is in equilibrium with the surrounding air. This does not mean that the material and the air have the same moisture content. It simply means that an equilibrium chemical potential exists between the material and the air. This equilibrium moisture content (*EMC* or *Me*) is a function of the temperature, the relative humidity, and the product. Numerous equations have been proposed to represent the EMC curves for various products (Iglesias and Chirfe 1982).

### 4.1.3. Water activity

The amount of water in foods and agricultural products affects the quality and perishableness of these products. However, perishableness is not directly related to moisture content. In fact, perishableness varies greatly among products with the same moisture content. A much better indicator of perishableness is the availability of water in the product to support degradation activities such as microbial action. The term “water activity” is widely used in the food industry as an indicator of water available in a product (Labuza 1984, Troller and Christian 1978). Water activity ($a_w$) is defined as:

$$a_w = \frac{P_w}{P_{ws}} = \frac{\phi}{100} \tag{3}$$

where:

$\Phi$= the relative humidity (water activity is equal to the relative humidity per 100 only if the material is at equilibrium with its headspace.), %

$P_w$ = the partial pressure of water vapor at the specified conditions, Pa

$P_{ws}$ = the partial pressure of water vapor at saturation at the specified temperature, Pa

For most foodstuffs a critical $a_w$ exist below which no microorganism can grow. This is in the range 0.6-0.7 (Stencl 1999). In general dehydrated foods have $a_w$ less than 0.6 semi-moist foods such as cereal grains, raisins and intermediate-moisture pet foods usually have $a_w$ between 0.62-0.92 (Stencl 1999). Fruit and vegetables which contain high (>80%) moisture content (like apple) have $a_w$ about 0.94-0.97 (Haas et al. 1975).

## 4.2. Controlling factors for air-drying

Two separate phenomena are involved in drying. First, moisture must move from the interior of a material to the surface of that material. Second, the surface water must be evaporated into the air. These two steps involve two very different phenomena (Beke 1997). Movement of water from the interior to the surface must occur in one of two manners—capillary action or diffusion. Movement by capillary action would only occur during early stages of drying. As the drying process continues, internal moisture movement would occur by molecular diffusion of water vapor within the material.

Removal of water from the surface involves evaporation of water from the surface into the surrounding air. The evaporation rate depends upon the condition of drying air (temperature, pressure, moisture content, and velocity of drying air) and the concentration of water at the surface. Air-drying involves the passing of air over the object(s) to be dried. Typically, the air is heated prior to entering the drying region (Wilhelm et al. 2004).

Consider the drying process for a high-moisture product (>80% wb) such as an apple slice. The surface of the slice will be visibly covered with water immediately after slicing. As this water evaporates, the surface becomes slightly dry. Moisture cannot move from the interior of the slice as rapidly as it can evaporate at the surface. Thus, the governing factor in later stages of drying is the diffusion rate of moisture within the slice (Wilhelm et al. 2004).

Factors affecting the drying rate will vary slightly depending upon the type of drying system used. However, in general, the following factors must be considered:

1. nature of the material: physical and chemical composition, moisture content, etc.;
2. size, shape, and arrangement of the pieces to be dried;
3. relative humidity or partial pressure of water vapor in the air (all are related and indicate the amount of moisture already in the air);
4. air temperature
5. air velocity

Another phenomenon that must be considered in drying solid materials is case hardening. This problem can occur if the initial stage of drying occurs at low relative humidity and high temperature. Under these conditions, moisture is removed from the surface of the material much

faster than it can diffuse from within the material. The result is formation of a hardened, relatively impervious layer on the surface of the material. Formation of such a layer causes subsequent drying to be much slower than it would otherwise be (Wilhelm et al. 2004).

Formerly, it was considered that water in a foods fell into one or the other of two categories, free water or bound water (Earle 1983). This now appears to be an oversimplification, and such clear demarcations are no longer considered useful. Water is held by forces whose intensity ranges from the very weak forces retaining surface moisture to very strong chemical bonds. In drying, it is obvious that the water that is loosely held will be removed most easily. Thus, it would be expected that drying rates would decrease as moisture content decreases, with the remaining water being bound more and more strongly as its quantity decreases. In many cases, a substantial part of the water is loosely bound. This water for drying purposes can be considered as free water at the surface (Beke 1997).

In air-drying processes, two drying periods are usually observed: an initial constant-rate period in which drying occurs as if pure water were being evaporated and a falling-rate period where moisture movement is controlled by internal resistances (Rao and Rizvi 1995). Figure 1 illustrates a commonly used drying curve, where part I-II represents the initial unsteady-state, warming up period, and II-III the constant-rate period (Rao and Rizvi 1995, Earle 1983). Constant-rate drying period has been reported for sweet potato, carrot and several fruits and vegetables (Saravacos and Charm 1962). Under typical drying conditions, the absence of constant-rate periods has also been reported for air drying of apples (Labuza and Simon 1970). The transition moisture content at which the departure from constant-rate drying is first noticed is termed the critical moisture content (indicated by III in Figure 1). At this point, the moisture content of the foods is not sufficient to saturate the entire surface. The critical moisture content generally increases with the thickness of the material and with the drying rate (Rao and Rizvi 1995). The drying period represented between III-IV is termed the first falling-rate period. During this period, the rate of liquid movement to the surface is less than the rate of evaporation from the surface and the surface becomes continually depleted of liquid water. Parts of the surface dry up by convective transfer of heat from the drying air, the surface temperature begins to rise, and vapor from inside the materials starts diffusing into the gas stream until point IV where all evaporation occurs from the interior of the food. Beyond point IV, the path for transport of both heat and mass becomes longer and more tortuous as the moisture content continues to decrease. This period is called the second falling rate period.

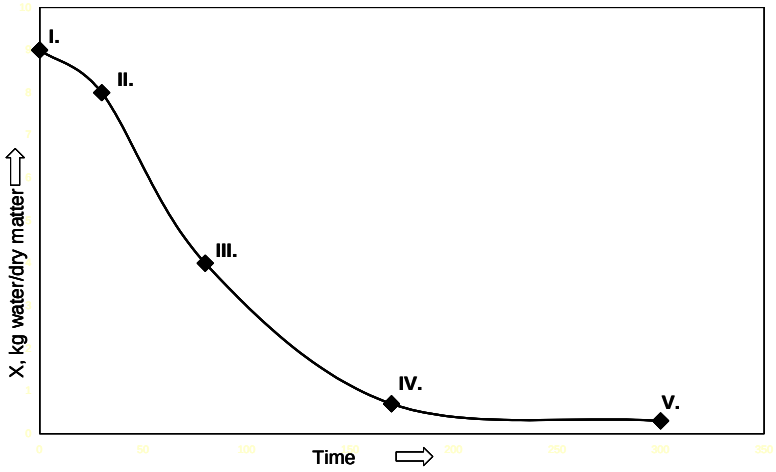


Figure 1. Drying curve, db moisture content versus time

The rate-controlling factors in the falling-rate period are complex, depending upon diffusion through the food and upon the changing energy-binding patterns of the water molecules (Rao and Rizvi 1995, Earle 1983). Finally, the vapor pressure of the food becomes equal to the partial vapor pressure of the drying air, and no further drying takes place. The limiting moisture content at this stage to which a material can be dried under a given drying condition is referred to as the equilibrium moisture content (Beke 1997, Wilhelm et al. 2004).

## 4.3. Drying of cereal grains and oilseeds

Drying has been the most common method for preserving grains and seeds. During drying, seeds go through physical and chemical changes caused by temperature and humidity gradients (Beke 1997, Neményi 2003). As an example, hydro and thermal stresses can appear and change properties such as density and porosity (Fortes & Okos 1980). Proper drying is a precondition for safe storage and delivery.

Cereal grains are usually dried in bin dryers with forced flow of the drying medium (Sharp 1982). A number of publications report studies of grain drying processes (Jayarman and DasGupta 1992, Wanaanen et al. 1993). Knowledge of thermal properties (specific heat capacity, thermal conduction factor, etc) of grain is essential for studying drying processes. Other papers deal with heat and mass transfers of cereal grains during drying with the final aim of enhancing the efficiency of dryers (Brooker et al. 1992, Bakker-Arkema et al. 1974, Boyce 1966, Neményi et al. 2000). The aim of these studies was to reduce the energy consumption and reduce the drying time without damaging the grain. França and Fortes (1994) developed a multidimensional model for grain fixed-bed drying simulation by expanding Brooker et al.'s (1992) model. Their model allows analyzing the airflow inside the dryer and includes the effect of temperature- and moisture-dependent properties. Czaba and Neményi (1997) modeled the heat and mass transfer within individual maize kernels during drying using finite element method. The main goal of this study was to give a

mathematical model with numerical solution to follow the heat and moisture distributions inside a cross sectional area of an individual maize kernel as a function of drying time with respect to the effects of the coupled heat and mass transfer processes. This mathematical model investigated maize hybrids with different drying characteristics during drying. The mathematical model with the boundary and initial conditions could reveal for example the difference between the fast and the slow drying hybrids (Czaba and Neményi 1997).

Mathematical models of the grain drying process, used mainly in simulations, describe convection drying of the raw material in the stationary bed under conditions of con-current or counter-current flow as well as in cross flow (Sharp 1982; Bertin and Blanquez 1986, Vagenas and Murinos-Kouris 1991).

Assessing the moisture content is one of the most critical grain quality measurements because of the direct economic significance of the fraction of the total product mass that is water and because moisture content largely determines the rate, at which the grain will degrade during handling and storage. Grains are bought and sold based on mass. The actual value of the grain is in the dry material, and accurate moisture determinations serve as the basis for appropriate price adjustments. Since grain deterioration due to microbial activity and insects is highly dependent upon moisture content and temperature, maximum moisture guidelines have been set for handling and storing grain (Funk 2001).

## 4.4. Importance of apple cultivation in Hungary

The apple is one of the most economically significant fruits in Hungary. The total area of production is close to 40000 hectares. By the data of the Hungarian Central Statistical Office, the biggest apple-yielding area is the North Hungarian Lowland with 22000 hectares. The South Hungarian Lowland follows with 5000 hectares. Several years ago, apple production was larger--more than 1.2 million tons. Nowadays this number is about 0.5-0.7 million tons per year, which is 4.2 percent of EU production and 0.9 percent of world total apple production (Harsányi et al. 2005).

The fruit contain a high percentage of their fresh weight as water (80-90%).Ginzburg (1978) found 86.5% wb moisture content for apple. He found total amount of carbohydrate is about 11.3%. The protein content is 0.4%, the fiber content is 0.6%, the acid content is 0.7%, the ash content is 0.5% and the carotene content is 0.1%. The C vitamin content is about 7 mg/100g (Ginzburg 1978). Accordingly, apples exhibit relatively high metabolic activity compared with other plant-derived foods such as seeds. This metabolic activity continues after harvesting, thus making most fruits highly perishable commodities (Atungulu et al. 2004).

## 4.5. Apple drying

One of the simplest methods to improve the shelf life of fruits is to reduce their moisture content to such extent that microorganisms cannot grow. Apples are consumed either fresh or in the form of various processed products such as juice, jam, marmalade, and as dried product, for example in muesli. Dried apple chips are a new tasty product in Hungary.

Several studies of apple drying characteristics have been carried out by Funebo and Ohlsson (1998), Wang and Chao (2002), Sacilik and Elicin (2005) and Velic et al (2004). Lengyel (1997) examined the change of the physical and chemical properties (carbohydrate, protein, ash and vitamin content) during air-oven drying. Lengyel (1997) has found the pectin and sugar content in Jonathan apples dried at 50 °C decreased in two different steps. In the first part, from 90% wb moisture to 40-50% wb moisture, large amounts of pectin and sugar migrate to the tissue surface with the evaporating water. Because of the higher temperature close to the surface, the pectin disintegrates. Because of the high sugar content and higher temperature close to the surface, Maillard reactions and caramelization occur. These reactions might cause the “bark” around the drying apple. In the second part, from 40-50% wb moisture until the equilibrium moisture, the pectin and sugar content decrease slowly. Lengyel also found that the acid and vitamin C content decreased uniformly during drying.

### 4.5.1. Apple drying methods

Usually for drying of apples or apple slices the air drying method (Beke 1997) is applied, but sometimes other alternative methods were developed. Infrared drying of apple slices was applied by Nowak and Lewicki (2004). Dielectric heating was applied by Feng and Tang (1998). Others (Simal et al. 1997) used pre-drying methods before air-drying. Several pre-treatment methodologies are commonly used in order to obtain high quality dehydrated foods. Osmotic dehydration of fruits and vegetables by immersion in liquids with a water activity lower than that of the food has received considerable attention in recent years as a pre-drying treatment to reduce energy consumption and to improve food quality (Jayarman and Das Gupta 1992, Torreggiani 1993, Karathanos et al. 1995). This method of dehydration, in which simultaneous movement of water and solutes from and into the material takes place (Yao and Le Maguer 1994), can be used as a pretreatment before air drying in order to reduce the water content of the food by 30 to 70% of the original amount (Lenart and Lewicki 1988). However, osmotic dehydration will usually not achieve sufficiently low moisture content for the product to be considered shelf-stable. This statement was concluded by Rahman and Lamb (1991) for pineapple samples.

### 4.5.2. Apple drying kinetics

In the air-drying process of capillary-porous colloidal foods (such as fruits and vegetables), two drying periods are usually observed: an initial constant-rate period, (constant moisture loss per unit time) in which drying occurs as if pure water were being evaporated, and a falling-rate period (decreasing rate of moisture loss) when moisture movement is controlled by internal resistances. Although several experimental and theoretical works about the drying of fruits (especially apples) were performed (Rao and Rizvi 1995), mathematical and physical description of a specific drying problem is rather difficult. Usually the material coefficients (viscosity, diffusion constant, etc.) are not known, and the structure of the drying object is continuously changing during dehydration. The same object can show various drying characteristics in various circumstances; the air-drying process of freshly harvested apples has a constant-rate and two falling-rate periods (Özilgen et al. 1995), while the drying of cold-stored apples does not contain a constant-rate period—rather two falling-rate periods (Labuza and Simon 1970, Üretir et al. 1996).

Low energy efficiency and lengthy drying time during the falling-rate period are major disadvantages of hot air drying of foods. Because of the low thermal conductivity of food materials in the falling-rate period, heat transfer to the inner section of foods during conventional heating is limited. The desire to eliminate this problem to prevent significant quality loss and to achieve fast and effective thermal processing has resulted in the increased use of microwaves for food drying. During microwave drying, local pressure and temperature rise continuously even though the loss factor of treated materials decreases with the reduction in moisture content. Although these increases of pressure and temperature can speed up the drying process, they may cause side effects such as bio-value degradation. Generally, the drying process of fruits is followed by weight loss (Özilgen et al. 1995, Rao and Rizvi 1995). Weight loss characterizes only the global moisture content of fruits or fruit slices and does not give information about the inner state of biological tissue. Usually scientists examine the microscope or electron microscope pictures of dried apple to get information about the inner state of the tissue. Wang and Chao (2002) observed the microscopic characteristics of irradiated and dried apple slices. They found that the microstructure and vacuole of 5mm stick apple slices was damaged after drying and irradiation. Other scientists (Bourvellec and Renard 2005) observed the electron microscope pictures of the cell wall materials and the oven-dried (100 °C) cell wall material of apple. They found the cell wall material was formed by a network of empty cells with thin walls and irregular shape. Oven-drying of the cell wall resulted in compaction and collapse of the network. The oven method changed the macro porosity of the material.

## 4.6. Electrical measurements

### 4.6.1. Electrical impedance

The application of a sinusoid voltage signal at single frequency to a sample results in a current of the same frequency. If the sample's impedance is purely resistive, the phase of the current is the same as that of the voltage. However, if the sample exhibits any capacitive or inductive reactance, a phase shift ($\varphi$) occurs. The impedance (Z, Equation 4) of a sample is the quotient of the alternating voltage ($U = U_o \cos \omega t + jU_o \sin \omega t$) across the sample and the alternating current ($I = I_o \cos(\omega t + \varphi) + jI_o \sin(\omega t + \varphi)$) through the sample. $U_o$ *and* $I_o$ are the peak values of voltage and current and *U and I* are the complex values of voltage and current at time *t*. $j = \sqrt{-1}$ is the imaginary operator, and $\omega = 2\pi f$ is the angular frequency, where *f* is the measuring frequency.

$$Z = U/I \tag{4}$$

Because of the phase shift ($\varphi$) between these two sinusoidal quantities, the quotient (equation 4) must be handled as a complex number (Z –Equation 5), having both real (resistance, *R*) and imaginary (reactance, *X*) parts (MacDonald 1987):

$$Z = |Z| \cdot \cos\varphi + j|Z| \cdot \sin\varphi = R + jX \tag{5}$$

Therefore, impedance can be plotted in the complex plane. |Z| and φ are the magnitude and the phase angle of impedance. This kind of representation of electrical impedance values, called a Wessel or an Argand diagram (Figure 2.) (Grimnes and Martinsen 2000, Macdonald 1987).

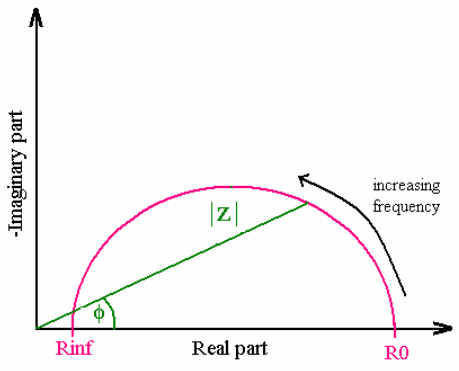


Figure 2. Typical Wessel or Argand diagram

Dielectic materials can be modeled with some simple electrical circuits. In ideal case, the dielectric material is not conducting material, but in biological tissues there is a conductance. These agricultural dielectric materials can be modeled with a simple parallel RC model (Figure 3.) (Sembery 2002, Grimnes and Martinsen 2000).

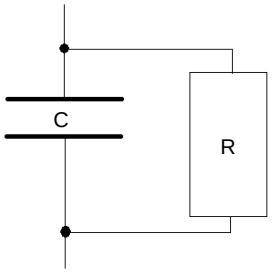


Figure 3. Simple parallel RC model

The reciproc of complex impedance of this model can be written as (equation 6):

$$\frac{1}{Z} = \frac{1}{R} + \frac{1}{-j\frac{1}{C \cdot \omega}} \tag{6}$$

Assuming that the area of the capacitor plate is A and d is the distance separating the electrode, the specific resistant is ρ and the relative dielectric constant is $\varepsilon'_r$, then we can write (equation 7):

$$\frac{1}{Z} = \frac{1}{\rho \cdot \frac{d}{A}} + \frac{1}{-j\frac{1}{\varepsilon_0 \cdot \varepsilon_r'} \cdot \frac{A}{d} \cdot \omega} \tag{7}$$

Because of the reciprocal of the specific resistance is equal of the specific conductance ($1/\rho=\sigma$) Equation 7 can be written as (equation 8):

$$\frac{1}{Z} = \sigma \cdot \frac{A}{d} + j \cdot \varepsilon_0 \cdot \varepsilon_r' \cdot \omega \cdot \frac{A}{d} \tag{8}$$

Introducing the relative complex electrical permittivity: ($\varepsilon'_r - \varepsilon''_r$), we get the complex capacitance (equation 9):

$$\overline{C} = \varepsilon_0 (\varepsilon_r' - j\varepsilon_r'') \cdot \frac{A}{d} \tag{9}$$

where $\varepsilon''_r$ is the dielectric loss factor, and $\sigma = \varepsilon_0 \cdot \varepsilon_r'' \cdot \omega$, the reciprocal value of impedance can be written as (equation 10):

$$\frac{1}{Z} = j \cdot \overline{C} \cdot \omega = j\varepsilon_0 \cdot (\varepsilon_r' - j\varepsilon_r'') \cdot \frac{A}{d} \cdot \omega = \varepsilon_0 \cdot \varepsilon_r'' \cdot \frac{A}{d} \cdot \omega + j\varepsilon_0 \cdot \varepsilon_r' \cdot \frac{A}{d} \cdot \omega \tag{10}$$

### 4.6.2. Dielectric properties

The application of an electric field to a material (such as the electric field within a capacitor) causes reversible and non-reversible motions of charges in the material. (Reversible changes are charge displacements that contribute to the dielectric constant. Non-reversible changes are charge motions that dissipate energy and contribute to the loss factor). These reactions are dependent on the properties of the material. Dielectric materials are usually insulators or they have small

electrical conductivity. The electrical properties of dielectric materials are called dielectric properties (Sembery 1994, Nelson 2003).

Many agricultural materials are treated as dielectric materials because they have low conductivity and can store electrical energy by polarization in an electric field. Electric polarization is characterized by the vector of electrical field intensity (E) and the vector of the dielectric displacement (D). The relationship between the two factors is Equation 11:

$$D = \varepsilon \cdot E \tag{11}$$

where $\varepsilon$ is the complex permittivity (MacDonald 1987). The value of the complex permittivity (Equation 12) depends on the material in the electric field.

$$\varepsilon = \varepsilon_0 \cdot \varepsilon_r \tag{12}$$

$\varepsilon_0$ is the permittivity of vacuum (8.854 x $10^{-12}$ Farad/meter)

$\varepsilon_r$ is the (dimensionless) relative permittivity

In a non-conducting material in an electrical field, a polarization effect will apply. During this effect, one side of the material would be positively charged and the other side would be negatively charged. The polarization works against (cancels part of) the applied electric field.

The complex relative permittivity is composed of two parts as shown in Equation 13:

$$\varepsilon_r = \varepsilon_r' - j \cdot \varepsilon_r'' \tag{13}$$

where $\varepsilon_r'$ is the real part, which is simply called “dielectric constant”, and $\varepsilon_r''$ is the imaginary part, which is called “loss factor” and j is the imaginary operator. The dielectric constant is proportional to the energy stored per cycle of an applied alternating electric field, and the loss factor is proportional to the energy dissipated as heat per cycle of the electric field. The ratio of these two factors (Equation 14) is the loss tangent (MacDonald 1987).

$$tg\delta = \frac{\varepsilon_r''}{\varepsilon_r'} \tag{14}$$

The dielectric constant and loss factor for a given material depend on the applied frequency. The dielectric constant always decreases as the measurement frequency increases. The loss factor may increase with frequency in some ranges and decrease with frequency in other ranges (Sembery 2002). Each local maximum in the loss factor is associated with a “relaxation mechanism,” and the frequency of the local maximum is the “characteristic frequency” for that relaxation mechanism. A material may have several different types of relaxation mechanisms present, and each type of relaxation mechanism may exhibit a broad distribution of characteristic frequencies. The particular frequency or frequencies that are chosen for dielectric measurements depend on which relaxation mechanisms provide useful information and which relaxation mechanisms are to be avoided because they interfere with the desired information.

The capacitance of a capacitor depends on the geometry and size of the capacitor and the dielectric properties of the material between the electrodes. The simplest geometry for a capacitor is the parallel-plate arrangement. The capacitance (Farads) of a parallel-plate capacitor (neglecting edge effects) is given by Equation 15 (The equations that define capacitance for other electrode geometries are generally much more complicated).

$$C = \frac{\varepsilon_0 \cdot \varepsilon_r \cdot A}{d} \tag{15}$$

If there is a vacuum between the electrodes, $\varepsilon_r$ is 1. The relative permittivity of air is also very nearly 1. If the material between the plates is conductive or "lossy," the relative permittivity is complex (both real and imaginary parts are non-zero), and the resulting capacitance is also a complex quantity.

### 4.6.3. Electrical impedance spectra and models

Electrical Impedance Spectroscopy (EIS) is becoming a popular tool in material research and development because it involves a relatively simple electrical measurement that can readily be automated and whose results may often be correlated with many complex material variables from mass transport, rates of chemical reactions, corrosion and dielectric properties, to defects, microstructure, and compositional influences on the conductance of solids. EIS can predict aspects of the performance of chemical sensors and fuel cells (MacDonald 1987). It is useful as an empirical quality control procedure, yet it can contribute to the interpretation of fundamental electrochemical and electronic processes. The disadvantages of EIS are primarily associated with possible ambiguities in interpretation. An important complication of analysis based on an equivalent circuit is that ordinary ideal circuit elements represent ideal lumped-constant properties. Inevitably, all electrolytic cells are distributed in space and their microscopic properties may be also independently distributed. Under these conditions, ideal circuit elements may be inadequate to describe the electrical response. Thus, it is often found that Z (ω) cannot be well approximated by the impedance of an equivalent circuit involving only a finite number of ordinary lumped-constant elements. It has been observed by many in the field that the use of distributed impedance elements (e. g., constant-phase elements (CPE)) in the equivalent circuit greatly aids the process of fitting observed impedance data for a cell with distributed properties (Macdonald 1987).

Electrical impedance spectroscopy of the lower frequency ranges (10 Hz - 1 MHz) has been applied extensively in medical science, and, in several cases, plant science (Grimnes and Martinsen 2000). In these frequency ranges (low and radio frequency), EIS of biological tissues presents α and β-dispersion bands. At higher frequencies (microwave frequency) γ and δ bands appear. The β-dispersion band was first investigated and recognized as a Maxwell-Wagner relaxation associated with membrane structures and is sensitive to tissue integrity and functionality (Martinsen et al.

2002, Kuang and Nelson 1998). A large magnitude, low frequency dispersion was observed by Schwan with muscle tissue and it is related in part at least to the tubular system (Schwan 1954). Colloidal particle suspensions also display this phenomenon (Schwan et al 1962). It is caused by the counterion atmosphere surrounding the charged particle surface. Rajewsky and Schwan (1948) noted a third γ-dispersion at microwave frequencies. It is caused by abundant tissue water. Several effects of smaller magnitude were later added by Schwan (1993). A number of β-dispersion effects of small magnitude occur at the tail of the β-dispersion. These effects are caused by proteins, protein-bound water (δ-dispersion), and cell organelles such as mitochondria (Stoy et al. 1982). A second Maxwell-Wagner dispersion is characteristic of suspended particles surrounded by a shell and is usually of small magnitude (Martinsen et al 2002). It occurs at frequencies well above those of the main β-dispersion.

The measured impedance spectrum of biological tissue usually can be modeled with equivalent circuits. In the simplest case, the measured impedance of tissue containing homogeneous cells can be described by a lumped model consisting of discrete resistors and capacitors representing the resistance and capacitance of cell compartments. Electrical behavior of tissue can be explained using the properties of these models (Grimnes and Martinsen 2000).

For most biological systems, it is observed that the centre of the impedance circular arc locus is situated below the real axis in the Wessel diagram (Figure 2). This was clear from the late 1920's, Cole and Fricke gave some diagrams and equations based upon a frequency independent phase angle (Cole 1928, Fricke 1932). But in 1940 Kenneth S. Cole proposed the empirical equation or distributed element so called Cole element or equation $Z = R_{\inf} + \frac{R_0 - R_{\inf}}{1 + (j\omega\tau)^{\alpha}}$ to describe the tissue impedance.

Where:

$R_0$ is the resistance at infinite frequency, ohm

$R_{inf}$ is the resistance at zero frequency, ohm

ω is the angular frequency, radian per second

τ is the relaxation time, 1 per second

α is a constant parameter

It is common observation that the value of Z for biological tissues decrease with frequency. $R_{inf}$ is the resistance value where the circular arc of the Cole-element intersects the real axis at "infinitely" high frequency (that is, far above the associated relaxation frequency f=2π/τ). The point

of intersection of this circular arc with the real axis at "zero frequency" (that is, far below the associated relaxation frequency) give the $R_o$ resistance. Choosing α as exponent in the Z equation (Cole 1940), the correct frequency dependence is taken care of with α always positive: $1 \geq \alpha \geq 0$. The parameter α is regarded as a measure of the distribution of relaxation times or as a measure of the deviation from an ideal resistor and capacitor in the equivalent circuit. Other interpretations are possible (Grimnes and Martinsen 2000). According to the first interpretation, the spread of relaxation times may due to: (a) different degrees of molecular interaction (minimal interaction corresponds to α=1 for impedance and α=0 for permittivity), (b) cellular interactions and properties of gap junctions, (c) anisotropy, (d) cell size, or (e) fractal dimensions. For impedance α=0 corresponds to the purely resistive case, for the permittivity α=1 corresponds to the no loss case. The parameter α is therefore analogous to the phase angle, 1-α to the loss angle (Grimnes and Martinsen 2000).

The Constant Phase Element (CPE) is a non-intuitive circuit element that was discovered (or *invented*) while looking at the response of real-world systems. The Cole equation does not allow an independent variable dc conductance in parallel with the CPE, but it allows as an independent series connection. In this case, the series-connected impedance of a constant Phase Element ($Z_{CPE}$) can be written as $Z_{CPE} = \Delta R(j\omega\tau)^{-\alpha}$ (Grimnes and Martinsen 2000 Macdonald 1987). In the Wessel diagram of a CPE is a simple one. For a solitary CPE, the locus of points is just a straight line, which makes an angle with the x-axis.

When biological tissues under investigation contain several components having a variety of different structures, then the measured impedance is affected by each structure. This resultant impedance can be successfully modeled using distributed (Cole) elements (Repo and Zhang 1993) containing a few parameters. However, the parameters for the distributed element model do not always relate to actual anatomical structures of sample tissue. The intercellular (apoplasmic) part and intracellular (symplasmic) parts of living tissue have mainly resistive characteristics, while the cell membrane impedance is essentially capacitive with very high resistivity. At low (~100 Hz) frequencies, current passes through the apoplasmic space of tissue where ions are the main current carriers. Cell membranes and other interfacial layers appear more conductive with increasing frequency, since the impedance of those capacitive barriers decrease. The apparent conductivity is dependent on the permittivity of the interfacial layers (Pething and Kell 1987). Accordingly, symplasmic space appears more conductive at higher frequencies. At high (above 100 kHz) frequencies, where the impedance of membranes is low and the resistance of the membrane can be

neglected, the symplasmic and apoplasmic resistances can be modeled as a parallel circuit (Grimnes and Martinsen 2000, Zhang and Willison 1991).

Electrical impedance spectra of materials are usually measured with a two-electrode arrangement. Such measurements are complicated by the fact that the measured impedance includes electrode polarization effects. When an electrode surface is immersed in an electrolytic medium, metallic ions migrate into the electrolyte and create a space-charge region near the surface. This space-charge region creates a potential barrier that opposes the flow of current. This shielding of the electrode by an ionic cloud is called electrode polarization (Scott et al. 2000). If the electric field is constant, the ions are distributed in a double layer as described by Debye and Hückel (1923). If the electric field is alternating, the ions respond to the reversal of charge on the electrodes at each half-cycle, but they are retarded by their frictional drag through the medium. The double layer then becomes sensitive to the frequency of the alternating field since electrode charge oscillating faster than the ions can respond leads to incomplete formation of the double layer. Thus, the effects of electrode polarization disappear at high frequencies. The electrode polarization impedance can be estimated and separated from the tissue impedance by measuring the same sample with different electrode spacing (Zhang and Willison 1991, Vozáry et al. 1996,).

Another method is available to eliminate the electrode polarization effect. This is the four-electrode impedance measurement. In this arrangement, the constant current flows through the sample between the outer electrodes and the voltage is measured between the two inner electrodes. In this case, the polarization on the inner pins cannot be observed because there is no current on the potential measuring pins. For this method, it is necessary to compensate the sample's impedance between the outer and the inner electrodes. (Schwan P.H. and Ferris D.C. 1968). Unfortunately, RCL meters (HP 4284 and 4285) at the Physics and Control Department cannot work in the four-electrode arrangement.

## 4.7. Moisture content determination of cereal grains and oilseeds

An extensive list of standards for moisture measurement is provided by the Association of Official Analytical Chemists (AOAC 1990), which is an international organisation. The technique used in a given instance depends upon the material being studied the equipment available, and the time available for the measurement.

### 4.7.1. Reference and basic methods

The air oven method is the most common reference method for grain wb moisture determinations. Air oven methods vary widely in procedures and results (Hungarian Standard

6367/3-83, Burden 1998), but all are based on heating the sample for a prescribed period at a prescribed temperature and measuring the loss of mass. The amount of mass lost is assumed the amount of water that was present in the sample. Unfortunately, the method is not that simple. Together with water, non-aqueous material is also driven off by heating. The heating times and temperatures parameters are determined by comparing the air oven method to other more basic (and difficult) methods such as the phosphorous pentoxide (ICC Standard 1976) ($P_2O_5$) method or the Karl Fischer titration method (ISO Standard, ISO 760 1978). Most air-oven methods require hours or days to complete. The $P_2O_5$ and Karl Fischer methods provide the most accurate results for moisture content but they are time consuming and require special apparatus, ground grain samples and different chemicals (Iod, $SO_2$, Pyridine). Clearly, grain producers, handlers, and processors need much more rapid methods to assess moisture content (Funk 2001).

### 4.7.2. Rapid indirect methods

Many different technologies have been tried for rapid grain moisture measurement. Rapid indirect methods all measure some physical parameters (dielectric constant, conductivity, reflection coefficient, absorbance by electrical or optical sensing) and predict moisture content with calibration equations or charts. Invariably, other sample constituents or sample geometry interfere with the signal (wavelength, voltage differences) caused by water. Temperature usually affects both the water signal and the interfering signals. Therefore, calibration equations attempt to achieve a best fit between the measured parameters and the moisture content as defined by an accepted moisture reference method. Accurate grain moisture measurements depend upon successfully overcoming the effects of the most important interfering factors, such as density, temperature, chemical composition, and impurities (Funk 2001, B. Gillay 2005, Trablesi and Nelson 1998).

#### 4.7.1.1.Near-infrared method

Near-infrared spectroscopy instruments sense the absorption of near-infrared radiation by water. The water absorption bands that are used for moisture determinations are at about 1.0, 1.4, and 1.9 micrometer wavelengths (Funk 2001, Williams and Norris 1987). Whole-grain near-infrared (NIR) instruments that are used for moisture determinations generally use one of the lower wavelength regions. Other grain constituents such as protein, oil, and starch have absorption bands that overlap the water absorption bands. Furthermore, differences in grain physical condition caused by growing conditions and grain handling strongly affect NIR instrument measurements. These interferences demand separate calibration equations for different grain types. Multivariate statistical methods such as multiple linear regression, principal components regression, partial least squares regression, polar qualification system and neural networks are used to develop NIR moisture

calibrations that achieve excellent accuracy in spite of these strong interferences (Funk 2001, Maertens et al. 2004, Kaffka et al. 1982, Kaffka and Seregély 2000, Seregély 2000).

#### 4.7.1.2.Conductivity method

The conductivity method for measuring grain moisture is based on the approximately linear relationship between grain moisture content and the logarithm of direct-current conductivity of grain kernels (Funk 2001). Conductivity-type instruments generally use a small sample size (ground samples) and depend upon compressing, crushing, or grinding the grain to achieve consistent moisture measurement results. Conductivity-type moisture meters are usually the lowest-cost alternative for moisture measurement because of their electronic simplicity, but they are quite inaccurate for measuring grain with non-uniform moisture distributions within the kernel (Funk 2001, Hunt and Pixton 1972).

#### 4.7.1.3.Microwave method (From about 300 MHz to 300 GHz)

Water absorbs microwave energy strongly (Trablesi at al 1998)--a fact routinely exploited to cook moist foods in microwave ovens. Microwave moisture measurement meters direct a beam of microwave radiation through the grain sample and measure signal parameters related to the attenuation and/or the phase shift of the microwave signal caused by the sample's presence (as compared to air). Calibration equations can be established to relate these measured parameters (along with sample type, density, and temperature) to moisture content as determined by routine reference methods (Funk 2001). The microwave method is a particularly attractive technology for online measurements of flowing grain (in transit through a pipe or on a moving belt) because the microwave beam can sense the average dielectric properties of a large cross-section of grain. Sample temperature measurements are easily achieved in flowing grain, but simultaneous density determinations are more difficult. Microwave systems that ignore density are unlikely to yield adequate accuracy for intended purposes. Simultaneous measurements of attenuation and phase shift provide enough data to calculate the complex permittivity of the sample (Nelson 2004). Several different density-independent functions of the complex permittivity have been tested and shown to yield good moisture measurement accuracy without explicit sample density measurements (Kraszewski et al. 1998, Trabelsi and Nelson 1998). Some of these functions also provide an estimate of the sample density (Kraszewski and Nelson 1992, Trabelsi et al. 1998). That work has also suggested an algorithm for unifying calibration equations for different grain types (Trabelsi et al. 1999). Proponents of the microwave method cite its relative immunity to sample conductivity effects as a major advantage over conductivity methods or RF dielectric moisture measuring

methods (Hasted 1973, Kraszewski 1996). The primary limitation of the microwave method has been the relatively high cost and complexity of microwave-based moisture measurement systems.

4.7.1.4. Radio-frequency dielectric method (From about 20 kHz to 300 MHz)

The radio-frequency (RF) dielectric method measures moisture content in grain by sensing the dielectric constant of grain samples. The dielectric constant is a measure of a material's ability to store electrical energy when placed in an electric field. Because of its molecular structure, water has a very high dielectric constant (approximately 80) compared to other grain constituents (protein, oil, starch, etc. -- 2 to 3) (Funk 2001, Venkatesh and Raghavan 2005). This wide difference in dielectric constants between water and other grain constituents should make the RF dielectric moisture method quite insensitive to sample composition. However, the RF dielectric moisture method is influenced significantly by grain kernel structure and composition and moisture distribution within kernels, necessitating individual calibration equations for different grain types and limiting measurement accuracy. In addition, the RF dielectric moisture method is expected to be more sensitive to grain conductivity (presumably ionic conductivity) than the higher frequency microwave methods (Funk 2001). Despite these limitations, the RF dielectric moisture method presents an attractive combination of good accuracy, close matching (standardization) among instruments within a model, relatively simple calibration development, and moderate manufacturing cost. (Funk 2001, Gillay B. 2005).

### 4.7.3. Dielectric grain moisture measurements

Electrical properties of grain seed have been utilized in devising electrical instruments, which can be used for quick tests for indication of moisture content or some other quality parameters (protein, oil, starch content). Dielectric properties have also been of interest because of their influence on energy absorption in dielectric heating studies. In still other possible applications, electrical properties, which influence static charge behavior, have been of interest in studies of electrostatic separation principles (Hamond et al. 1961, Matthes and Boyd 1969). There has been much interest in electrical properties of grain and seed for many years because of the possibility for measuring or sensing moisture content or other quality factors. Interest generally focused on the influence of a grain or seed sample on the response of an electrical circuit, and, in the case of moisture measurement, the instrument readings were calibrated with values measured by oven techniques or other standard methods.

General principles employed by electrical moisture testers for grain and seed have been discussed by Zeleny (1954, 1960) and Nelson (1973) and differences were noted in the performance of conductance and capacitance-type moisture meters. The influence of various factors on the accuracy of capacitance type moisture meters was carefully considered by Matthews (1963) and

design requirements developed for such an instrument on the basis of these studies. Using a d-c resistance measuring meter and a capacitance-type meter in combination, a measure of the moisture distribution in corn kernels was obtained by Holaday (1964) and used successfully to detect heat damage (protein deanaturation) in artificially dried corn. Frequency and moisture dependence data on a similar selection of grain and seed have been reported for the audio frequency range, 250 Hz to 20 kHz (Corcoran et al. 1970, Stetson and Nelson 1972a) Dielectric constant decreased while frequency increased. They supposed this is as an evidence of a dispersion phenomenon. Extensive studies have been conducted comparing results of moisture content values provided by various electrical meters with those of approved oven testing procedures or other standards. Such a comparison was reported for a conductance-type meter and two capacitance-type meters, which have had USDA approval for grain inspection work (USDA 1963). Hart and Golumbic (1966) have been reported such comparisons for seed other than grain. Such studies on dielectric-type meters widely used in Europe have also been reported (Moller 1971). In general, the accuracies of capacitance-type meters can be approximately 0.5 percent within limited moisture ranges when clean grain samples of usual characteristics are being tested.

The temperature dependence of dielectric properties of grain is important especially when a new prototype moisture meter is developed. Lawrence et al. (1990) were working on the temperature correction of several grain types at wide (0.1 MHz-110 MHz) frequency range.

For the measurement of microwave electrical properties of wheat and corn, a prototype system was developed at the Budapest University of Technology and Economics Department of Microwave and Telecommunications (Sembery and Völgyi 1989).

In numerous publications in which the precisions of different types of dielectric moisture meters are compared with each other and with a reference method (in most cases with the air-oven method).

A comparison of the dielectric properties of three varieties of alfalfa seed at 39 MHz and 2.45 GHz has been reported by Stetson and Nelson (1972b). The measurements showed somewhat lower dielectric constants at the higher frequency and considerably lower loss factors at 2.45 GHz than at 39 MHz. The variability components for determining precision of moisture meter to oven comparisons were determined by Hurburgh et al. (1980). They reported the standard deviations of individual drops from the mean of three drops increased linearly with moisture increases from 0.1 % point at 15% wb moisture to 0.34% point at 35% wb moisture. Hurburgh et al. (1981) compared moisture meter readings to oven determinations for 879 samples of 1979 and 1980 harvested corn. At that time, all of the meters tested had calibration biases ranging from 1.5 percentage points above to 3.5 percentage points below the air oven.

Paulsen et al. (1983) found moisture meter biases for corn from +0.1 to +0.6% points in the 12 to 14% wb moisture range and from –0.6 to –3.0% points in the 30 to 32% wb range. The meter biases became more negative as moisture increased.

Hurburgh et al. (1985) measured three factors affecting the variability of moisture meter measurements. Those factors were the oven, moisture meter, and sample variance. Oven variance was constant across all moistures and contributed about 4% or less of the total variance. Moisture meter variance increased as moisture increased but was always less than 12.5% of the total variance. The remaining 83.5% of variance was attributed to the samples. Overall variance approached a minimum between 15 and 20% wb moisture content. They concluded that more knowledge of grain compositional quality relative to dielectric properties would aid in improving moisture meter accuracy.

Other scientists were working on developing new prototype instruments, test cells, and methods. The tendency of the new developments in dielectric moisture meters shows that the measurement frequency is moving into the higher region. Radio or microwave frequencies are used instead of audio frequencies to avoid the low frequency polarization effect (Funk 2001, 2000, Funk et al 2005, Nelson 2003, 2004, Gillay Z. and Funk 2003, 2005, Gillay B and Funk 2002, 2003).

## 4.8. Grains quality and approved moisture measurement methods in the U.S.A., in the E.U. and in Hungary

Because of the huge amount of grain trading all over the world, strict rules are important in trading. In the U.S. marketing system, quality requirements for grain exports are governed by both contract specifications and a complex, constantly evolving government-regulated system of guidelines that cover the inspection, sampling, grading and weighing of grains. These grain standards and inspection procedures are designed to ensure a uniform product and to facilitate the trading and marketing of U.S. grains. Congress passed the U.S. Grain Standards Act in 1916 at the request of local trade and governments that wanted a national inspection program and, for the first time, a national weighing program.

The Federal Grain Inspection Service (FGIS) is an organization of the U.S. Department of Agriculture’s (USDA) Grain Inspection, Packers and Stockyards Administration (GIPSA). FGIS administers a system for officially inspecting and weighing grain and other commodities through 12 field offices and two federal/state offices in the United States and Canada.

US Grain Standards exist for 12 grains: corn, wheat, soybeans, sorghum, barley, oats, rye, flaxseed, sunflower seed, canola and triticale. Commodities such as rice, pulses and hops have similar standards for grade and quality factors. With a few exceptions, the official inspection of export grains is mandatory. Official personnel employed or licensed by GIPSA obtain

representative samples using approved equipment. The grade is reported on a certificate, which represents the entire lot inspected. (U.S. Grains Council Importer Manual. Chapter 4 1986)

In the USA it is determined by GIPSA which rapid moisture meter is accepted for an official moisture measurement. The method, which is applied to measure the moisture content of grain, is also determined officially. The moisture content in the grain is determined only by a standardized DICKEY-john Grain Analysis Computer (GAC2100). Moisture does not influence the numerical grade or any special grades. However, it is determined on all shipments and reported on the official certificate. The process how to use the GAC2100 is also determined by USDA. (U.S. Grains Council Importer Manual 1986)

In the European Union, grain quality standards are determined in intervention standards. The most recent standard is the intervention for grain quality control and quality assurance that was developed in 2000 (824/2000 EC Comission Regulation). This regulation is valid in each member of the European Union. Therefore, at this moment this is the official standard in Hungary if somebody would like to sell grain in the EU. In this Comission Regulation there is an appendix number three about moisture measurements. The definitive moisture measuring technique is the Air Oven method. In questionable cases, only the results of the air oven method are accepted (appendix 2). Instruments, which apply dielectric spectroscopy or NIR method, are also accepted for grain moisture content determination. These equipment types have to conform to the ISO 712:1998 standard. These fast moisture meters have to be calibrated in accredited laboratories. The limit of validity of the calibration is usually 2 years. For reliable results, the calibration has to be checked in every half year with 3-5 reference samples and the instrument has to be recalibrated if necessary. EU standard require that the moisture content measured by a fast method has to be determined by the average of three repeated measurements. The differences between the measurements cannot be greater than 0.5%. If the result is greater this value, the whole process has to be repeated.

## 4.9. Unified Grain Moisture Algorithm

The radio-frequency (RF) dielectric method is used to measure moisture content in grain for forty years by The United States Department of Agriculture—Grain Inspection, Packers and Stockyards Adminstration (USDA-GIPSA). In Hungary and in other countries of Europe, large grain receiving stations are also using this type of technology to measure the moisture content of grain samples because the method presents an attractive combination of good accuracy, relatively simple calibration development (for one grain type), and moderate manufacturing cost. However, the technology is burdened by the need for separate calibrations for each grain types or classes and yearly checking of calibrations to ensure continuing accuracy.

Research collaboration between USDA-GIPSA and USDA-Agricultural Research Service (Athens, GA) over the period of 1995 to 2001 resulted in an improved RF dielectric moisture measuring method that effectively combined many diverse grain types or classes calibration into a single "unified calibration" (USDA-GIPSA 2005 Annual report to congress Federal Grain Inspection Service). This method was found capable of moisture measurement accuracy equal to or better than what was achievable for grain-specific calibrations with current instruments. In this method, similar grain classes and types were placed in grain groups that could be measured without knowing the specific grain class. (Funk 2001)

A total of 2714 grain samples were tested by the technical staff at the United States Department of Agriculture—Grain Inspection, Packers and Stockyards Administration (GIPSA) in the course of the original research. That research utilized the samples that were collected through GIPSA's Annual Moisture Calibration Survey in the United States. (USDA-GIPSA 1999) That program provides a uniquely extensive, broad, and representative sample set to ensure accurate calibrations for official grain moisture measurements—and it is ideally suited for research to measure dielectric properties that affect moisture measurement and to develop improved moisture measurement algorithms.

### 4.9.1. Application of the Unified Moisture Algorithm

The first generation of Unified Moisture Algorithm was developed by Funk in 2001 and is described more detailed in his dissertation (Funk 2001). The advantage of the single measurement frequency is that an instrument based on an algorithm that could achive excellent moisture measurement performance with a single measurement frequency should much less expensive to design and manufacture than one requiring multiple widely-spaced frequencies. The advantage of an algorithm that uses a single measurement frequency is the simplicity of the calibration process (Funk 2001). The square of linear correlation (squared Pearson's r) was calculated between the density corrected dielectric constant for yellow-dent field corn at 149 MHz and at 1 to 251 MHz and air-oven moisture content. Above 70 MHz the the correlation was greater than 0.999, but at lower frequencies the conductivity effect was higher. Therefore, the optimum measurement frequency was determined at 149 MHz.

#### 4.9.1.2. Materials and methods for Unified Moisture Algorithm

The dielectric data for the 2714 grain samples were measured with a special test cell that was configured as a parallel-plate transmission line with a matched (50-ohm) termination. A Hewlett Packard HP-4291A RF Material/Impedance Analyzer sensed the complex reflection coefficient at the input to the test cell. The test cell was mathematically modeled using a signal-

flow-graph, and an iterative solver (written in Mathcad) was used to convert complex reflection coefficients to relative complex permittivity (dielectric constant and loss factor).

Other research showed that the measured dielectric constant need to be corrected for two effects (empty cell correction with $\varepsilon_{ec}$ and Filling Factor FF correction) that are caused by the test cell design (Gillay Z. and Funk 2003). The presence of dielectric materials in proximity to the test cell (specifically the cell "gate") caused the calculated dielectric constant of the empty test cell to be other than 1.000. To correct this, an offset value $\varepsilon_{ec}$ (dielectric constant of the empty test cell) was subtracted from the measured relative complex permittivity ($\varepsilon_{meas}$) as shown in Equation 16. Secondly, the parallel-plate transmission-line test cell did not support a true transverse-electric-magnetic (TEM) mode when grain is in the test cell. A filling factor *FF* was needed to convert the measured relative complex permittivity to actual relative complex permittivity. The real part of the relative complex permittivity (dielectric constant) $\varepsilon_r$ was used for further calculations.

$$\varepsilon'_r = \mathrm{Re}\left(\varepsilon_{meas} - \varepsilon_{ec}\right) \cdot FF + 1 \tag{16}$$

4.9.1.3. Density correction in the Unified Moisture Algorithm

Dielectric constant is inherently a volume-based parameter (Nelson 1992), but grain moisture is expressed as the percent of the total grain mass (water and dry material). Assuming an average bulk density for each grain type causes large moisture measurement errors because the bulk density of grain samples within most grain types varies by more than twenty percent of the nominal value. Across grain types, bulk density varies by more than a factor of three (Funk 2001). Thus, some means of density correction must be incorporated in a grain moisture meter to achieve good accuracy.

Funk's research confirmed Nelson's assessment (1992) that Equation 17 was highly effective for estimating the dielectric constant at a second bulk density (target) from the measured dielectric constant at an original bulk density. Hereafter in this dissertation, Equation 17 (a restatement of the Landau and Lifshitz, Looyenga mixture equation by Nelson (1992)) will be referred to as the "cube-root density correction" (Funk 2001).

$$\varepsilon_c = \left[\left(\varepsilon'^{\frac{1}{3}}_r - 1\right) \cdot \frac{\rho_{target}}{\rho_{sample}} + 1\right]^3 \tag{17}$$

*where:*

$\varepsilon_c$ is the density-corrected dielectric constant
$\varepsilon_r'$ is the measured dielectric constant
$\rho_{target}$ is the target density (g/cm$^3$)
$\rho_{sample}$ is the sample density (g/cm$^3$)

4.9.1.4. Slope, Offset and Translation adjustment in the unifyied calibration

Figure 4A shows the dielectric constant values at 149 MHz for 2714 samples representing 15 grain groups and three crop years and Figure 4B shows the same data after applying the cube-root density correction to the dielectric constants. Each sample in each grain group was density-corrected to the average sample density for that group (Funk 2001).

The effects of applying different target sample densities to each grain group were tested. It was found that the error in the linear fit between density-corrected dielectric constant and moisture content was essentially independent of the target sample density chosen. However, varying the target sample density adjusted the slope of the linear regression. Therefore, target sample densities were chosen for each grain group to make the linear regression (between density-corrected dielectric constant and moisture content) be exactly 6.000 % moisture per unit of density-corrected dielectric constant. This was essentially a reverse slope adjustment step (hereafter in this dissertation, reverse slope correction will be referred to as slope correction). Figure 4C shows the results of this adjustment. All grain types essentially coalesced into two groups.

After that slope correction, it appeared that the differences among the groups were essentially offsets along the vertical (dielectric constant) axis. A separate offset parameter *OP* was applied to the density-corrected dielectric constants in each grain group (Equation 18) to minimize the average differences among grain groups. The results are shown in Figure 4D.

$$\varepsilon_{adj} = \varepsilon_c + OP \tag{18}$$

After applying the offset adjustments, the density-corrected dielectric constant versus moisture curves were very nearly superimposed for all grains. However, some differences were visible in the very low moisture region. Slope changes were observed for each grain group at or below about 10 % wb moisture. The bend for sunflower seeds occurred at about 7 % wb moisture, the bend for soybeans was at about 8.5 % wb moisture, and the bend for the cereal grains was at about 10 % wb moisture (or slightly higher). It was recognized that these bends were occurring at about the same moisture levels where conductivity caused much more dramatic bends in the dielectric constant versus moisture curves at much lower frequencies (Funk 2001). This change in slope was found to be stable over the range of 100 to 250 MHz. It was concluded that this slope change was due to two different water phases (monolayer water and higher layers of water) that have different dielectric constants. This commonality of slopes in both regions suggested one last correction to bring all grain types together in a single prediction equation.

Starting from the condition portrayed in Figure 4D, the data for soybeans were translated along the common line (slope = 6.000) by +1.5 % moisture content and +1.5/6.0 = 0.25 units of dielectric constant; and the data for sunflower seeds were translated by +3.0 % wb moisture content

and +3.0/6.0 = 0.50 units of dielectric constant to get the close agreement among grain groups shown in Figure 4E. The translation unifying parameter *TP* was applied according to Equations 19 and 20. No translation unifying parameter was applied to the cereal grains.

$$x_{adj} = x_{ref} + Ktc \cdot (t - 25) + TP \tag{19}$$

$$\varepsilon_{adj} = \varepsilon_c + OP + \frac{TP}{6} \tag{20}$$

$x_{ref}$ is the reference (air oven) wb moisture value

$x_{adj}$ is the reverse temperature-corrected air-oven wb moisture value

*Ktc* is the temperature correction coefficient (% wb moisture per degree Celsius)

*T* is the measured sample temperature

A 4th-order polynomial equation was fitted to $x_{adj}$ and $\varepsilon_{adj}$ to create a "unified" calibration equation. (Equation 21). Note that the temperature correction (*Ktc*) and the translation unifying parameter (*TP*) are subtracted in Equation 21 to get the final predicted wb moisture value.

$$x_{tc} = \sum_{r=0}^{4} (\varepsilon_{adj})^r \cdot CC_r - Ktc \cdot (T - 25) - TP \tag{21}$$

$CC_r$ is the *r* order polynomial regression coefficient

Figure 4F shows the predicted wb moisture measurement error for this calibration model. The overall standard deviation of differences for the calibration was 0.29 % wb moisture.

Funk's research (2001) introduced a new type of calibration process (for 2714 grain samples) for dielectric grain moisture meter, which effectively combined many grain types calibration into a single unified algorithm. He showed the basic steps of the Unified Moisture Algorithm, but he opened some questions for further research. These questions were:

1. How can the test cell be scaled and retain calibration compatibility?
2. In a transmission-line test cell, what length of air-filled line is required?
3. What tolerances are required for measured parameters to retain conformity with VHF algorithm?
4. What mechanical and electronic tolerances are necessary for conformance with the VHF algorithm and other existing specifications?
5. How to effectively develop unifying parameters for additional grain types and classes?
6. How can unifying parameters be determined directly from grain chemical and physical characteristics?
7. How to develop a "master" instrument, reference materials, and processes to validate dielectric measurements for commercial instruments.
8. What are the effects of cell coatings/corrosion on the measurment?
9. What materials are suitable for the test cell?
10. Can coaxial and single-sided parallel geometries be used with the algorithm?

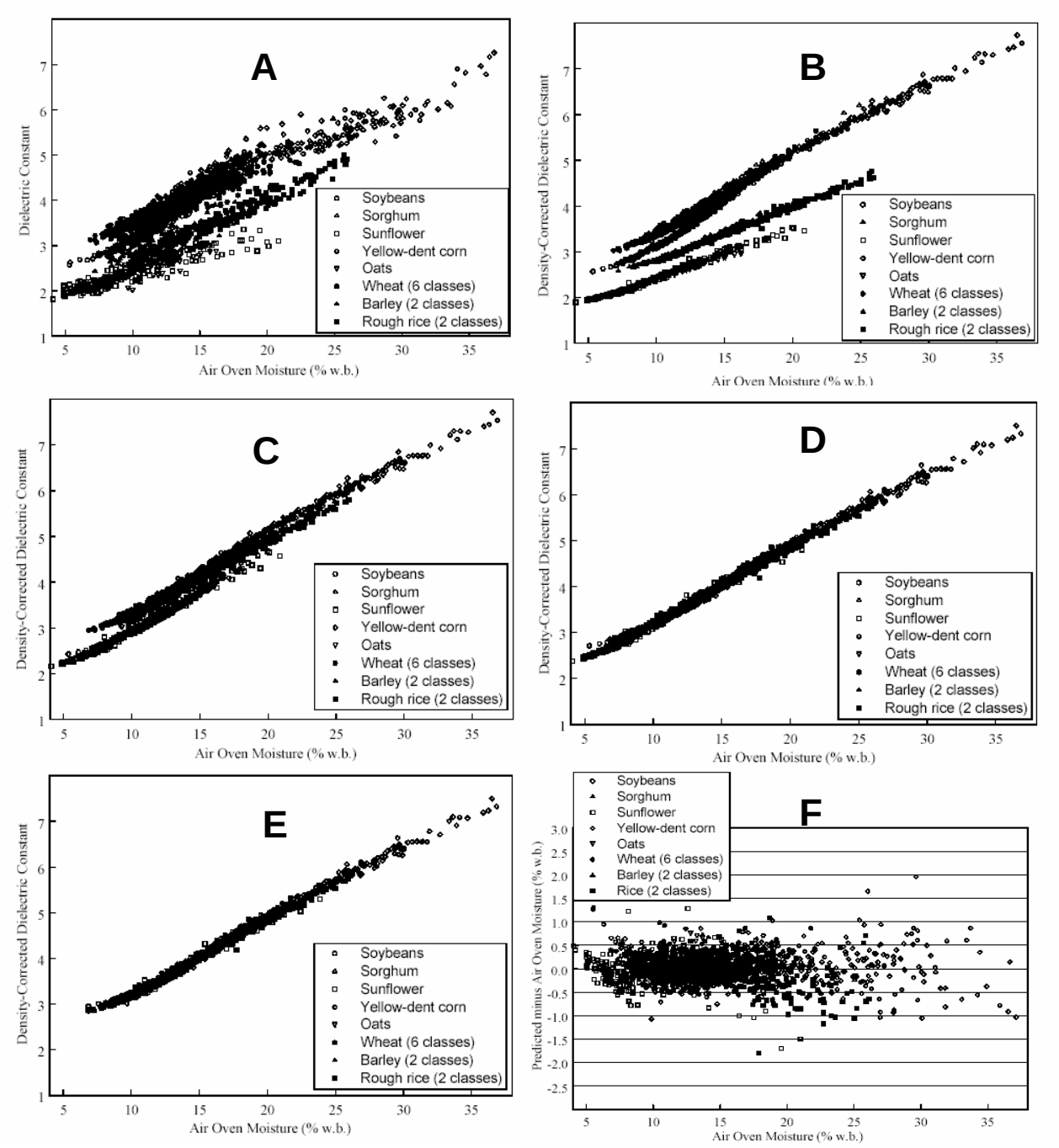


Figure 4. Details of the Unified Moisture Algorithm. A) Dielectric constant without density correction. B) Plot of density corrected dielectric constant (Each grain group density-corrected to the average density for that grain group). C) Same as in previous plot except each grain group density-corrected to a value selected to yield slope of linear regression equal to 6.000 % wb moisture per unit of density-corrected dielectric constant. D) Each grain group density-corrected to give a slope of 6.000 (% wb moisture per unit dielectric constant) and biased according to the intercepts found by linear regression. E) Same as previous plot except the data were translated along the common slope line to align the curve shapes in the low moisture region with 4th order polynomial calibration curve. F) Performance of the Unified Moisture Algorithm (predicted minus reference wb moisture) (Used with permission from Funk (2001).)

## 4.10. Temperature corrections of dielectric measurements

Sample temperature is one of the most important factors influencing dielectric grain moisture results since temperature affects the dielectric constant of water, the degree of hydrogen bonding between water and other molecules, and the magnitude of interfering factors such as ionic conductivity (Funk 2001, Nelson 1973). The effects of sample temperature are further complicated by the phase change of "free" water at zero Celsius. Ice has a much lower dielectric constant than water in the RF and higher frequency ranges (Hasted 1973).

Grains are often harvested at high moisture contents and requires drying to moisture levels that allow long-term storage without spoilage. Accurate moisture measurements before drying are needed to set drying parameters that yield the desired output moisture contents after drying. Since some types of grains are sometimes harvested during cold weather, the grain may be very cold (grains temperature can be 0 to -5 °C) when harvested. Storage in very cold weather (with or without prior drying) may also cause the grains temperature to be very low when the grain is removed from storage for sale (especially during wintertime). In other cases, grain may be harvested at high temperatures and taken directly to market. Grain is also very warm at the output of grain dryers. Waiting for grains to equilibrate to near room temperature to obtain accurate moisture measurements causes unacceptable delays in handling. Therefore, it is very desirable to be able to make accurate moisture measurements on grain that is very warm (above 35°C) or very cold—even below the freezing point of water (Funk 2001, Lawrence et al. 1990).

In a series of papers, Nelson (1984, 1985a, b, 1986a, b) published mathematical models for estimating the dielectric constant of cereal grains and oilseeds at 24 °C. Only limited data are available relating to the temperature dependence of the dielectric properties of grains. Caugh et al. (1973) found a positive linear correlation between moisture content and temperature for moisture contents from 0.5 to 25% wb over a temperature range from -20° to 80° at frequencies of 2.45 and 9.0 GHz. Jones et al. (1978) reported a positive temperature coefficient of approximately 0.02 units per degree Celsius at 30 MHz for the dielectric constant of wheat at moisture contents of 13.4 to 21.2% wb in the temperature range from 4° to 40° Lawrence et al. (1989, 1990) reported complex permittivity measurements for soft red winter wheat at frequencies from 0.1 to 110 MHz and moisture contents ranging from 8.2 to 23.4% wb. These measurements were taken at 10° C intervals from 0° to 50° C. In addition, Lawrence et al. (1991) reported a temperature-dependent model to calculate the dielectric constant of soft red winter wheat. They found that the dielectric constant of soft red winter wheat in the frequency range from 0.1 to 100 MHz generally increases nonlinearly with increasing temperature in the range from 0° to 50° C and with increasing temperature coefficients as moisture content increases in the range from 8 to 23% wb.

Funk (2001) found that a simple temperature correction function (Equation 22.*)* was reasonably effective for correcting temperature effects on predicted wb moisture values in the first generation of the Unified Grain Moisture Algorithm.

$$x_{tc} = x_{pred} - Ktc \cdot (T - 25) \tag{22}$$

$x_{pred}$ is the wb moisture value calculated from dielectric characteristics

$x_{tc}$ is the predicted wb moisture content with temperature correction

That is, the temperature correction required was linear with temperature and independent of moisture content (to a reasonable approximation). When developing moisture calibration equations it was found advantageous to reverse-correct the reference moisture values for temperature, as shown in Equation 19, instead of forward-correcting the dielectric constant values. This simplified calibration development, especially when multi-term (polynomial or other) non-linear equations were used to fit dielectric data to air oven results.

There are also some unanswered questions about the temperature correction of dielectric moisture tests in Funk's dissertation (2001). These were:

1. What are the temperature effects for different grain types at 150 MHz?
2. What are the freezing point (moisture) limits for different grain types?

# 5. OBJECTIVES

The United States Department of Agriculture- Grain Inspection, Packers and Stockyards Administration has supported continuing research at Corvinus University of Budapest, Physics and Control Department, for the purpose of improving the Unified Grain Moisture Algorithm method for optimizing the necessary unifying parameters and developing methods that make the calibration process easier in the future for new grain types and classes which have not yet been fit in the calibration. Our purpose was to extend the application of this calibration to very low (-25 °C) and to high (50 °C) temperature range.

During the dielectric grain moisture measurements relatively low moisture content (about 10-35 % wb) samples were obtained, but it is also important to measure the electrical properties of high (80-90% wb) moisture content agricultural product, like fruits. Dielectric moisture meters at different measurement frequencies are widely used for moisture content determination all over the world. The question arises whether some kind of electrical parameter at lower frequencies (30 Hz – 800 kHz) is suitable to follow on-line or off-line the moisture content changes in a high moisture content fruit during drying.

Because of the moisture distribution changes in fruit samples during the drying process, the parralell plate test cells (used for grain dielectric measurements) were changed to the pin electrode measurement, which can give more information about the inside properties of the tissue.

Ice has a much lower dielectric constant than free water in the RF and higher frequency ranges, which cause a discontinuity in dielectric spectra measured as a function of temperature.

There are different periods (constant-, falling-rate), during the drying of high moisture content fruit. Therefore, it was also interesting to us whether we can find relationships between the electrical parameters, model parameters, and the periods of fruit drying.

Main goals of the study in detail:

1. Improving the Unified Grain Moisture Algorithm. Reducing the number of grain groups and minimizing the calibration error. Examining the goodness and precision of the fitted calibration.
2. Developing new calibration methods to minimize the calibration error (for 4887 data measured by GIPSA staff) by the recalculation of the calibration parameters.
3. Developing new calibration algorithm to simplify the calibration process when more grain types and classes are fitted in the calibration and to minimize the calibration error.
4. Determining the dielectric constant and loss factor of grains and oilseeds at low and high frequencies. Measuring the dielectric parameters of several grains and oilseeds at high (149

MHz) frequency with a transmission line test cell by a Very High Frequency (VHF) prototype and at low frequencies (1-20MHz) with capacitive test cell by LCR meter in temperature range of -25 to 50 °C. Determining the wb moisture content by developing temperature correction. Comparing the temperature correction at low and high frequencies.

5. Determining the wb moisture limits for low and high frequency dielectric measurements, where the free water has frozen in the sample, and below which the dielectric measurement is applicable for grain moisture content determination. Comparing the wb moisture threshold values at low and high frequencies.
6. Collecting physical and chemical parameters of grains from the literature. Predicting unifying parameters (Slope, Offset, Translation, moisture-independent and moisture-dependent temperature correction) from physical and chemical parameters. Validating models, which used unifying parameters calculated from physical and chemical parameters.
7. Developing methods for impedance measurements in apple slices during drying. Measuring the magnitude and phase angle of impedance in drying apple slices.
8. Comparing changes in magnitude and phase angle of impedance with changes in moisture content during various periods of apple drying. Distinguishing two falling rate periods of apple drying by impedance parameters.
9. Modeling the measured impedance values of apple slices by one or two distributed elements. Comparing the changes in moisture content with changes of model parameters in drying apple slices.

# 6. MATERIALS AND METHODS

## 6.1 Materials

There are four different kind of data set, which were examined in this dissertation. The first data set (dielectric parameters, wb air-oven moisture content, temperature and sample mass) was measured on more than 5000 grain samples by the staff at the United States Department of Agriculture—Grain Inspection, Packers and Stockyards Administration. The second data set (dielectric parameters, wb air-oven moisture content, temperature and sample mass) on six major Hungarian grain types (130 samples) and the third data set the impedance of apple slices during drying were measured at the Corvinus University of Budapest Physics and Control Department. The fourth data set (physical and chemical properties of grains and oilseeds) was collected from the literature.

### 6.1.1. Cereal grains and oilseeds

More than 5000 grain samples were tested by the technical staff at the United States Department of Agriculture—Grain Inspection, Packers and Stockyards Administration (GIPSA). Appendix 1 summarizes the grain types and numbers of samples that were tested during each crop year. This research utilized the samples that were collected through GIPSA's Annual Moisture Calibration Survey (USDA-GIPSA 1999) in the United States between 1998 and 2002. This program provides a uniquely extensive, broad, and representative sample set to ensure accurate calibrations for official grain moisture measurements—and it is ideally suited for research to measure electrical parameters to develop improved moisture measurement algorithms. Figure 5 summarizes the measured parameters of the huge amount of samples, which were tested by the USDA-GIPSA stuff.

For the dielectric tests (130 dielectric and temperature tests) which were developed at Corvinus University of Budapest Physics and Control Department, six bulk grain samples were obtained from grain receiving stations in Hungary (Herceghalmi Rt. and Tápánszentkereszt Gabona Kutató Kht). The grain types tested included:

I. Oilseeds: soybeans (*Glycine soja*), sunflower (*Helianthus annuus*), rapeseed (*Brassica napus*),
II. Cereal grains: soft wheat (*Triticum aestivum*), autumn barley (*Hordeum vulgare*) and oats (*Avena sativa*).

Some of these samples (sunflower, soybeans) were collected after harvesting at high wb moisture contents (>20%) and they were cleaned and cooled down to 4-6 °C immediately to avoid

spoilage. Others were dried (12-15 % wb moisture content) after harvesting. These samples needed re-wetting before dielectric tests to reach high (>20% wb moisture content). The moisture contents of the samples were adjusted as necessary by allowing the samples to air-dry under room ambient conditions or by adding distilled water to the samples, mixing the samples thoroughly in sealed containers, and allowing them to equilibrate under refrigeration for at least one week prior to testing (Lawrence et al 1990, Nelson 1978, ISO 7700:1 1984, ISO 7700:2 1987, OIML IR59 1984).

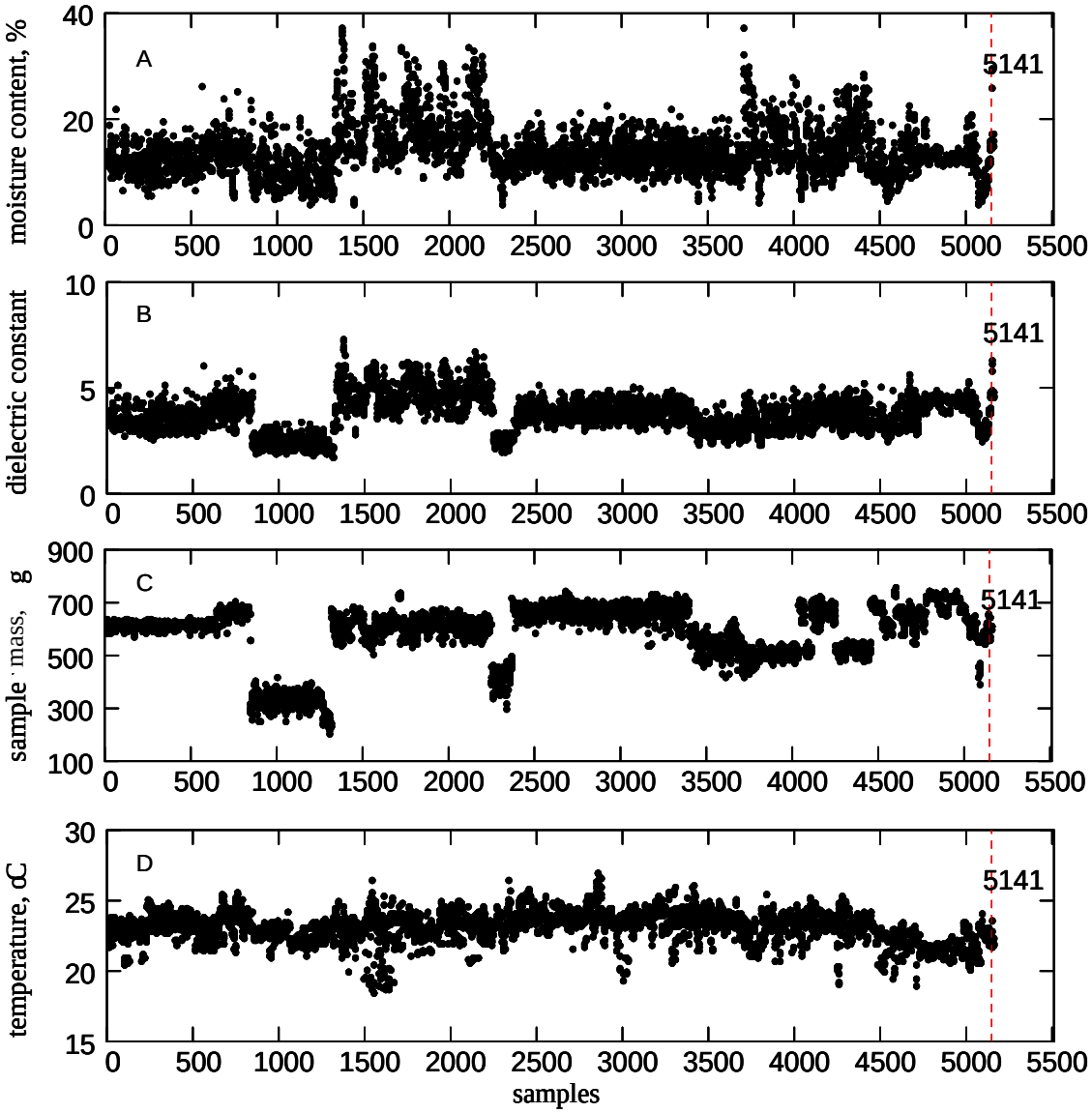


Figure 5. Measured parameters of grains and oilseeds samples by the USDA-GIPSA stuff A) Wet basis Air-Oven moisture content versus sample number B) Real part of the dielectric constant versus sample number C) sample mass (g) versus sample number D) sample temperature versus sample number

### 6.1.2. Physical and chemical properties of cereal grains and oilseeds

The physical and chemical parameters (Appendix 5) for 10 grain types were collected from many different references. Some literature sources did not include values for each physical and

chemical parameter. In these cases the average value (calculated from other literature) was substituted. Tables 1-2 show the average values for each grain type. (See Reference Numbers in Table 1 and notes below Table 2.). The values shown in Appendix 5 Tables 1A) and 1B) are rounded to approximately two significant characters for ease of comparison.

Table 1. Average chemical properties of grain types

| Grain type | Reference Numbers | Protein, % | Oil/Fat, % | Ash, % | Starch, % | Moisture, % |
|---|---|---|---|---|---|---|
| Soy | 1, 2, 3, 19, 20, 21 | 40 | 22 | 4.9 | 24 | 9.80 |
| Sorghum | 1, 2, 4, 5, 22 | 8.4 | 3.0 | 1.4 | 72 | 13.90 |
| Sunflower | 1, 6, 7, 8, 20 | 19 | 45 | 3.8 | 22 | 10.90 |
| Corn | 1, 2, 9, 10, 11, 12, 13, 20, 21 | 9.9 | 3.0 | 1.3 | 76 | 10.41 |
| Oats | 1, 2, 6, 10, 11, 14, 19 | 13 | 6.0 | 3.3 | 60 | 15.33 |
| Wheat | 1, 2, 9, 10, 11, 15, 16, 20 | 10 | 1.2 | 1.7 | 71 | 15.12 |
| Barley | 6, 10, 11, 17 | 16 | 3.2 | 2.5 | 70 | 9.00 |
| Rice | 1, 2, 6, 10, 11, 14 | 8.2 | 1.8 | 1.5 | 80 | 9.02 |
| Flaxseed | 14 | 23 | 42 | 3.9 | 25 | 6.00 |
| Rapeseed | 17, 18, 20 | 26 | 42 | 6.3 | 15 | 11.52 |

Table 2. Average physical properties of grain types

| Grain type | Bulk Density ($g/cm^3$) | Seed mass (mg) | Seed volume ($mm^3$) | Kernel Density ($g/cm^3$) | Major axis (mm) | 2nd Axis (mm) | 3rd Axis (mm) |
|---|---|---|---|---|---|---|---|
| Soy | 0.73 | 157 | 125 | 1.25 | 7.3 | 6.5 | 5.5 |
| Sorghum | 0.73 | 32 | 25 | 1.26 | 4.2 | 3.7 | 3.1 |
| Sunflower | 0.35 | 66 | 64 | 1.03 | 14.1 | 7.2 | 4.1 |
| Corn | 0.73 | 330 | 250 | 1.31 | 11.2 | 7.6 | 4.5 |
| Oats | 0.48 | 31 | 24 | 1.31 | 10.5 | 2.8 | 2.1 |
| Wheat | 0.73 | 34 | 24 | 1.35 | 6.3 | 3.3 | 2.9 |
| Barley | 0.62 | 42 | 35 | 1.20 | 8.9 | 3.5 | 2.5 |
| Rice | 0.71 | 31 | 22 | 1.40 | 7.6 | 2.7 | 2.4 |
| Flaxseed | 0.68 | 4.3 | 3.5 | 1.15 | 5.6 | 2.9 | 1.2 |
| Rapeseed | 0.69 | 3.7 | 3.0 | 1.12 | 1.6 | 1.6 | 1.5 |

1. Nelson 2002 2. IGP 1998 3. Milani 2000 4. Lee 2003 5. Lupien 2004 6. Paliwal 1998 7. Duke 2003 8. Santalla 2003 9. Nelson 1978 10. Győri and Mile 1998 11. Lásztity 1998 12. U.S. Grains Council 2001-2002 13. Klein 2003, 2004 14. Doug 2004 15. Kajdi 2003 16. Satterlee 2000, 2002 17. Canadian Grain Comission 2003 18. Kansas State University 2003 19. Muir 2004 20. Kocabiyik 2004 21. Delate et al. 2002 22. Cagampang and Kirleis 1984

### 6.1.3. Apple

Jonathan apples *(Malus domestica)*, were obtained from a local market. Samples were stored in refrigerator at about 5-7 °C temperature. Samples were removed from the refrigerator and were placed in the Lab area for 2-3 hours to reach the room temperature before impedance measurements. For the measurements, approximately 20 mm x 20 mm x 10 mm slices were cut from the apples before testing. The mass of each slice was measured at the before drying and after drying--before the impedance measurements. Assuming an average 89 % wet basis moisture content of whole apple (Mohsenin 1980 Sass and Horn 1974), the dry-basis moisture content (kg of water per kg of dried matter), *X*, of slices after drying was calculated by the formula (Equation 23):

$$X = \frac{m - 0.11\, m_0}{0.11\, m_0} \tag{23}$$

The values of $m_o$ and $m$ are the mass of slices before and after drying, respectively.

## 6.2 Instrumentation

### 6.2.1. Electrical measurements on grains at Grain Inspection, Packers and Stockyards Administration

At GIPSA, grain samples were tested by a HP-4291A RF Material/Impedance Analyzer (Figure 6.), which is a single-port RF instrument. Measurements, which data were used for the calculation of the unifying parameters, were performed on this instrument. Complex reflection coefficients with high precision from 1 to 501 MHz were measured (Funk 2001). Measurement voltage was a constant low value (500 mV). The instrument included software to calculate correction parameters to calibrate the instrument with standard networks (open, short, and 50-ohm load) at the instrument's test port and to extend that calibration to other reference planes—in this case the grain test cell is described below. The instrument had the capability to store data to a floppy disk or send it to an external computer through the GPIB interface. A digital thermometer (Shore Sales Digital Thermometer Model LT-207) (for room temperature tests) and alcohol-in-glass thermometers (for extreme-temperature tests) were used to determine sample temperature immediately before pouring the sample into the loading funnel.

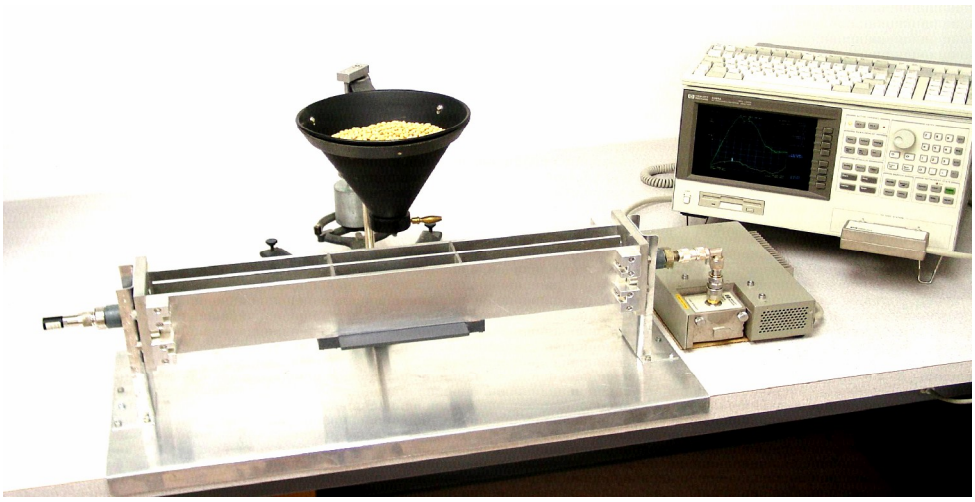

Figure 6. A 50 ohm transmission-line test cell and HP-4291A RF Material/Impedance Analyzer

### 6.2.2. Electrical measurements on grains at Corvinus University of Budapest

At the Physics and Control Department, the grain samples at different moisture contents were tested by means of a HP-4285A Precision LCR Meter (Figure 7.) at 51 frequencies in the range of 75 kHz to 30 MHz. The measurement voltage was constant low value (1V). The temperature sensor was a series-connected pair of 1N914 silicon diodes fed by a 1 mA current source. A HP-3457A Digital Multimeter was used to measure the temperature sensor voltage. The

HP-4285A and the HP-3457A were connected to a computer through a GPIB interface to permit unattended data collection as controlled by a proprietary QBasic program (written by David Funk).

Figure 7. Instrumentation for the low frequency
(75 kHz – 30 MHz) dielectric moisture tests

Dielectric characteristics at 149 MHz were measured by a prototype moisture measurement system (Figure 8). This system included a VHF signal generator type G4-107 a parallel-plate transmission-line test cell, three directional couplers to sample drive signal level and the incident and reflected signals, and an Analog Devices type AD8302 Gain/Phase Detector integrated circuit (evaluation board) to sense the relative gain and phase of the incident and reflected signals. An HP-3457A Digital Multimeter was used to measure the drive signal level, gain, and phase voltages and the current from an Analog Devices type AD-590 temperature sensor (1 μA/K), which was located in the test cell. Automatic data collection was performed by a QBasic program (written by Viktor Jagasits and David Funk)

Figure 8. VHF prototype system

Figure 9. shows the block diagram of the prototype reflectometer-type system. In our system, we used three directional couplers. In general, a directional coupler is a device that allows most of the signal to pass from the input to the output terminal and “samples” that signal. The “sampled” signal appears at the “coupled” output (Mini-Circuits 1999).

The first directional coupler was used to sample the drive signal. The coupled output of that 10 dB directional coupler (meaning that the output at the coupled port is 10 dB lower than the input signal level) was connected to a diode detector, which converted that RF signal to a DC voltage that was measured to sense the generator drive signal. The 10 dB attenuator between the first directional coupler and the second directional coupler served two functions. First, it decreased the drive signal by 10 dB so that the signal going into the second directional coupler was at the same level as the signal measured by the diode detector (from the 10 dB coupler). Secondly, the attenuator would prevent signals that were reflected back to the source (from the other directional couplers and test cell) from being re-reflected back to the directional couplers and test cell—and thereby confusing the measurement. The 10 dB attenuator prevented this by attenuating the reflected signal by 10 dB on the way back towards the source (generator) and again by 10 dB if any of that signal was reflected from the source.

The second directional coupler was used to sample the forward signal and send that RF signal to the Gain/Phase detector as a reference signal. The coupled output of the “forward” coupler went through a 20 dB attenuator to reduce that “reference” signal level to approximately the level of the “reverse” signal that was sampled from the third directional coupler. Attenuating the reference signal was necessary because of the limited (60 dB) “dynamic range” of the AD-8302 Gain/Phase Detector circuit (Analoge Devices Inc. 2002).

The third directional coupler was placed “backwards” in the signal path so its coupled output contained very little of the “forward” signal from the previous directional coupler’s output, but it sensed the reflected signal from the test cell.

The AD-8302Gain/Phase Detector provided output voltages that were: 1) proportional to the logarithm of the ratio of the two input voltages (approximately 0.60 volts per decade of voltage ratio), and 2) proportional to phase difference between the two RF signals (approximately 10 mV per degree) (Analog Devices Inc. 2002).

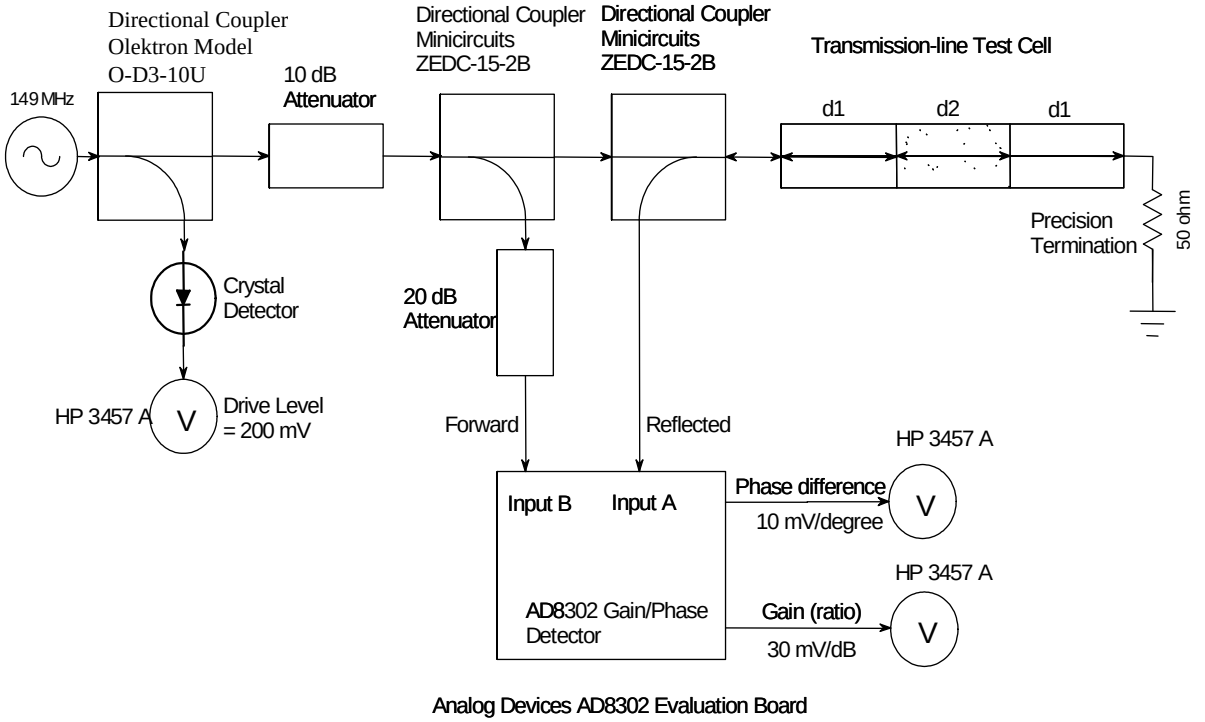


Figure 9. VHF prototype sensor block diagram

### 6.2.3. Apple impedance measurements

The magnitude ($Z_M$) and phase angle ($\varphi_M$) of electrical impedance in the apple slices were measured by an HP 4284A Precision LCR meter (Figure 10) at 44 frequencies in the frequency range of 30 Hz to 800 kHz. The measurement voltage was constant low value (1V). The LCR meter was connected to a computer via a GPIB interface. Data collection was performed by a proprietary QBasic program (written by David Funk). Open (measuring air--$Z_O$, $\varphi_O$) and short (measuring short circuit-- $Z_S$, $\varphi_S$) corrections were applied to minimize measurement errors (Honda 1989). Equations 24 to 29 were applied to calculate the open-short corrected impedance and phase angle ($Z_C$, $\varphi_C$).

$$ZO = Z_O \cdot \cos\varphi_O + j(Z_O \cdot \sin\varphi_O) \tag{24}$$

$$ZS = Z_S \cdot \cos\varphi_S + j(Z_S \cdot \sin\varphi_S) \tag{25}$$

$$ZM = Z_M \cdot \cos\varphi_M + j(Z_M \cdot \sin\varphi_M) \tag{26}$$

$$ZC = \frac{ZO \cdot (ZM - ZS)}{ZO - (ZM - ZS)} \tag{27}$$

$$Z_C = \sqrt{(\mathrm{Re}\,ZC)^2 + (\mathrm{Im}\,ZC)^2} \tag{28}$$

$$\varphi_C = \arctan\left[\frac{(\mathrm{Im}\,ZC)^2}{(\mathrm{Re}\,ZC)^2}\right] \tag{29}$$

The temperature inside the apple slices was monitored with a copper-constantan thermocouple during drying. The thermocouple voltage was measured by a Solartron–Schlumberger 7066 voltmeter with ice-bath reference junction compensation.

Figure 10. Instrumentation for the impedance measurements

### 6.2.4. Apple air oven tests

A Venticell 111 air oven was used for apple drying tests. Apples were placed on the air-oven latticed tray, so the moving hot air in the oven could contact with almost the whole surface of the samples. Apple slices were dried at 50 °C. This moderate drying temperature is commonly used in practice (Üretir et al 1996).

### 6.2.5. Grain air oven tests

The grain moisture measurements (prepared at Corvinus University of Budapest, Physics and Control Department) were performed by the appropriate Hungarian Ministry of Agriculture standard air oven method (Hungarian Standard 6367/3-83 --- Appendix 2.). For these tests, a QC-128 type laboratory grinder was used to grind cereal grains and oilseeds. A Mettler AE-200 analytical balance was applied to measure the sample mass before and after the drying and samples were dired in a Venticell 111 type air oven.

For the grain analyses at GIPSA, the reference wb moisture value for each test sample was determined by GIPSA technical staff using the appropriate USDA standard air oven method (Burden 1998).

## 6.3. Test cells and electrodes

### 6.3.1. Electrical measurements on grains at GIPSA

The test cell used at GIPSA (Figure 11.) was constructed as a 50-ohm transmission line (Lawrence et al. 1999). It consisted of three parallel aluminum plates. The ends of the plates were connected to endplates from a Hewlett-Packard 805A Slotted Line. Each endplate contained a 50-ohm transition from a Type-N coaxial connector with a threaded stud that was connected directly to the center plate. The test cell was designed to permit transmission coefficient measurements as well as reflection coefficient measurements.

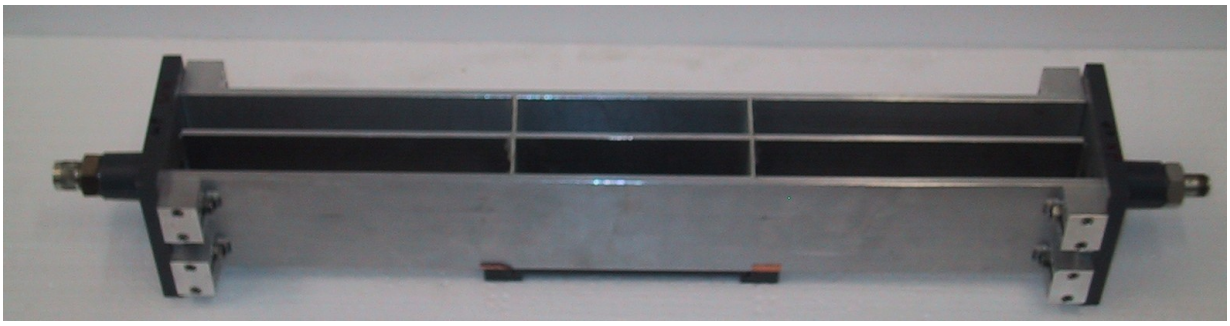

Figure 11. 50-ohm transmission line test cell

### 6.3.2. Electrical measurements on grains at Corvinus University of Budapest

Two types of test cells were used at the Physics and Control Department. For the low frequency (75 kHz-30 MHz) measurements, the test cell (Figure 12) was a special parallel-plate capacitive test cell from a GAC-II moisture meter (Dickey-john Corporation, Auburn, Illinois, USA). The volume of the test cell was 342 $cm^3$. For the capacitive test cell, the sample temperature was sensed by measuring the voltage drop across a pair of series-connected silicon diodes within the test cell, with a constant current source of 1 mA.

For the high frequency (149 MHz) dielectric moisture measurements, the test cell (Figure 13) was a special parallel-plate transmission line consisting of two outer parallel copper plates (76 mm x 229 mm x 0.8 mm) and a center electrode (also 76 mm x 229 mm) made of 0.8 mm thick double-sided copper-clad circuit board. The volume of this test cell was 393.6 $cm^3$. At each end of the center electrode, a one-cm-wide strip of the copper (both sides) was removed except for where the electrode was soldered to the SMA-type chassis coaxial connector. The spacing between electrodes was set at 25.4 mm to achieve a characteristic impedance of very nearly 50 ohms. The test cell was terminated with a precision 50-ohm load. Rigid polystyrene foam insulation (Owens-Corning PINK®) was used as spacers between the electrodes to define the grain-filled section (101.6 mm long) and as insulation around the test cell to minimize the rate of heat transfer during the

temperature tests. The polystyrene foam's very low dielectric constant (<1.1) was an advantage because of the small effect on the dielectric constant measurements.

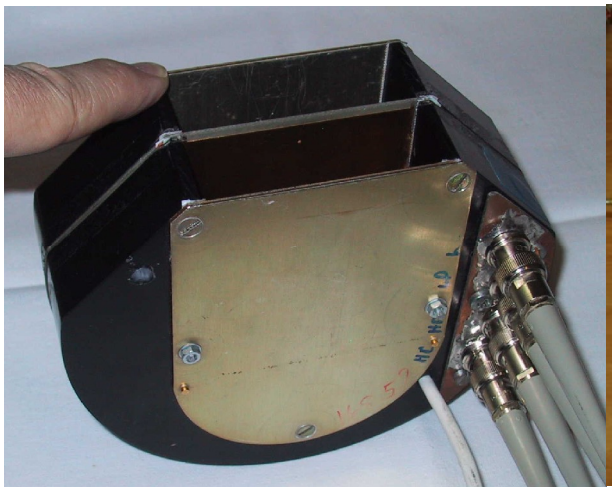

Figure 12. Parallel-plate capacitive test cell (for the low frequency 75 kHz to 30 MHz dielectric tests)

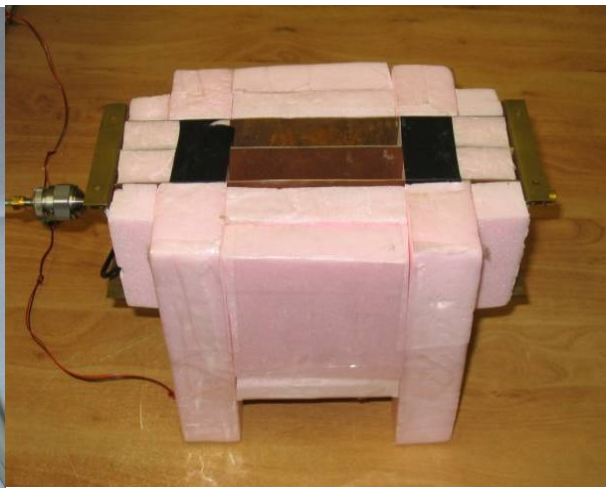

Figure 13. Transmission-line test cell (for the high frequency 149 MHz dielectric tests)

### 6.3.3. Electrodes for apple impedance measurements

The impedance spectra were measured with a two-pin electrode (Figure 14.) arrangement. Three different electrode spacings (1.8 mm, 4.6 mm and 6.8mm) were used. The thickness and the length of the gold-plated copper pins (from Socapex plugs) were 0.6 mm and 14 mm, respectively. The electrodes were connected to BNC jacks by copper wires with Teflon isolation, and the BNC jacks were joined to the HP-4284A LCR meter by a special 1 m length shielded cable (HP-16048A can be seen on Figure 10.).

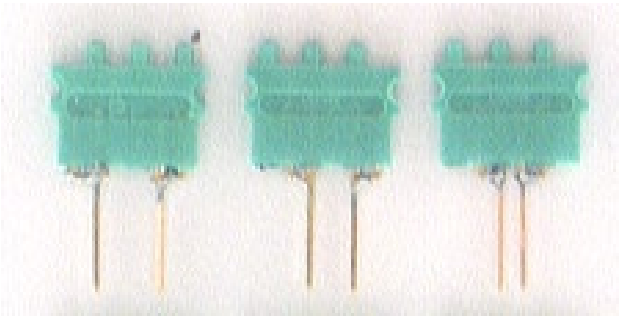

Figure 14. Pin electrodes for impedance measurements

## 6.4. Methods

### 6.4.1. High frequency (1-501 MHz) grain measurements at GIPSA

At GIPSA, the data set was collected by the following process. The sample was loaded into the test cell with a process intended to achieve a moderate packing density. Grain was allowed to flow from the filled funnel into the center of the test cell and completely over-filled the test cell.

The excess was removed by striking off the test cell with the type of striker used by the USDA for official test weight (bulk density) determinations. This established a fixed volume for the test. Complex reflection coefficient ($\Gamma$) measurements from 1 to 501 MHz were recorded using the HP-4291A. The test cell was emptied by removing a sliding gate below the grain-holding section, and the sample was weighed. The measured data were converted from complex reflection coefficients to relative complex permittivity by means of an iterative solver in a custom-designed Mathcad (Mathsoft 2000) program (Z. Gillay 2003). The conversion was based on a signal flow-graph analysis of the test cell. (Funk 2001) The calibration parameters for the conversion algorithm were determined from the results of tests performed by Dr. Kurt Lawrence, ARS-Athens, GA, using reagent-grade alcohols. He measured dielectric parameters of the test cell filled with air, methanol, propanol, n-butanol, n-pentanol, n-hexanol and n-decanol with HP-8753C vector network analyzer. He calculated the complex dielectric constants at each frequency for each material from the complex transmission coefficients (Lawrence et al 1998). Further analysis of the data (Funk 2001) showed a single frequency, approximately 149 MHz, to be the most suitable for RF grain moisture measurements. That measurement frequency was used for the present work.

### 6.4.2. Low frequency (75 kHz-30MHz) grain measurements at Corvinus University of Budapest

At the Physics and Control Department, the low frequency dielectric data were collected by the following process. The sample was loaded into the test cell with a process intended to achieve a high packing density. Grain was poured slowly into the test cell while the test cell was vigorously shaken horizontally. The excess was removed by striking off the test cell with a striker. After loading, the top of the test cell was sealed (with wide plastic adhesive tape with $\varepsilon'=1$ which has no influence for the dielectric moisture measurement) to minimize moisture loss. Differences between the loading processes, which were used for the GIPSA and for the Corvinus University measurements, were not important because the density correction (Equation 17.) minimized the effects of this problem (Nelson 1984, 2002, Funk 2001).

The test cell was placed in a two-piece insulating enclosure made of expanded polystyrene. The test cell (in the bottom half of the enclosure) and the (removed) top half of the insulating enclosure were placed in a laboratory freezer (set to approximately –25 °C) and allowed to equilibrate for at least 12 hours. After the equilibration period, the insulated test cell assembly was removed from the freezer, closed, transported to the laboratory area (approximately 22 °C), connected to the HP-4285A and HP-3457A, and allowed to warm to room temperature.

Sample temperature was sensed by measuring the voltage drop across a pair of series-connected silicon diodes within the test cell with a constant current source of 1 mA. Because of the insulating enclosure around the test cell, the sample temperature changed slowly (approximately

0.25 °C per minute), and temperature gradients (approximately 1-4 °C) within the test cell were minimized. The temperature was automatically checked every 30 seconds and a set of dielectric measurements was initiated each time the sample temperature changed by more than 0.5 degree C from the temperature of the previous data set.

The parallel capacitance (*C*) and conductance (*G*) of sample measurements at 51 logarithmically-spaced frequencies between 79 kHz and 29 MHz were obtained and stored automatically. When the grain had warmed to near room temperature, the automatic data collection sequence was terminated. The grain was emptied from the test cell and weighed so that the sample density could be determined. The data were processed using custom-designed software written in Mathcad. (Mathsoft 2000)

The equations 30 to 33 were applied to convert the parallel capacitance (C) and conductance (G) to complex permittivity ($\varepsilon_r$), dielectric constant ($\varepsilon'_r$), and loss factor ($\varepsilon''_r$).

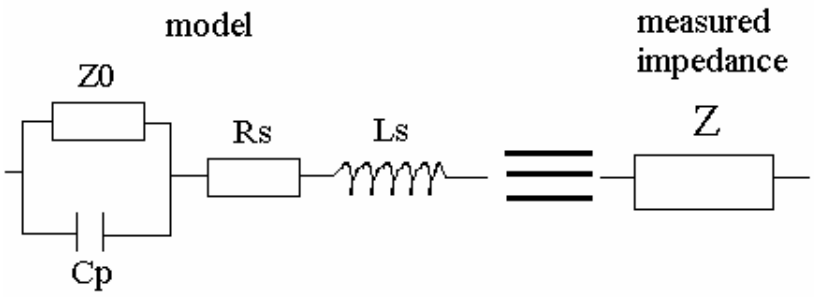


Figure 15. Electrical model of grain moisture measurement at low frequency (1-20 MHz)

First, the complex impedance (Z) of the test cell was calculated from Equation 30 and then expressed (Equation. 33) in terms of the model (Figure 15) (B. Gillay and Funk 2005).

$$Z = (G + j \cdot \omega \cdot C)^{-1} \tag{30}$$

$$\frac{1}{Z_0} = \frac{1}{-j\dfrac{1}{C_0 \cdot \dfrac{\varepsilon_r}{\varepsilon_0} \cdot \omega}} = j \cdot C_0 \cdot \frac{\varepsilon_r}{\varepsilon_0} \cdot \omega \tag{31}$$

$$\varepsilon_r = \varepsilon_0 (\varepsilon_r' - j\varepsilon_r'') \tag{32}$$

$$Z = \left[ j \cdot \omega \cdot \left( C_p + C_0 \cdot \varepsilon_r \cdot \varepsilon_0^{-1} \right) \right]^{-1} + R_s + j \cdot \omega \cdot L_s \tag{33}$$

where:

*j*: the complex operator

$\omega$: the radian frequency of the measurement

$C_0$: capacity of the test cell in vacuum

$C_p$: the parallel stray capacitance (5.9 pF)

$R_s$: the residual series lead resistance (2.5 ohm)

$L_s$ : the residual series lead inductance (27.5 nH)

Equation 33 means that the measured value of complex impedance (calculated directly from measured parallel capacitance and conductance) includes the reciprocal of the admittance of the "ideal" test cell plus the impedance of the apparent series resistance and inductance of the test leads beyond the point where open/short corrections were performed. The values of $R_s$ and $L_s$ were determined from measurements of air and distilled water. Model parameters ($C_0$, $C_p$, $R_s$, and $L_s$) were adjusted to cause the model to yield the theoretical values for dielectric constant of distilled water ($\varepsilon_r$`=78.5 at 25 C)* and air ($\varepsilon_r$`=1.000)* (Hasted 1973). The theoretical dielectric loss factor for air is zero. Conductivity effects (electrode polarization) cause some loss to be evident at lower frequencies, but the loss factor was assumed to be essentially zero in the 1-20 MHz range, because the relaxation frequency of water is at about 15 GHz (Hasted 1973), and the dielectric constant was assumed to be constant.

Solving Equation 33 for complex permittivity yields Equation 34 whose real part (divided by $\varepsilon_0$) is the dielectric constant (Equation 35) and imaginary part is the dielectric loss factor (Equation 36).

$$\varepsilon_r = \varepsilon_0 \cdot (\varepsilon_r' - j \cdot \varepsilon_r'') = \frac{-\varepsilon_0 \cdot \omega \cdot C_p \cdot (Z - R_s - j \cdot \omega \cdot L_s) - j \cdot \varepsilon_0}{\omega \cdot C_0 \cdot (Z - R_s - j \cdot \omega \cdot L_s)} \tag{34}$$

$$\varepsilon_r' = \mathrm{Re}\left[\frac{-\omega \cdot C_p \cdot (Z - R_s - j \cdot \omega \cdot L_s) - j}{\omega \cdot C_0 \cdot (Z - R_s - j \cdot \omega \cdot L_s}\right] \tag{35}$$

$$\varepsilon''_r = \mathrm{Im}\left[\frac{-\omega \cdot C_p \cdot (Z - R_s - j \cdot \omega \cdot L_s) - j}{\omega \cdot C_0 \cdot (Z - R_s - j \cdot \omega \cdot L_s}\right] \tag{36}$$

Model parameters can be determined from Equation 35-36 after air and distilled water measurement in the test cell. Model parameters were then used with Equation 30 and Equation 35. to compute sample dielectric constant from measurements of capacitance and conductance.

Predicted wb moisture values were determined from the dielectric measurements. The calibration coefficients used for the predictions were calculated from dielectric data and reference wb moisture values obtained from research performed by David Funk at the United States Department of Agriculture--Grain Inspection, Packers and Stockyards Administration. These data were developed based on samples representing all growing areas of the United States in 1999 (USDA 1999). The calibration process is shown in the Appendices (Appendix 3.)

The reference wb moisture value for each Hungarian test sample was determined by the appropriate Hungarian Ministry of Agriculture standard air oven method (Hungarian Standard 6367/3-83 — Appendix 2).

### 6.4.3. Very high frequency (VHF-149 MHz) dielectric measurements at Corvinus University of Budapest

For the VHF (149 MHz) tests, the measurements were performed by the following process. The sample was loaded into the test cell with a process intended to achieve a relatively high packing density. Grain was poured slowly into the test cell while the test cell was shaken to settle the sample. The excess was removed by striking off the test cell with a striker. After loading, the top of the test cell was sealed (with wide plastic adhesive tape) to minimize moisture loss. The test cell was placed in a laboratory freezer (set to approximately –25 °C) and allowed to equilibrate for at least 12 hours. After the equilibration period, the insulated test cell assembly was removed from the freezer, covered with a piece of polystyrene foam, transported to the laboratory area (approximately 22 °C), connected to the measuring system, and allowed to warm to room temperature. Dielectric measurements were performed at each time when the sample warmed up by 0.5 °C. When the grain had warmed to near room temperature, the automatic data collection sequence was terminated. After that, the test cell was placed in a laboratory oven, which was set to approximately 50 °C, and allowed to equilibrate for at least 6 hours. Then the test cell was again moved to the laboratory area and connected to the measuring system. Dielectric measurements were performed at each time when the sample cooled down by 0.5 °C. When the grain had cooled to near room temperature, the automatic data collection sequence was terminated. The grain was emptied from the test cell and weighed so that the sample density could be determined.

The data were processed using custom-designed software written in Mathcad. (Mathsoft 2000). The gain and phase data voltages were converted to complex reflection coefficient ($\Gamma$) using Equation 37. The gain voltage with the reflectometer output shorted ($\Gamma$ = -1) was 1.45 volts. The phase sensitivity of the reflectometer was 87.609 degrees per volt, and the gain sensitivity was 0.60 volt per decade of voltage ratio change (Analog Devices Inc. 2002). The 51.033 value came from the calibration of the test cell versus the Agilent E4991 Material/Impedance Analyzer.

$$\Gamma = \left[ 10^{\left(\frac{V_G - 1.45}{0.6}\right)} \cdot e^{\left(j \cdot (51.033 + 87.609 \cdot V_P)\right)} \right] \tag{37}$$

where:

$V_G$ is the gain voltage from the AD-8302 gain/phase detector circuit

$V_P$ is the phase voltage from the AD-8302 gain/phase detector circuit

$j$ is the complex operator

The complex reflection coefficient values were converted to complex dielectric constant ($\varepsilon'_r$) with an iterative solver based on signal-flow graphs as shown by Funk (2001). The corrected dielectric constant values ($\varepsilon_c$) were adjusted for effects of surrounding dielectric materials and non-TEM modes by Equation 38 (This equation came from Equation 16 on page 31. The empty cell

correction value was 1.04 and the Filling Factor for this test cell was 1.25 (Gillay Z. and Funk 2003))

$$\varepsilon_c = (\varepsilon_r^{'} - 1.04) \cdot 1.25 + 1 \quad (38)$$

### 6.4.4. Data processing to determining the unifying parameters from grain physical and chemical properties

The relationships between the physical and chemical properties of grains (independent variables) and the target values for unifying parameters (third generation of unifying parameters SP -slope, OP- offset, TP –translation) and temperature correction coefficients (dependent variables) were modeled using step-up multiple linear regression.

Multiple linear regression (usually simply called multiple regression) may be regarded as an extension to simple linear regression when more than one explanatory variable is included in the regression model. For each individual, there is information on its values for the outcome variable, *y*, and each of *k*, say, explanatory variables, $x_1$ , $x_2$, ..., $x_k$. Usually, focus is centred on determining whether a particular explanatory variable, $x_i$, has a significant effect on *y* after adjusting for the effects of the other explanatory variables. Furthermore, it is possible to assess the joint effect of these *k* explanatory variables on *y*, by formulating an appropriate model, which can then be used to predict values of *y* for a particular combination of explanatory variables. The multiple linear regression equation in the population is described by :$Y = \alpha + \beta_1 x_1 + \beta_2 x_2 + ... + \beta_k x_k$ (Petrie at all 2002)

With forward (step-up) selection, the first step is to create a simple model with one explanatory variable which gives the best $R^2$ *and F-test* result when compared with all other models with only one variable. In the next step, a second variable is added to the existing model if it is better than any other variable at explaining the remaining variability and produces a model which is significantly better (according to some criterion) than that in the previous step. This process is repeated progressively until the addition of a further variable does not significantly improve the model.

The best three (highest correlation with unifying parameters) independent variables were chosen to model each of the unifying parameters and the temperature coefficient. The reasons for choosing three factors included: 1) The F-test was generally highest for three factors. 2) The multiple correlation coefficient results did not increase significantly for more factors. 3) The small number of grain types to be fitted caused a high risk of over-fitting the data with more than three factors.

The prediction models were tested by cross-validation. After the best three factors were determined to model each dependent variable, separate multiple linear regressions were performed leaving out each grain type one at a time. The resulting models were applied to the excluded grain

types to estimate the prediction error for unknown grain types. The data were processed using custom-designed program written in Mathcad. (Mathsoft 2000)

### 6.4.5. Electrical impedance measurements of apple slices

The impedance spectra of apple slices during drying were determined in two ways. In the first experiment (method I), single slices, with measuring electrodes inserted, were placed in the 50 °C air oven (one slice at a time) and impedance was measured every 10 minutes during drying. More than ten repetitions of this method were performed on different apple slices. Automatic data collection was performed by a QBasic program (written by David Funk). The electrode spacing in this experiment was 1.8 mm. Sample temperature was monitored with a thermocouple inserted into the slice. The total drying time for each slice was 780 minutes (13 hours).

For the second experimental method (method II), multiple slices were (166 sample obtained in six independent measurement) placed in the 50 °C Venticell air oven, and every 20 minutes one sample was removed from the oven for testing. The sample was sealed in cellophane and allowed to equilibrate to room temperature for 20 minutes prior to testing. The db moisture content of the sample was calculated from the sample mass, which was measured before and after drying. Then the sample impedance spectrum was measured. In some measurements, the impedance of each slice was measured with each of the three electrode spacings. The total drying time for this experiment was also 780 minutes (13 hours).

### 6.4.6. Modeling of impedance spectra of apple slices

In the first method the measured impedance spectra and in the second method the tissue impedance spectra were evaluated with respect to an equivalent electrical model. A model consisting of series-connected one or two Cole-elements (circular arcs) and a constant phase element ((CPE) straight line) (Grimnes and Martinsen 2000) was used for fitting the spectrum of each measurement (Figure 16).

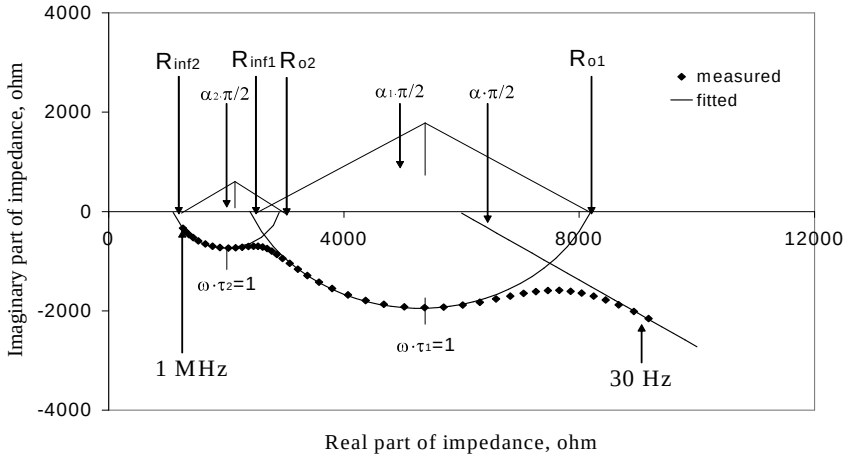


Figure 16. The measured impedance values (points) and a model consisting of two Cole-elements and one constant-phase element (line). Model parameter definitions are indicated on the figure.

The spectra obtained in the first falling-rate period of drying contained only one Cole-element and a CPE. In the second falling-rate period, a second Cole-element appeared at the high frequency range of the spectra, and the constant phase element disappeared. The model consisting of two Cole-elements and one CPE was described by the expression:

$$Z = R_{\inf 1} + \frac{R_{01} - R_{\inf 1}}{1 + \left(j\omega\tau_1\right)^{\alpha_1}} + R_{\inf 2} + \frac{R_{02} - R_{\inf 2}}{1 + \left(j\omega\tau_2\right)^{\alpha_2}} + R_0 (j\omega\tau)^{-\alpha} \qquad (39)$$

In this expression, the first two terms and the second two terms describe the impedance of the first and the second Cole-element, respectively, and the last term is the impedance of the CPE. $R_{inf1}$ and $R_{inf2}$ are the resistance values where the circular arcs of the first and second Cole-elements intersect the real axis at "infinitely" high frequency (that is, far above the associated relaxation frequency $f_1=2\pi/\tau_1$ or $f_2=2\pi/\tau_2$ ). The points of intersection of these circular arcs with the real axis at "zero frequency" (that is, far below the associated relaxation frequency) give the $R_{o1}$ and $R_{o2}$ resistances. The $\alpha$, $\alpha_1$, and $\alpha_2$ parameters (which vary between 0 and 1) describe the distributions of $\tau$, $\tau_1$, and $\tau_2$ relaxation times. If the value of $\alpha_1$, for example, is 1.0, the associated relaxation is described by a single relaxation frequency. Lower values correspond to increasingly broad distributions of relaxation frequencies. The MathCad curve-fitting program estimated the $R_o$, $R_{o1}$, $R_{o2}$, $\tau$, $\tau_1$, $\tau_2$, $\alpha$, $\alpha_1$ and $\alpha_2$ parameter values.

# 7. RESULTS AND DISCUSSION

In 2001 and 2002 the calibration database (2714 data) made in the USDA-GIPSA was filled up with thousands of new measurements. Many new grain types were tested, so the first generation of unifying parameters required a refining process. USDA-GIPSA has been supporting research at Corvinus University of Budapest, Faculty of Food Science, for the purpose of developing methods for optimizing the necessary unifying parameters. The following few chapters (7.1– 7.3) explain the roles of the unifying parameters in the new moisture measurement method and the processes for developing the unifying parameters. Specific optimized values for the unifying parameters for different grain groups are given, and the performance improvements achieved by optimizing the parameters are shown.

## 7.1. Optimizing the first generation unifying parameters

The new database for the calibration included 4887 data measured by GIPSA staff and represented over 2000 more grain samples, more crop years, lower wb moisture samples, and many new grain classes and types. These included confectionary sunflower, popcorn, short grain rough rice, many classes of processed rice, peas, mustard, many classes of edible beans, and triticale. The optimization of the calibration process was performed at the Corvinus University of Budapest in Mathcad program. The aim of the optimization was to improve moisture accuracy and to reduce the number of variables in the calibration (put together as many grain classes and types as possible without sacrificing moisture measurement accuracy).

At the beginning of the optimization there were 15 separate grain groups (soybean, sorghum, sunflower seed, corn, oats, wheat, barley, rice, durum wheat, confectionary sunflower, peas, mustard, edible beans, processed rice, and triticale). Analyzing the behavior of the grain types and classes in the calibration suggested reducing the number of groups to 13. Confectionary sunflower was grouped with oil-type sunflower seed and durum wheat was grouped with rice based on similar unifying parameters.

## 7.2. Evaluation of the fitted calibration curve

Different models were fitted on the adjusted and density-corrected dielectric constant versus reverse temperature-corrected air oven wb moisture content (Figure 17), to find the best calibration curve. In the polynomial regression the density-corrected dielectric constant is the independent variable and the reference air oven moisture content is the dependent variable, but traditionally (Funk 2000, 2001 Nelson 1973, 2003 Lawrence 1999, Trablesi and Nelson 1998) the reference air oven moisture content is placed on the x-axis. Evaluating the goodness of the fitted model, methods

grouped into two types: graphical and numerical. Plotting residuals and prediction bounds are graphical methods that aid visual interpretation, while computing goodness-of-fit statistics and coefficient confidence bounds yield numerical measures that aid statistical reasoning.

Figure 17 presents different polynomial calibration curves. Temperature correction was applied in reverse to the air-oven moisture to see only the effects of the three unifying parameters. From this figure it is obvious that the $4^{th}$ and $6^{th}$ order polynomial calibration curves practically are not the best choice because the curve "rolled-over" at or near the highest moisture levels in the calibration. This might cause problems in the moisture prediction for samples that are at the edge of the calibration range. It is better for the predicted moisture to increase sharply rather than decrease sharply above the calibration range. In this case, the instrument will identify samples that are outside the calibration range and give an error message. If the calibration curve rolls over, the predicted moisture may be within the calibration range even if the actual moisture is outside the range. The undesirable alternative is to specify a dielectric constant calibration range instead of a moisture calibration range. This would be unpleasant and incomprehensible for users. The original 4th-order polynomial had another problem. The fitting was not very good at very low moisture levels because there is not enough curvature at the knee point at the low moisture region (5-10% wb). The $3^{rd}$ and $5^{th}$ order polynomial equations could deal with the roll-over problem. In both case the fitted curve was increasing continuously. The fifth order polynomial equation was increasing more sharply than for the $3^{rd}$ order polynomial. In those extreme cases when the moisture was above 38% wb (out of the calibration range) the moisture meter would give a warning message. In the low moisture range the $5^{th}$ order polynomial was working better than the $3^{rd}$ order one, which could not follow the curvature below about 8% wb moisture.

Figure 18 shows the residual errors of the A) $3^{rd}$ order, B) $4^{th}$ order, C) $5^{th}$ order and D) $6^{th}$ order polynomial equations. Assuming the fitted model to the data is correct, the residuals approximate the random errors. Therefore, if the residuals appear to behave randomly, it suggests that the model fits the data well. However, if the residuals display a systematic pattern, it is a clear sign that the model fits the data poorly. The largest errors can be seen below about 8% for the 3rd order polynomial errors and get progressively smaller for the higher order polynomials. There is a decreasing tendency in the error plot between 3 and 8% wb moisture, which also mean that the model fits the data poorly. There are some differences on the error plot in this low moisture range between $4^{th}$, $5^{th}$ and $6^{th}$ order polynomial (differences in the error are bigger between the $4^{th}$ and $5^{th}$ order polynomial than between $5^{th}$ and $6^{th}$ order polynomial). Above 8% wb moisture, there are no significant differences in the error between Figures 18 B, C and D. Figure 18. A) also presents higher residual error above 8% wb moisture than the other polynomial.

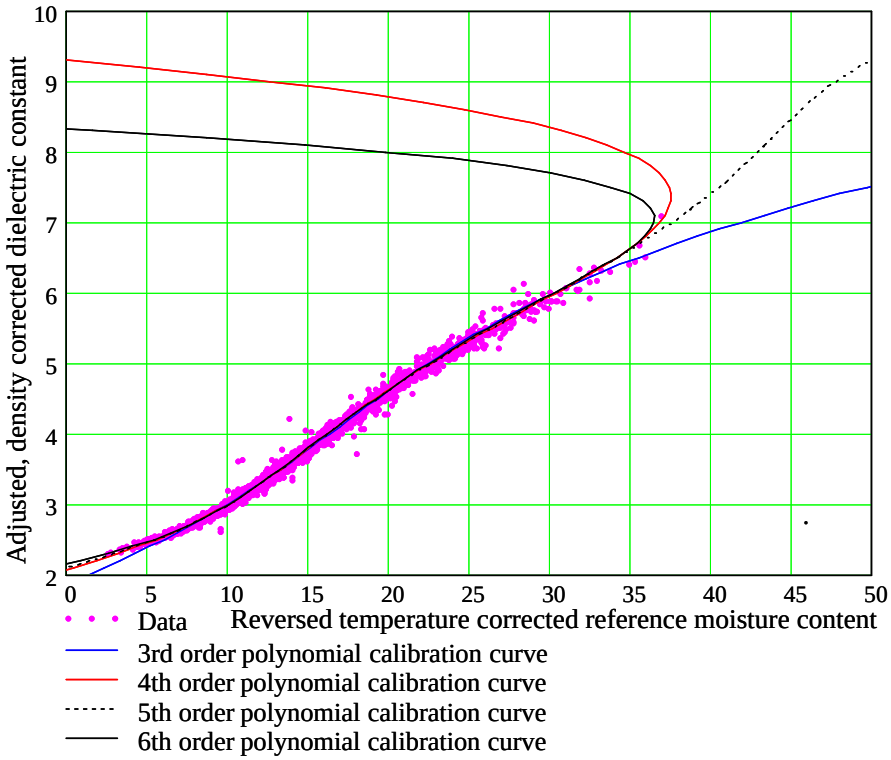


Figure 17. Adjusted density corrected dielectric constant versus reversed temperature corrected reference wb moisture content with different order polynomial calibration curves

After using graphical methods to evaluate the goodness of fit, it was necessary to examine the goodness-of-fit with parametric statistics. For this purpose some statistical parameters were calculated (Table 3.). The Sum of Squares Due to Error measures the total deviation of the response values from the fit to the response values. It is also called the summed square of residuals and is usually labeled as *SSE*. R-Square ($R^2$) measures how successful the fit is in explaining the variation of the data. Put another way, R-square is the square of the correlation between the response values and the predicted response values. It is also called the square of the multiple correlation coefficient and the coefficient of multiple determination. Root Mean Squared Error (RMSE) is also known as the fit standard error and the standard error of the regression. It is an estimate of the standard deviation of the random component in the data. Table 3 presents some statistical parameters of the fitted polynomials. The $R^2$ values are high (above 0.99) in each case and show not too much difference between the fitted polynomials. Both SSE and RMSE values show bigger differences. Both statistical parameters are the highest for the 3$^{rd}$ order polynomial and they are also high for the 4$^{th}$ order polynomial. There are only small differences in these parameters between the 5$^{th}$ and 6$^{th}$ order polynomials.

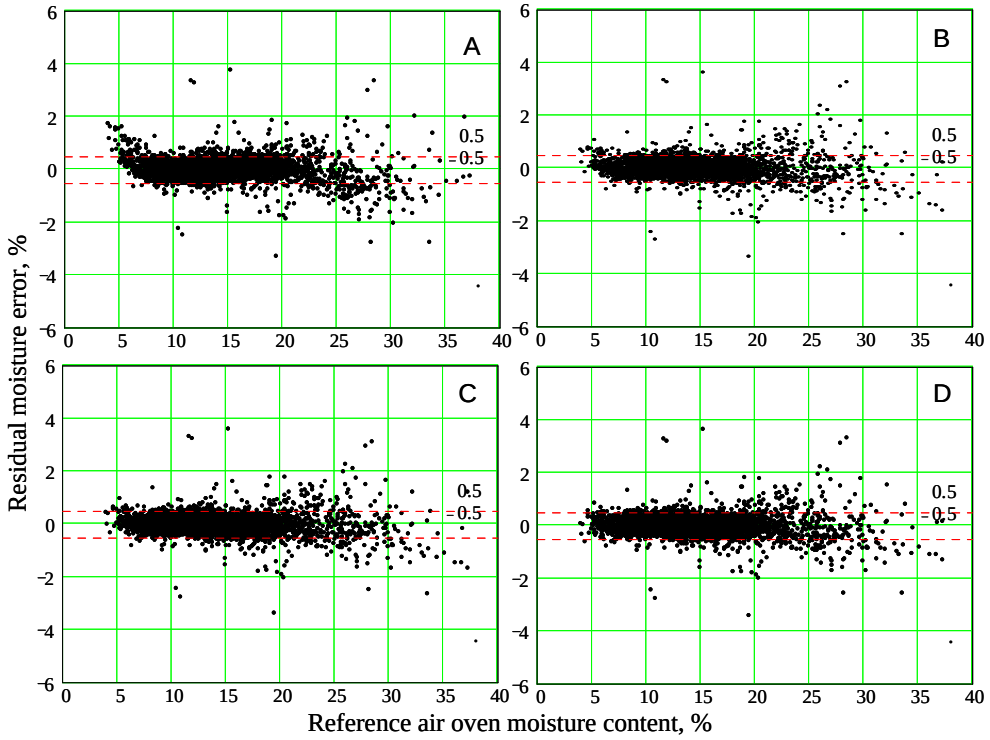


Figure 18. Residual wb moisture errors with A) 3rd , B) 4th , C) 5th and D) 6th order polynomial versus air oven wb moisture content.

Table 3. Statistical parameters of the fitted polynomials

| | SSE | R2 | RMSE |
|---|---|---|---|
| Third-order polynomial | 734.28 | 0.9930 | 0.3875 |
| Fourth-order polynomial | 602.66 | 0.9940 | 0.3511 |
| Fifth-order polynomial | 598.82 | 0.9943 | 0.3498 |
| Sixth-order polynomial | 592.26 | 0.9943 | 0.3480 |

The Durbin Watson (DW) statistical test was also performed to test the presence of autocorrelation in the residuals of the regression equation. The test compares the residual for time period t with the residual from time period t-1 and develops the q statistic that measures the significance of correlation between these successive comparisons. The Durbin Watson test result is exactly 2 when there is no autocorrelation and becomes smaller or larger as the serial correlations increase.

With 4887 data points, the Durbin Watson test result was 1.637 for the 3rd order polynomial, 1.832 for the 4th order polynomial, 1.839 for the 5th order polynomial and 1.853 for the 6th order polinomyal equation. The lowest value, which belongs to the 3rd order polynomial, indicates some problem with this curve fitting.

In our case, the density of the data set is uneven. There are thousands of measurements between 10 and 20 % wb moisture content and there are only several hundreds below 10 % and above 20% wb moisture. A Durbin Watson map was introduced to show the big data matrix divided

in smaller parts. The residual values were calculated for 4887 data at each polynomial, then the Durbin Watson test was performed using sets of 100 adjacent data points. This representation might help to see the goodness of the fitted calibration curves in a smaller moisture range.

Figure 19. shows the result of the Durbin Watson test at the $\alpha$=0.05 significance level using different order polynomial models. Each point in the graph is the DW number of 100 samples. On the X axis the wb moisture content is increasing from left to right. Upper (purple line) and lower (blue line) critical values of DW statistic, dU and dL have been tabulated for different values of k (the number of explanatory variables) and n (sample number). If the DW number is out of the purple range (DW<dU or DW>4-dU) then the residual show autocorrelation (positive or negative) and model fit poorly. If the DW number is between the blue and purple line (between dU and dL) than the test is inconclusive. If DW number is between the blue lines (between dL and 4-dL) than the model fit well at the given significance level on the data. This Figure also can show us that which wb moisture content fit the model well or poorly on the data set. In Figure 19. A it can be seen that many DW numbers are out of the critical values, they are smaller than two, so it is a positive autocorrelation in the case of the 3rd order polynomial. The smallest value (0.582) can be found in the low moisture region 3.89-6.57%. Results are much better for the other three polynomials. The 4th order polynomial has still some problem in the lowest moisture range. The 5th and 6th order polynomials seem to fit the data set well. Their DW maps are similar.

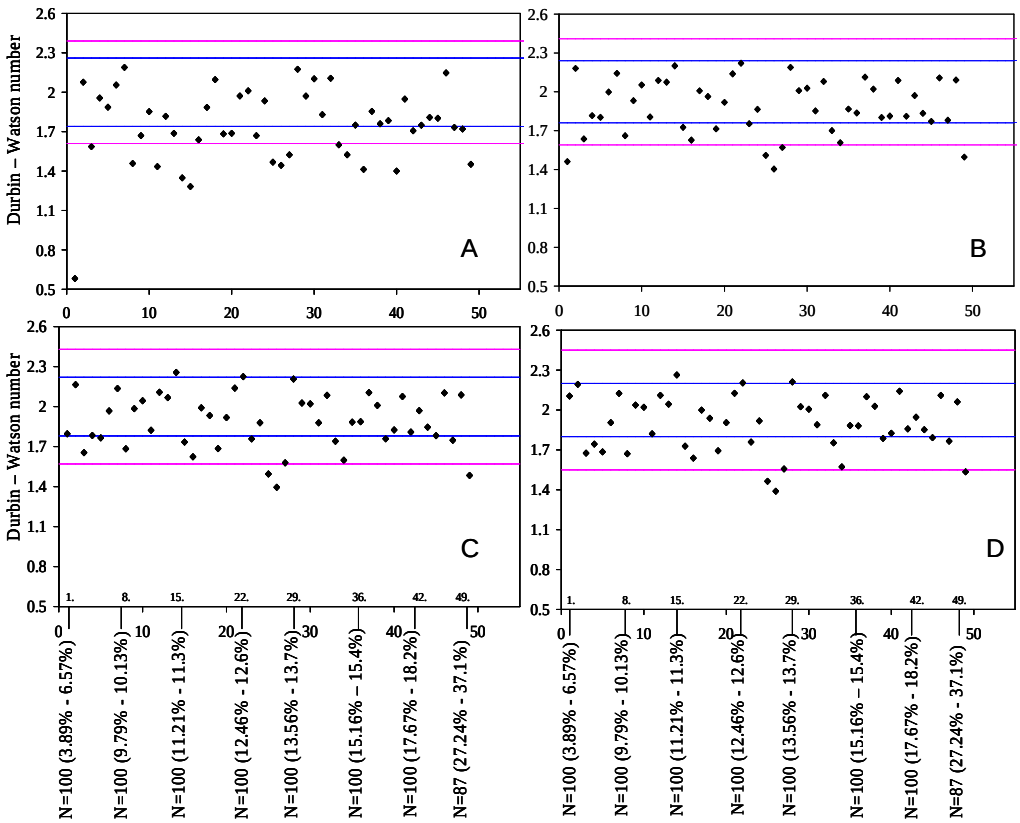


Figure 19. Durbin Watson map (each point is a DW number for 100 samples) for A) 3rd B) 4th , C) 5th and D) 6th order polynomial

In the unified algorithm, for the density-corrected and adjusted dielectric constant a fifth-order polynomial calibration curve yielded a substantially better fit to the data than the previous fourth-order equation—especially at very low and very high moisture levels. The 6th order polynomial didn't improve significantly the calibration statistics (this polynomial curve is also rolled-over at the high moisture range)—by the statistical and practical reasons it was concluded that the 5th order polynomial equation seems to give enough degrees of freedom.

The best achievable overall standard deviation of differences with the $5^{th}$ order polynomial in the case of the first generation of unifying parameters was 0.349 percent wb moisture as compared to 0.29 with the original (much more limited only 2714 samples) data set.

## 7.3. Second generation unifying parameters

For this study, 4887 grain samples representing almost 50 classes of U.S. cereal grains, pulses and processed rices for the 1998-2002 crop years were tested by GIPSA stuff. Figure 20A is a plot of dielectric constant versus reference wb moisture for those samples.

A new approach was developed for defining the unifying parameters at the Corvinus University of Budapest. Instead of selecting a separate target density for density-correcting the samples in each grain group, as in Figure 4C (page 34.), a single target density (approximately the average for all samples tested) was used for density-correcting all grain samples of all groups. The resulting density-corrected dielectric constant values are plotted versus adjusted reference, reverse temperature-corrected wb moisture values in Figure 20B. This figure suggested that a simple slope correction might “unify” the data effectively.

For each grain group, the slope (% wb moisture per unit density-corrected dielectric constant) was calculated for the portion of the samples with reference wb moisture values between 10 and 20 % wb moisture. The samples below 10 % wb moisture and above 20 % wb moisture were excluded because the “standard” curve shape was quite non-linear in those regions. The slope unifying parameter *SP* was defined as the correction factor needed to adjust the slope of each grain group to 6.000 in the 10 to 20 % wb moisture range. The data for the different grain groups appeared to rotate about a point (%M = 5, $\varepsilon_c$ = 2.5) so an offset unifying parameter *OP* of approximately 2.5 was presumed. Figure 20C shows the data with the slope unifying parameter applied. The offset unifying parameter was iteratively adjusted for each grain group, resulting in Figure 20D. A translation unifying parameter *TP* was needed to align the curve shapes for the different grain groups in the low moisture region. After applying the three unifying parameters to each grain group, the data appeared as in Figure 20E. A fifth-order polynomial was fit to the data as shown in Figure 20F. The overall mean differences for 4887 data was $3.233*10^{-11}$ and the best

overall calibration error with this method was 0.3066 percent wb moisture (standard deviation of differences with respect to reference wb moisture values).

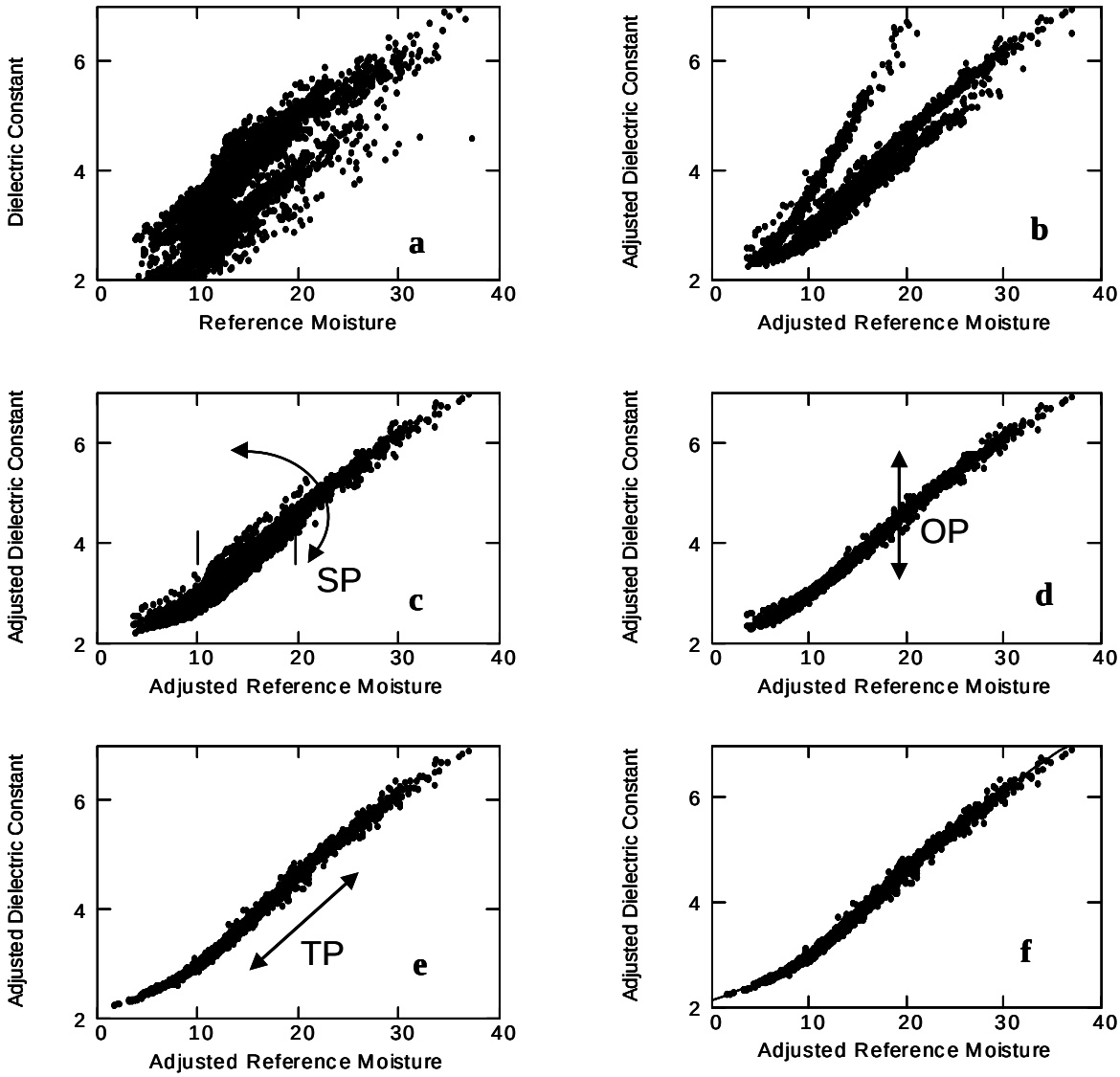


Figure 20. Details of the second generation Unified Moisture Algorithm. a) Plot of dielectric constant versus reference wb moisture for 4887 samples representing about 50 classes of U.S. cereal grains, oilseeds, pulses, and processed rices for the1998-2002 crop years. b) Same as previous plot except all dielectric constant values are density-corrected to a common density and the reference wb moisture values are temperature corrected (in reverse). c) Same as previous plot except each grain group is adjusted for a common slope (percent wb moisture per unit dielectric constant) in the 10-20 % wb moisture range. d) Same as in previous plot except each grain group is offset to minimize the average predicted moisture errors. e) Same as previous plot except the data are translated along the common slope line to align the curve shapes in the low moisture region. f) Same as previous plot except with the best-fit 5$^{th}$ order polynomial calibration curve superimposed on the adjusted dielectric constant versus moisture data plot.

$$\varepsilon_{adj} = (\varepsilon_c - OP) \cdot SP + 2.5 + \frac{TP}{6} \quad (40)$$

$$x_{adj} = x_{ref} + Ktc \cdot (T - 25) + TP \quad (41)$$

$$x_{pred} = \left( \sum_{r=0}^{5} (\varepsilon_{adj})^r \cdot CC_r \right) - TP \quad (42)$$

$$x_{tc} = x_{pred} - Ktc \cdot (T - 25) \quad (43)$$

Equations 40-43 are used for the second generation unifying parameters. The variables are defined above. The calibration performance statistics and unifying parameters calculated by the second generation algorithm for each grain group are listed in Table 4. Mean differences are the air-oven wb moisture minus the predicted wb moisture content. Group mean differences are low at each grain type, which means a really good prediction of the moisture content from the dielectric constant. The SDD values of grain groups are also under 0.5. The group slope values are the slopes of predicted versus reference wb moisture content. These three statistical parameters help to find the best unifying parameter for a grain group.

Table 4. Calibration statistics and unifying parameters calculated by the second generation algorithm

| *Group name* | *Slope parameter* | *Offset parameter* | *Translation parameter* | *Mean differences* | *Standard deviation of differences* | *Slope* |
|---|---|---|---|---|---|---|
| Soybean | 0.83 | 2.150 | -0.5 | -0.002 | 0.208 | 0.997 |
| Sorghum | 1.10 | 2.456 | 0.5 | 0.002 | 0.213 | 1.021 |
| Sunflower | 0.54 | 2.715 | 1.5 | -0.004 | 0.354 | 0.998 |
| Corn | 1.00 | 2.553 | 0 | 0.003 | 0.367 | 0.997 |
| Oats | 1.07 | 2.379 | 0.5 | -0.001 | 0.265 | 0.987 |
| Wheat | 1.15 | 2.390 | 0.5 | -0.001 | 0.214 | 1.006 |
| Barley | 1.07 | 2.299 | -0.5 | 0.006 | 0.279 | 0.987 |
| Rice | 1.12 | 2.424 | 0.5 | -0.002 | 0.427 | 1.008 |
| Peas | 1.22 | 2.194 | -1.5 | -0.003 | 0.105 | 0.968 |
| Mustard | 0.88 | 2.399 | 0.5 | -0.002 | 0.297 | 0.936 |
| Edible Beans | 0.92 | 2.200 | -0.5 | -0.001 | 0.342 | 0.996 |
| Triticale | 1.22 | 2.368 | 0.5 | 0.003 | 0.171 | 0.942 |
| Processed rice | 1.20 | 2.622 | 0.5 | 0.003 | 0.251 | 0.955 |

## 7.4. Third generation unifying parameters

In this stage of the research, several additional grain types and classes were added to the unified calibration (Canola, Safflower, Flaxseed, and High-Oil corn, some new classes of Processed Rice and Edible Beans). Therefore, in the third generation of unifying algorithm, grain types were regrouped. The second generation unifying parameters provided good moisture measurement

performance, but further simplification of the process was needed to be able to add more grain classes and types efficiently. The second generation method required iteratively optimizing the offset parameter OP and the translation parameter TP for each grain group and the fifth-order polynomial equation for all grain groups together each time a new grain type or class was added.

The key insight in moving to the third generation approach was that the curve shape should be fixed and the curve of the additional grain types or classes should simply be adjusted to match the existing standard curve shape (Equation 44). To do this, it was necessary to compare the measured adjusted dielectric constant (Equation 40) to the predicted adjusted dielectric constant calculated from the adjusted reference wb moisture value (Equation 41). This was accomplished by cubic spline interpolation. Cubic spline interpolation means that between each two points, there is a piecewise cubic curve. When we string these curves together, we set the second and first derivatives at the endpoints of each piecewise cubic curve equal to that of the adjacent cubic curve's second and first derivatives thus providing for a continuous second derivative. This gives a smooth curve that passes through each point, thus interpolating them. For any value of adjusted reference wb moisture, interpolation gave the associated adjusted dielectric constant value. Interpolation was done in Mathcad. The unifying parameters were adjusted to minimize the differences between the measured adjusted dielectric constant values (Equation 40) and the values predicted from cubic spline interpolation

$$x_{pred} = -12.222 + 12.449 \cdot \varepsilon_{adj} - 4.7724 \cdot \left(\varepsilon_{adj}\right)^2 + 0.93685 \cdot \left(\varepsilon_{adj}\right)^3 - 0.090096 \left(\varepsilon_{adj}\right)^4 + 0.0034250 \left(\varepsilon_{adj}\right)^5 \qquad (44)$$

Figure 21 illustrates the process (with synthetic data used for clarity). To begin the process, the dielectric constant data were density-corrected (using Equation 17 and the standard target density). Select a tentative temperature correction coefficient *Ktc* based on the known *Ktc* values for other grain types with similar chemical compositions. Select initial unifying parameter values based on those of similar grain types (though the initial unifying parameter values are not important). Calculate the adjusted dielectric constant values (Equation 40) and the adjusted reference wb moisture values (Equation 41) based on the initial parameters and the measured data. Calculate the predicted adjusted dielectric constant values (from the adjusted reference wb moisture) by cubic spline interpolation. Plot the differences between the measured and predicted adjusted dielectric constant values. Figure 21A shows typical values at this stage. The data will likely be offset vertically from the zero (target) line and show two regions with distinctly different slopes.

Adjust the slope unifying parameter *SP* to cause the slope of the high-moisture part of the curve (above about 12 % wb moisture) to be parallel to the zero line as shown in Figure 21B**.** Then set the translation unifying parameter *TP* to cause the low-moisture part of the curve (below about 12 % wb moisture) to be parallel with the zero line as shown in Figure 21C**.** Finally, adjust the

offset unifying parameter so that the average difference is zero as in Figure 21D. That completes the process of optimizing the unifying parameters for that grain type.

Besides the relative simplicity, sensitivity, and accuracy of this process, it has the advantage of not affecting the moisture measurements for any other grain group because the standard curve (Equation 44) is not recomputed in the process. After adjusting the unifying parameters for each grain group with this method, the overall calibration error (standard deviation of differences- SDD) was 0.308 percent wb moisture, which is insignificantly higher value than the SDD of the second generation of unified algorithm (4887 data SDD=0.3066); the third generation database (5141 data) contains 254 more data points than the second generation database (4887). The calibration performance statistics and unifying parameters calculated by the third generation algorithm for each grain group are listed in Table 5.

Table 5. Calibration statistics and estimated unifying parameters for the combined grain groups.

| Group Name | Number of Samples | Types in Group | Slope Unif. Para. | Trans. Unif. Para. | Offset Unif. Para. | Mean differences | St. Dev. of differences (% x) | Slope |
|---|---|---|---|---|---|---|---|---|
| Soybeans | 642 | 1 | 0.80 | -1.0 | 2.100 | -0.0120 | 0.169 | 0.996 |
| Sorghum | 193 | 1 | 1.10 | 0.5 | 2.456 | $-1.53\cdot10^{-6}$ | 0.214 | 1.022 |
| Sunflower | 472 | 2 | 0.54 | 1.5 | 2.715 | 0.0070 | 0.342 | 0.995 |
| Corn | 926 | 3 | 1.00 | 0.0 | 2.553 | 0.0080 | 0.365 | 1.000 |
| Oats | 125 | 1 | 1.07 | 0.5 | 2.378 | 0.0050 | 0.264 | 0.988 |
| Wheat | 1027 | 5 | 1.15 | 0.3 | 2.388 | -0.0002 | 0.212 | 0.999 |
| Barley | 308 | 2 | 1.07 | -1.0 | 2.288 | -0.0355 | 0.296 | 0.954 |
| Rice & Durum | 746 | 4 | 1.12 | 0.5 | 2.424 | -0.0021 | 0.427 | 1.009 |
| Peas | 81 | 3 | 1.10 | -1.5 | 2.146 | -0.0061 | 0.249 | 0.995 |
| Mustard | 33 | 2 | 0.88 | 0.5 | 2.399 | -0.0021 | 0.297 | 0.936 |
| Edible Beans 1 | 141 | 9 | 0.92 | -0.5 | 2.213 | 0.0097 | 0.403 | 0.962 |
| Triticale | 12 | 1 | 1.22 | 0.5 | 2.368 | 0.0018 | 0.171 | 0.942 |
| Processed Rice | 260 | 11 | 1.20 | 0.5 | 2.622 | 0.0369 | 0.273 | 0.969 |
| LG Proc. Rice | 56 | 2 | 1.30 | 0.5 | 2.830 | -0.0164 | 0.228 | 0.986 |
| Edible Beans 2 | 30 | 2 | 0.92 | -0.5 | 2.480 | -0.0010 | 0.416 | 0.949 |
| Canola | 16 | 1 | 0.60 | -2.0 | 2.420 | -0.0064 | 0.249 | 1.091 |
| Safflower | 12 | 1 | 0.60 | 0.0 | 3.010 | -0.0128 | 0.450 | 0.860 |
| Flaxseed | 28 | 1 | 0.60 | -0.2 | 2.460 | 0.0187 | 0.123 | 0.966 |
| High-Oil Corn | 33 | 1 | 1.01 | 0.5 | 2.827 | -0.0032 | 0.177 | 0.993 |
| Summary | 5141 | 53 | | | | $1.899\cdot10^{-5}$ | 0.308 | |

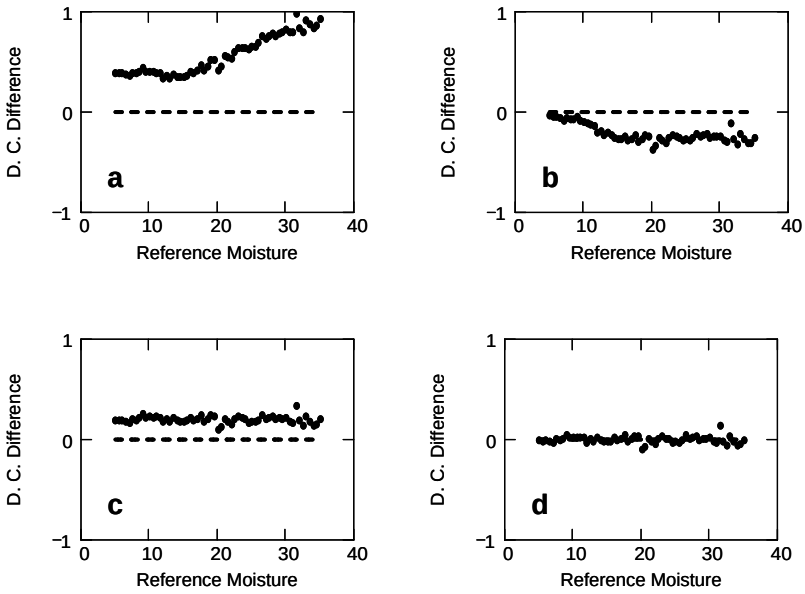


Figure 21. Details of the third generation Unified Moisture Algorithm illustrated with synthetic data. a) Initial differences between the measured adjusted dielectric constant and predicted adjusted dielectric constant. b) Same as previous plot except the slope parameter is adjusted to minimize slope error above 12 % wb moisture. c) Same as previous plot except the translation parameter is adjusted to minimize the slope error in the moisture range below 12% wb. d) Same as previous plot except the offset parameter is adjusted to achieve zero mean error between the measured and predicted adjusted dielectric constant values.

## 7.5. Temperature correction for dielectric moisture tests for several grains and oilseeds at low (1-20 MHz) and high (149 MHz) measurement frequencies

Sample temperature is one of the most important factors influencing dielectric grain moisture results since temperature affects the dielectric constant of water, the degree of hydrogen bonding between water and other molecules, and the magnitude of interfering factors such as ionic conductivity. Waiting until the grains achieve a standard (usually near room) temperature to obtain accurate moisture measurements causes unacceptable delays in grain handling. Therefore, it is very desirable to be able to make accurate moisture measurements on grain that is very cold—even below the freezing point of water.

Figure 22 demonstrates the extreme importance of temperature correction in dielectric grain moisture measurement. Predicted moisture values from dielectric measurements (by appendix 3.) of sunflower seeds at 20 MHz are shown without and with temperature correction. Without temperature correction (Figure 22A), the predicted moisture changes by approximately 3 percent wb moisture from -25 to +20 °C. The slopes of the curves (for the part of the curves above zero Celsius) are similar for all of the sunflower samples. For samples at 12 percent wb moisture and below, approximately the same slope persists down to -25 °C. However, for the two samples above 12 percent wb moisture, a significant discontinuity is observed at zero Celsius. Also, below about -15 °C, the curve for the 17.68 percent sample merged with the curve for the 13.82% sample.

Figure 22B shows how a simple temperature correction function (Equation 45) successfully corrects this slope over a wide range of temperatures--if the wb moisture content is below the "threshold." The resulting corrected wb moisture values are less dependent on temperature.

$$\%x_{tc} = \%x - Ktc \cdot (t-25) \quad (45)$$

Where:

$\%x_{tc}$ is the temperature-corrected wb moisture content
%x is the wb moisture content without temperature correction
Ktc is the temperature correction coefficient
t is the measured sample temperature in degrees Celsius

Figure 23A presents the information in Figure 22B in an expanded form. In this figure, the predicted wb moisture value for each sample at 20 °C is subtracted from the predicted values at all other temperatures. This presentation permits a more detailed view of the residual errors after temperature correction. Figures 23B-23F give the test results for five other types of Hungarian grain in the same format as Figure 23A.

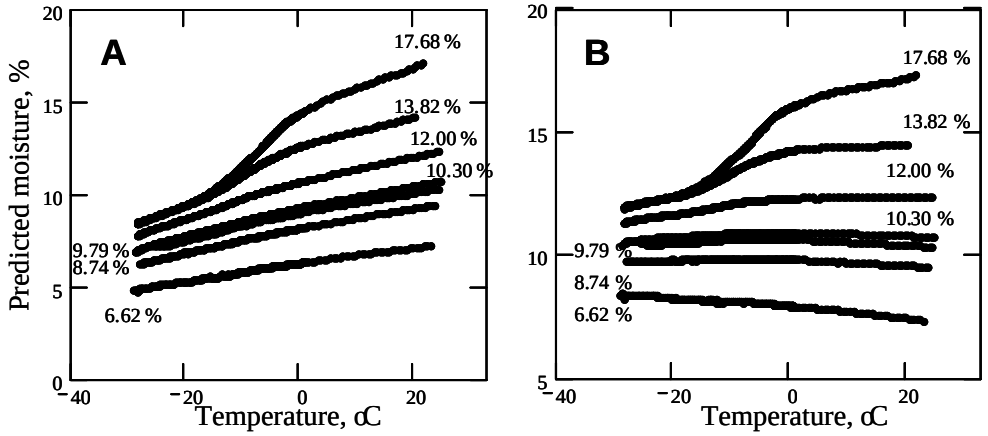


Figure 22. Predicted wb moisture values for sunflower samples at 20 MHz
A) without temperature correction, and B) with temperature correction

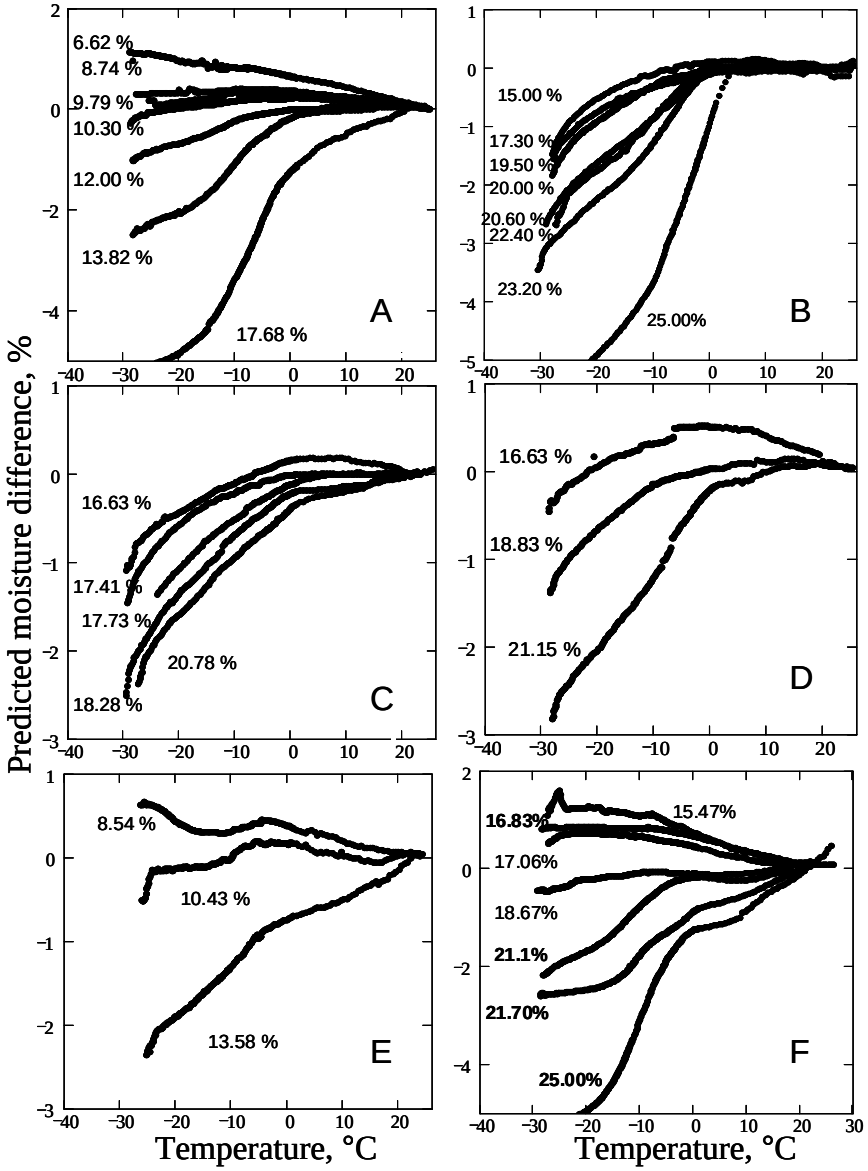


Figure 23. Predicted wb moisture difference at 20 MHz (with respect to the predicted value at 20 °C) versus temperature for A) sunflower, B) wheat, C) autumn barley, D) oats, E) rapeseed, and F) soybeans at the indicated wb moisture levels.

The optimal temperature correction, which minimized the moisture prediction error over the 0 to 30 C temperature range, was calculated for each grain sample for each of the six grain types. The optimal temperature coefficient for a grain type was determined as the average of the all sample temperature coefficients for samples of the grain type. In general, the average temperature coefficients were lower in magnitude and much more consistent among grain types and moisture levels at higher measurement frequencies. This is believed to be due to the reduced effects of sample conductivity at higher frequencies. Calculated temperature coefficients (Ktc) for three measurement frequencies (2 MHz, 20 MHz, 149 MHz) are shown in Table 6.

Table 6. Optimum temperature correction coefficients at three measurement frequencies.

| *Grain type* | *Ktc@ 2MHz* | *Ktc@ 20MHz* | *Ktc@ 149MHz* | *KTC0* | *KTCS* | *KTC01* | *KTCS1* | *KTCQ* |
|---|---|---|---|---|---|---|---|---|
| Wheat | 0.099 | 0.094 | 0.088 | 0.159 | -0.0051 | 0.1201 | -0.0044 | -0.0021 |
| Barley | 0.143 | 0.11 | 0.11 | 0.159 | -0.0035 | 0.1774 | -0.0050 | -0.0014 |
| Soybeans | 0.167 | 0.14 | 0.107 | 0.226 | -0.0099 | 0.1366 | -0.0072 | -0.0022 |
| Sunflower | 0.088 | 0.088 | 0.054 | 0.092 | -0.0028 | 0.0868 | -0.0026 | -0.0004 |
| Oats | 0.244 | 0.127 | 0.143 | 0.155 | -0.0014 | 0.1844 | -0.0051 | -0.0014 |
| Rapeseed | 0.173 | 0.105 | 0.081 | 0.134 | -0.0058 | 0.1745 | -0.0098 | -0.0013 |

Because of the moderate effectiveness afforded by Equation 45 at low frequencies, the same temperature correction strategy was applied to the 149 MHz data (Figure 24). Again, the temperature correction was moderately effective, but the high and low moisture samples still showed significant errors in predicted wb moisture content. At 149 MHz the low moisture samples were under-corrected and the high moisture content samples were overcorrected (above zero degrees Celsius). This was opposite to the residual errors observed at 20 MHz and below.

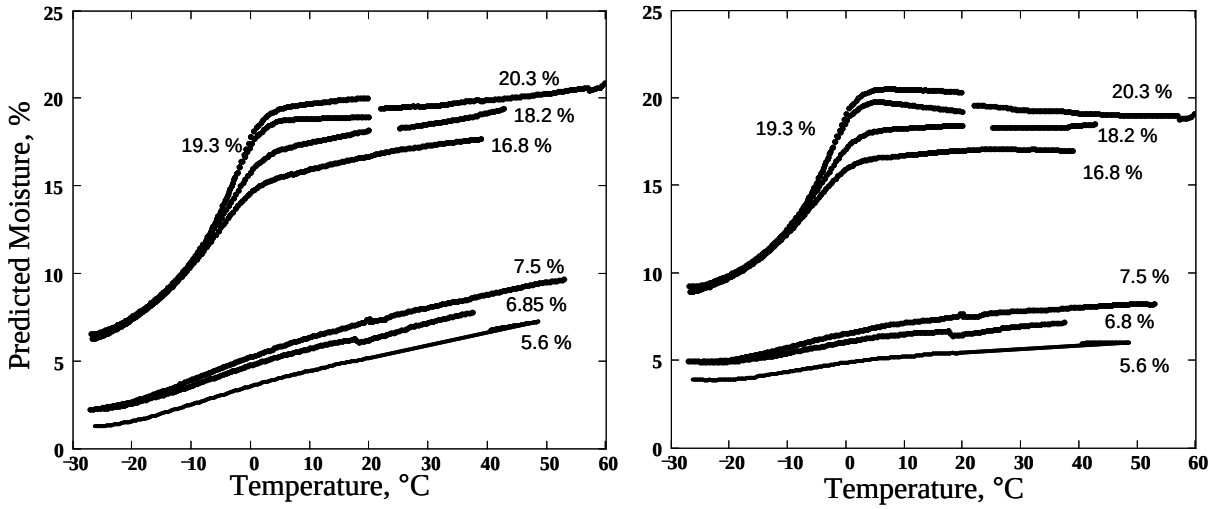


Figure 24. Predicted wb moisture values for sunflower samples at 149 MHz: a) without temperature correction, and b) with temperature correction (Equation 45).

To obtaine a better temperature correction function, the optimum temperature coefficients (percent per degree Celsius) for grain samples were analyzed as a function of wb moisture content at three different frequencies (2 MHz, 20 MHz, and 149 MHz). Figure 25 shows that the optimum sample temperature correction coefficient increased with wb moisture content for low frequency measurements and decreased with wb moisture content for VHF measurements. These figures also demonstrate greater variability and larger magnitudes for Ktc at lower frequencies.

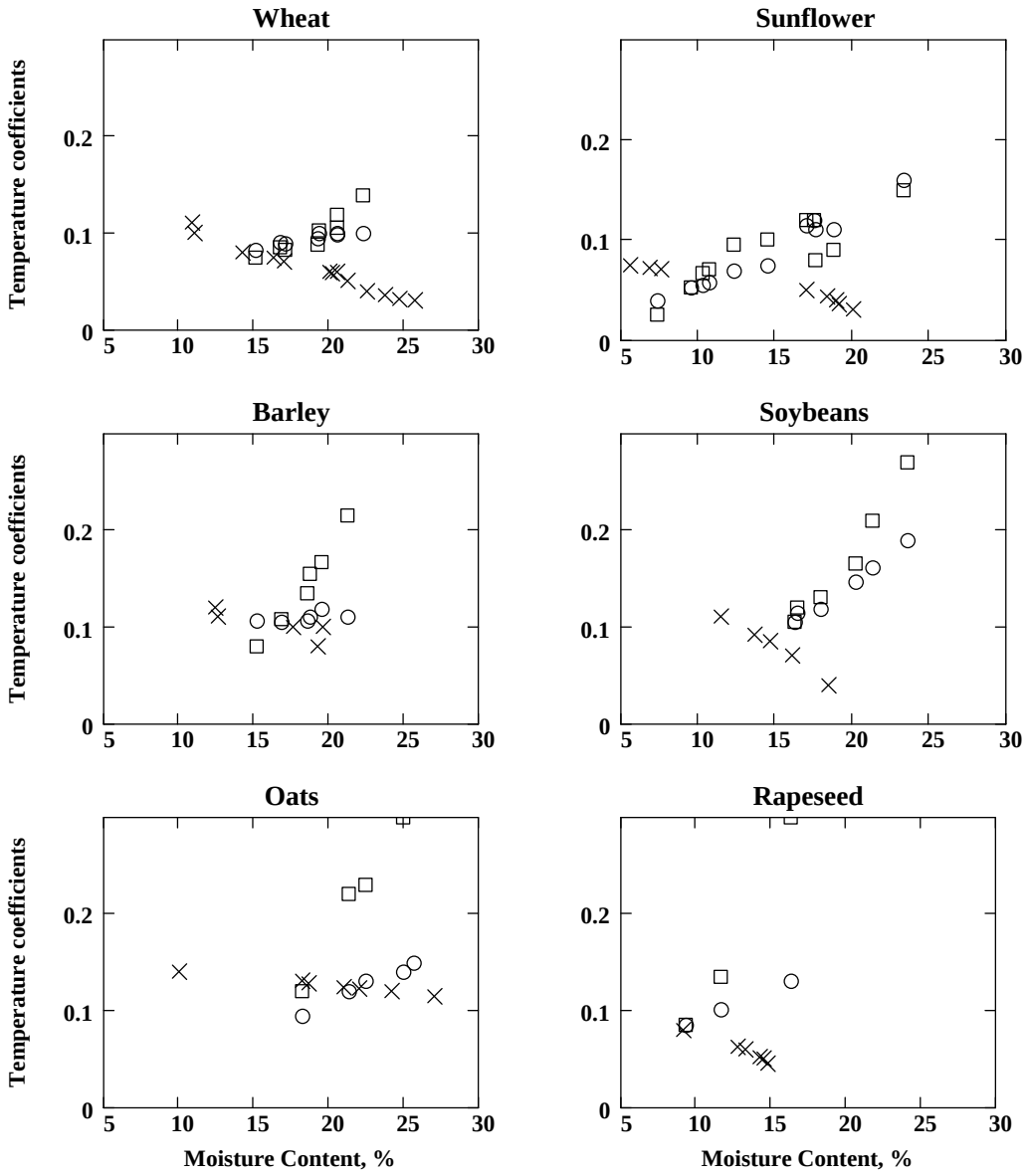


Figure 25. Optimum sample temperature coefficients (Ktc) versus wb moisture content for six grain types at 2 MHz (□), 20 MHz (o), and 149 MHz (x).

A hypothesis was developed to explain the differences in temperature coefficients at different frequencies. The increase in temperature coefficient with wb moisture at low frequencies was probably due to increased conductivity at higher temperatures and higher moisture content. An experiment was performed to investigate the source of the increase in the needed temperature correction with wb moisture content for lower frequencies. Figure 26 shows dielectric spectra (dielectric constant and loss factor) for a 25% wb moisture wheat sample at four temperatures. At -30 °C, the loss factor is low and shows a maximum near 1 kHz. This is the expected frequency range for dipolar relaxation of ice (Hasted, 1973). The dielectric constant decreases slowly and gradually from 100 Hz to 100 kHz and is nearly constant from 100 kHz to 1 MHz. Note that the loss factor is very low at frequencies above 100 kHz.

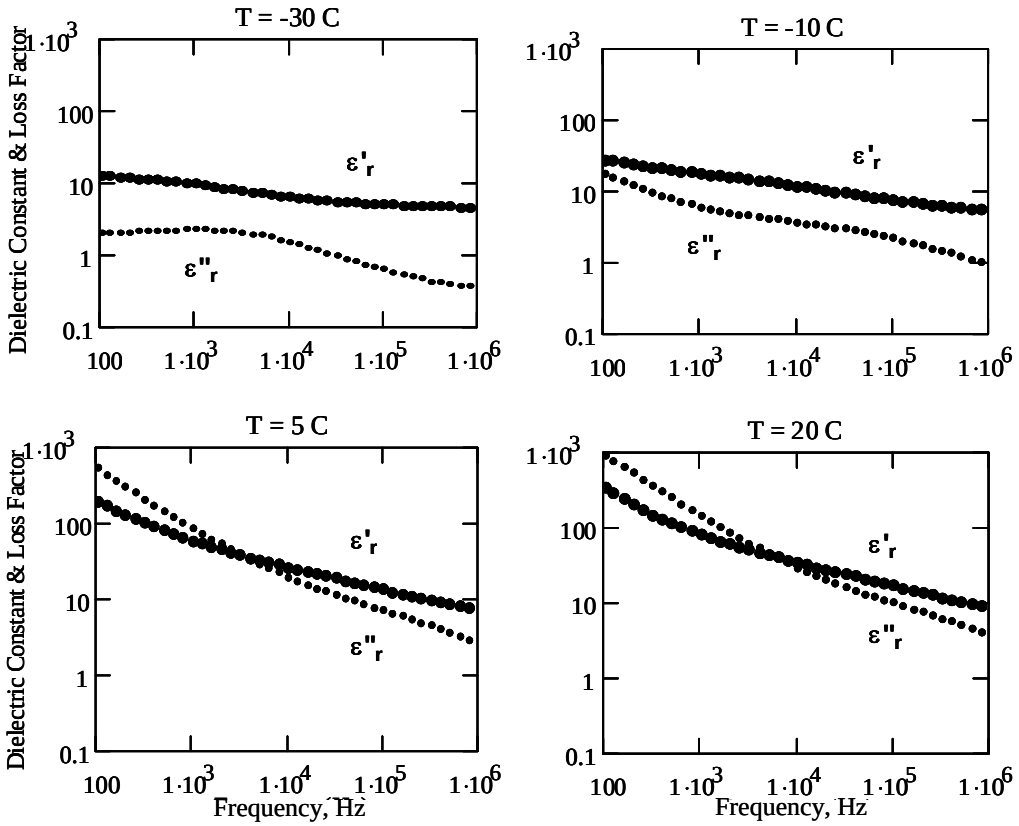


Figure 26. Dielectric spectra of wheat 25 % wb moisture wheat sample at four temperatures.

At higher temperatures, there is a dramatic increase in the loss factor that is typical of dc conductivity through the sample. Electrode polarization causes a huge (50 times) increase in dielectric constant at 100 Hz for the sample shown. Note that the sloping dielectric constant and loss factor curves, which are characteristic of electrode polarization (Grimnes S. Martinsen O.G. 2000), extend throughout the entire frequency range for the higher temperature measurements. Although the change at 1 MHz (about a factor of 2) is much smaller than at lower frequencies, the change is very large in terms of its effect on moisture predictions.

This test indicates that electrode polarization effects (though usually considered not so significant in the 1 to 20 MHz region) (Schwan 1964), are actually large enough to contribute to the change in dielectric characteristics. The decrease in temperature coefficient with wb moisture at VHF frequencies is probably because electrode polarization is dramatically reduced in the VHF region and the negative coefficient of free water is more significant at higher moisture levels. “Bound water” relaxation contributes to the observed temperature effects across the entire frequency range.

Inspection of Figure 25 revealed that the temperature correction at 149 MHz was dependent on moisture level. The effect of using a moisture-dependent linear function (Equation 46) instead of Equation 45 was tested. The effect of the moisture-dependent temperature correction function can be seen for six grain types in Figure 27. Linear regression was used to determine the optimum

*KTCO* and *KTCS* coefficients (for each grain type) for Equation. 46. Applying those coefficients in Equation 46 to the predicted wb moisture data gave the results that are shown in Figure 27.

$$\%x_{tc} = \%x - (KTC0 + KTCS \cdot \%x') \cdot (t - 25) \tag{46}$$

where : *KTC0* is the intercept value and *KTCS* is the slope value

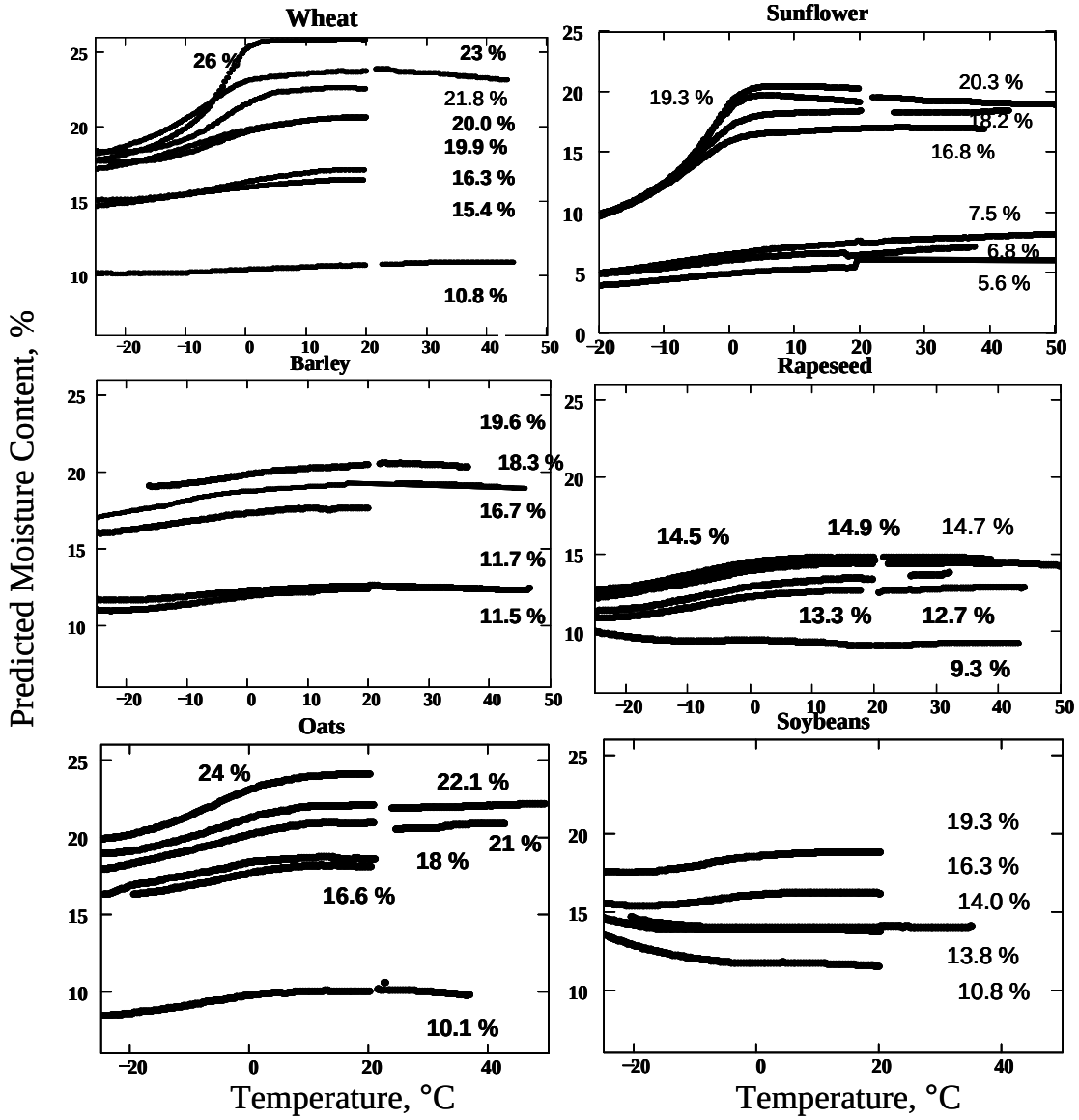


Figure 27. Predicted wb moisture content versus temperature for six grain types using the moisture-dependent temperature correction function **(**Equation 46**).**

Because of the uncorrected error at temperature extremes, a third alternative temperature correction function was also tested. This was a linear moisture-dependent temperature correction with quadratic temperature term (Equation 47). Polynomial regression was used to determine the optimum *KTCO1, KTCS1* and *KTCQ* coefficients (for each grain type) for Equation. 47. The effectiveness of the three alternative temperature correction functions was compared.

$$\%x_{tc} = \%x - (KTC01 + KTCS1 \cdot \%x') \cdot (t - 25) - KTCQ \cdot (t - 25)^2 \tag{47}$$

Applying Equation (46) and (47), *%x* is used for *%x'* (estimated temperature-corrected moisture) initially and the calculated value of $x_{tc}$ is iteratively substituted for *%x* until $\%x_{tc}$ converges. Alternatively, (48) and (49) (found by setting *%x'* equal to $\%x_{tc}$) can be used in place of (46) and (47), respectively, without iteration.

$$\%x_{tc} = \frac{\%x - KTC0 \cdot (t - 25)}{1 + KTCS \cdot (t - 25)} \tag{48}$$

$$\%x_{tc} = \frac{\%x - KTC01 \cdot (t - 25) - KTCQ \cdot (t - 25)^2}{1 + KTCS1 \cdot (t - 25)} \tag{49}$$

Figure 28 shows typical results for one of the grain types that were tested (soft wheat). Each curve represents the data for one sample. For some samples, only the low temperature part of the test was done. Curves are labeled with the corresponding samples' air-oven wb moisture values.

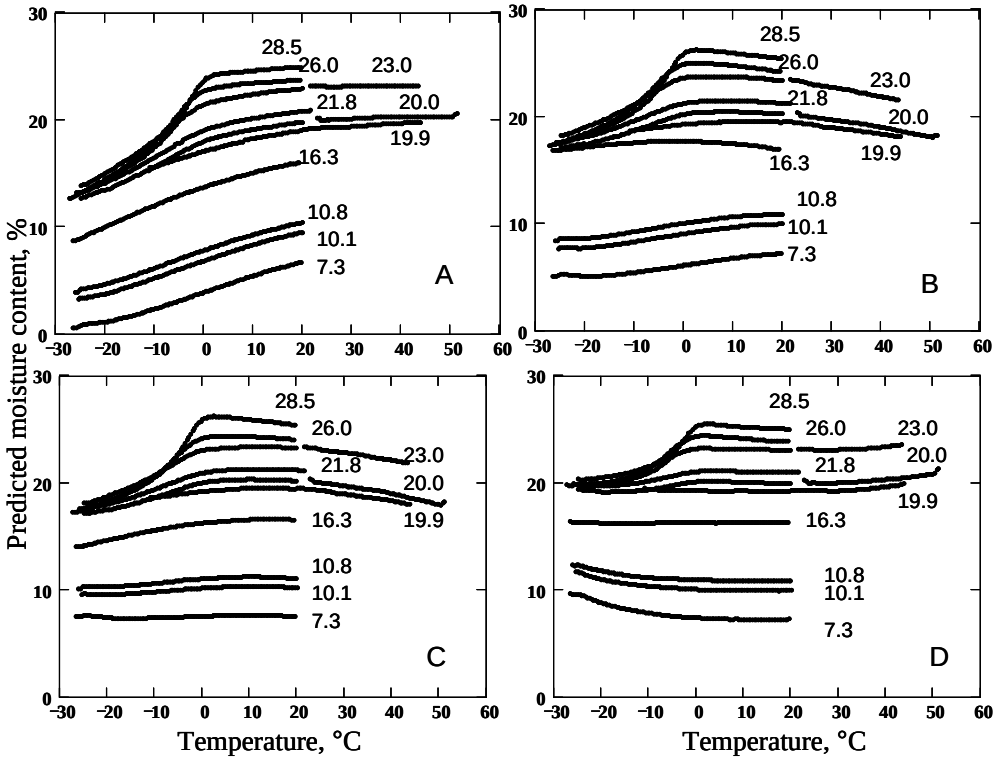


Figure 28. Predicted wb moisture values for wheat samples at 149 MHz with four different temperature correction methods. A) no temperature correction; B) constant temperature correction (Equation 45); C) linear moisture-dependent temperature correction (Equation 46); D) linear moisture-dependent temperature correction with quadratic temperature term (Equation 47).

Figure 28A presents the predicted wb moisture values without temperature correction. The predicted values increased with increasing temperature for all samples. The wheat samples at moisture levels above 20 percent wb showed slope discontinuities at zero Celsius. Those discontinuities are believed to be due to the phase change of the free water in the samples. The average slope (% wb moisture per degree Celsius) for the 0 to 50 C temperature range was calculated for each sample. The average slope for all samples (of the same grain type) was used as

the *Ktc* value in the correction defined by Equation 45. Figure 28B shows the effects of that temperature correction approach. The average slope for temperatures above zero Celsius was forced to zero, but individual samples exhibit significant residual slope errors.

Applying the linear moisture-dependent temperature correction (Equation 46), the predicted moisture data gave the results that are shown in Figure 28C. The slopes of the curves for all the samples are near zero in the 0 to 30 °C temperature range, but some curvature can be seen at temperature extremes.

Coefficients (*KTC01, KTCS1 and KTCQ*) for Equation 47 were calculated for each sample by polynomial regression. The quadratic temperature term provided by Equation 47 reduced the error at temperature extremes, as shown (for wheat) in Figure 28D. With the temperature correction provided by Equation 47, the predicted moisture errors (relative to predicted moisture content at 24 oC) were less then 0.6% wb moisture for all grain samples at temperatures above zero degree Celsius. For samples with moisture levels below the "free" water limit (approx. 20 % wb for wheat), the useable temperature range is extended to -20 °C or lower. The coefficients (*KTCQ*) of the quadratic term that were calculated for each sample were not highly correlated to sample moisture content, so an average value was selected for each grain type. A constant, moisture-independent *KTCQ* (per grain type) avoided a major increase in model complexity. The optimum values (based on the available samples) for the coefficients for Equations 45–47 are given in Table 6.

The measure of success of a temperature correction algorithm is how closely the corrected wb moisture values at other temperatures compare to the predicted wb moisture values at the reference temperature (typically 25 °C). One way of quantifying that agreement is to calculate the residual slope after temperature correction (slope of the corrected moisture predictions versus temperature). Table 7. presents the residual slope values for sunflower and soybean (Appendix 4. show the other four grain types) samples for temperature corrections based on Equations 45 - 47. Zero residual slope, of course, was the goal. The residual slopes that are shown were calculated for sample temperatures between 0 and 40 °C. Note the two different fonts. Bold number indicate tests that included only the low (from 0 to -25 °C) temperature range. Table 7. shows that, in general, the residual slope values are closer to zero for the moisture-dependent corrections than for the moisture-independent corrections. The advantage provided by the extra quadratic temperature term (*Equation 47*) is not evident as in Figure 28D because the temperature range for the slope calculations did not extend below zero Celsius.

Table 7. The residual slope after temperature correction for soybean and sunflower (slope of the corrected moisture predictions versus temperature).

| | *Residual (uncorrected) slope of the predicted moisture curve (from 0 to + 40 °C)* | | | | |
|---|---|---|---|---|---|
| Grain type | Moisture content wb | No temperature correction | Constant temperature correction (Equation 45.) | Linear moisture-dependent temperature correction (Equation 46.) | Linear moisture-dependent temperature correction plus a quadratic temperature term (Equation 47.) |
| Soybean | **10.8** | **0.138** | **0.0310** | **0.0200** | **0.0180** |
| | **13.8** | **0.118** | **0.0110** | **0.0180** | **0.0140** |
| | **14.0** | **0.091** | **-0.0160** | **0.0110** | **0.0057** |
| | 16.3 | 0.104 | -0.0033 | 0.0044 | 0.0350 |
| | **19.3** | **0.062** | **-0.0450** | **0.0017** | **-0.0059** |
| Sunflower | 5.6 | 0.070 | 0.0160 | -0.0086 | -0.0005 |
| | 6.8 | 0.078 | 0.0240 | 0.0037 | -0.0033 |
| | 7.5 | 0.080 | 0.0260 | 0.0069 | 0.0150 |
| | 16.8 | 0.013 | -0.0410 | -0.0250 | -0.0210 |
| | 18.2 | 0.063 | 0.0091 | 0.0150 | 0.0140 |
| | 19.3 | 0.019 | -0.0350 | -0.0210 | -0.0130 |
| | 20.3 | 0.055 | 0.0011 | 0.0110 | 0.0120 |

The measure of goodness of the different temperature correction functions is to calculate the residual moisture content (predicted moisture minus air oven moisture) at different temperature for each correction functions and plot these values versus the reference air-oven moisture content. In Figure 29 can be seen the residual moisture content versus the air oven moisture content at four different temperature (-20 °C in Figure 29A), -10 °C in Figure 29B), 20 °C in Figure 29C) and 40 °C in Figure 29D) and for the three different temperature correction function for the wheat samples. The linear moisture-dependent temperature correction was better at all temperature than the moisture-independent function, but the quadratic form was the best–especially at temperature extremes. The same conclusion was found for the other measured grain types.

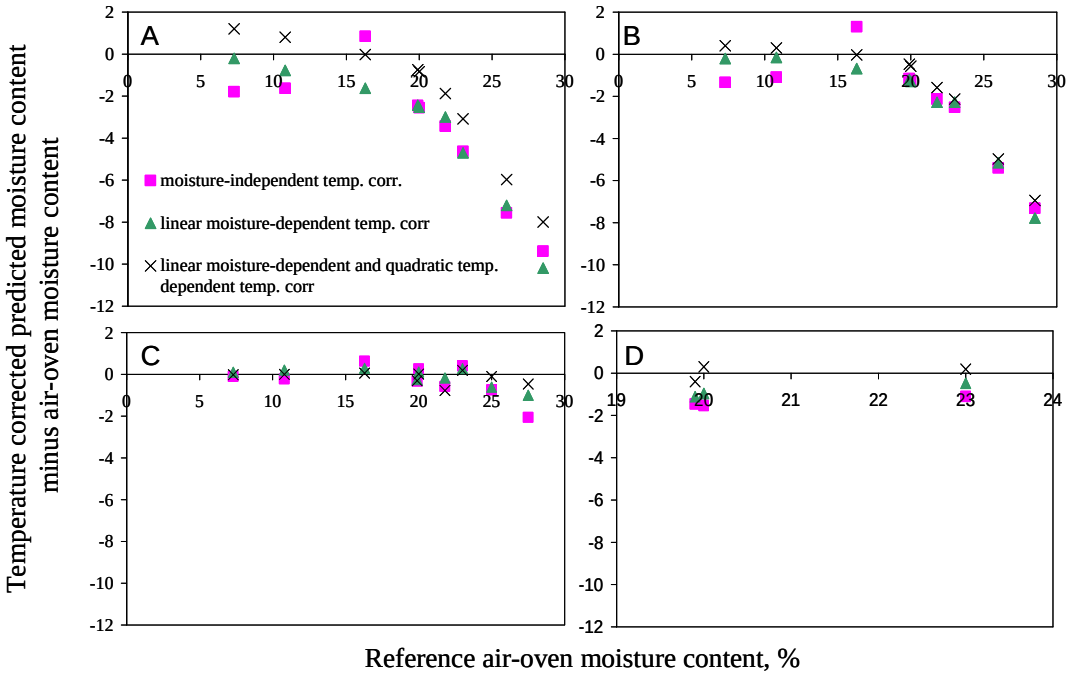


Figure 29. Residual moisture content (temperature corrected predicted moisture minus the reference air oven moisture) versus the reference air-oven moisture content for wheat at A) -20 °C, B) -10 °C, C) 20 °C and D) 40 °C temperature

## 7.6. Moisture limits of dielectric moisture measurements for several grains and oilseeds at low (1-20 MHz) and high (149 MHz) frequencies

The effects of sample temperature are further complicated by the phase change of “free” water at zero Celsius. Ice has a much lower dielectric constant than water in the RF and higher frequency ranges. Figure 30 shows typical dielectric characteristics (at 149 MHz) that were measured as samples warmed slowly to room temperature. Moist sand (14 % M) showed the expected discontinuity in dielectric characteristics at zero Celsius because of the dramatically different relaxation frequencies of ice and "free" water. Grain samples did not show such a discontinuity. Much of the water in grain is associated more or less tightly with polar sites on grain constituents through hydrogen bonding. Such water does not show a dramatic discontinuity in the dielectric constant value at zero Celsius. For dry to moderately moist grain samples, where virtually all of the water is bound to grain constituents, the variation of dielectric constant with temperature is nearly constant over a wide range of temperature that extends well below zero Celsius. However, at high wb moisture contents, some of the water in the grain is capable of changing phase and becomes invisible to the dielectric method at temperatures below the freezing point of water. (Funk et al 2005.)

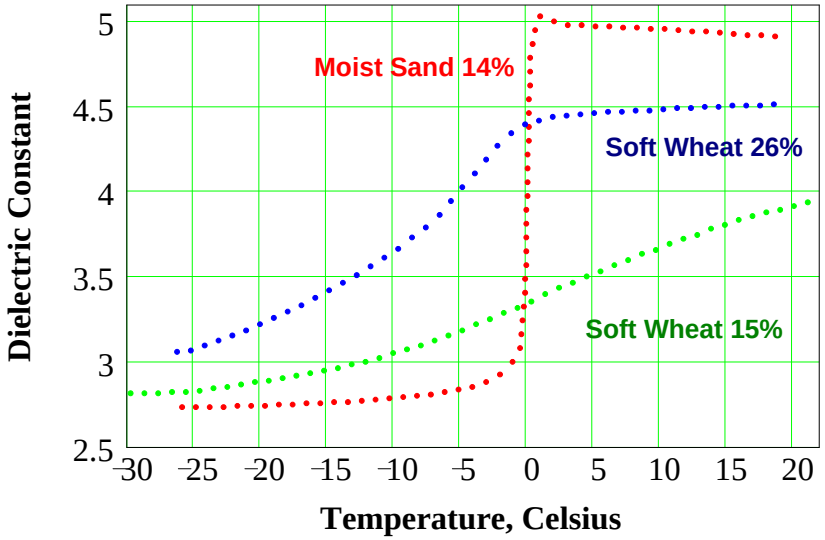


Figure 30. Dielectric constant versus temperature for moist sand and two wheat samples.

Figures 31A and 31B show the moisture-independent temperature-corrected predicted moisture contents at -20, 0 and +20 °C temperature for wheat samples and oat samples, respectively. The slope values between -20 °C and 0 °C and between 0 °C and +20 °C were determined. The slope value differences were calculated between these two temperature ranges. The upper moisture limit (below which moisture can be determined below zero Celsius) for each grain type was determined by the slope differences and the residual moisture content at -20 °C (Figure

31). For this test, the moisture-independent temperature correction was applied because at this moment all dielectric grain moisture meter manufacturers apply this temperature correction and these information are helpful to them. When these slope differences were above 0.08 and the absolute value of residual moisture content was higher than 2 at -20 °C then the discontinuity appeared in the dielectric characteristic at about 0 °C. For some grain types, more data are needed to further refine the limits. Table 8 gives the approximate wb moisture limit for each grain type. The minimal differences in the upper wb moisture limits for high and low frequency measurements are probably due to the different measurement systems and calibration procedures that were used for the two data sets.

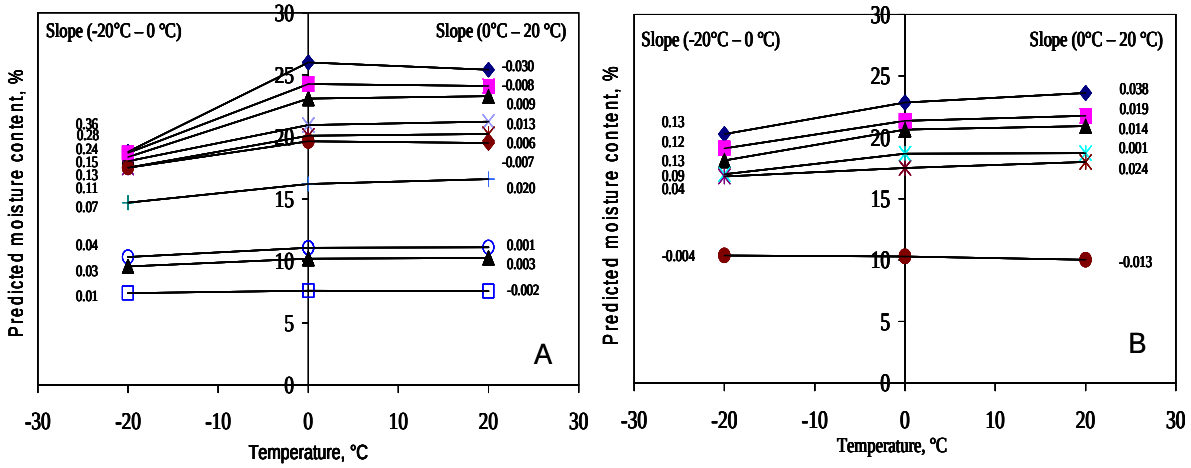


Figure 31. Moisture-independent temperature-corrected predicted moisture content at -20, 0 and +20°C versus temperature for A) wheat samples, B) oats samples (slope values between -20 – 0 °C and 0 - +20 °C are indicated on the Figure)

Table 8. Estimated wb moisture limits for moisture measurements below zero Celsius for six grain types.

| *Grain type* | *High moisture limit wb@ 20 MHz (%)* | *High moisture limit wb @ 149 MHz (%)* |
|---|---|---|
| Rapeseed | 11 % | 10 % |
| Barley | 19 % | > 19 % |
| Sunflower | 12 % | 10 % |
| Wheat | 20 % | 17 % |
| Oats | 19 % | 17 % |
| Soybeans | 19 % | > 19 % |

## 7.7. Developing unifying parameters from grain physical and chemical properties

The goal of this research was to determine whether the third generation unifying parameters for the Unified Grain Moisture Algorithm could be predicted from the typical chemical and physical properties (Appendix 5.) of different grain types. When a new grain type or class is fitted into the calibration set the cost of the calibration development (dielectric measurements, air-oven measurements and data analysis) is high, and the process is time-consuming. Because the dielectric parameters are depending on the physical and chemical properties of the grain type (Nelson 1973),

it is assumed that the differences in the dielectric constant between grain types, which can be corrected by the slope, offset, and translation parameters, are correlated with the grain physical and chemical properties. A viable process for accurately predicting unifying parameters for new grain types would greatly reduce the cost of calibration development.

The relationships between the physical and chemical properties of grains (Soybean, Sorghum, Sunflower, Corn, Oats, Wheat, Barley, Rice, Flaxseed, and Rapeseed as the independent variables) and the target values for third generation of unifying parameters (OP, SP, TP) and temperature correction coefficients were modeled using step-up multiple linear regression (detailed in the Material and Methods in section 6.4.4. – page 52).

Table 9 gives calibration and cross-validation statistics for predictions of Slope, Offset, and Translation parameters from grain chemical and physical parameters for 10 grain types. Results are shown for three-factor prediction models for each unifying parameter. Equations 50-52 show the selected model factors and the coefficients for predicting Slope, Offset, and Translation parameters for 10 grain types (soy, sorghum, sunflower, corn, oats, wheat, barley, rice, flaxseed, and rapeseed).

The fit for the Slope parameter was considerably better than for the other two parameters, as evidenced by the higher $R^2$ values for the calibration results. Note that the $R^2$ values for cross-validation are significantly lower that those for calibration for the Offset and Translation parameters. This is another warning sign regarding the reliability of those estimates. Figures 32 and 33 compare the calibration and cross-validation results graphically. Each point in the graphs represents one grain type. These results suggest that the Slope parameter may be predicted successfully from the grain chemical and physical parameters, but the other two parameters cannot be predicted reliably.

Table 9. Statistical results for step-up multiple linear regressions for SP, OP and TP parameters with three factors.

| Statistical Tests | Slope Parameter (SP) | Offset Parameter (OP) | Translation Parameter (TP) |
|---|---|---|---|
| F-test | 4468 | 199 | 82 |
| Standard error of calibration | 0.017 | 0.050 | 0.406 |
| Multiple correlation coefficient ($R^2$) | 0.993 | 0.897 | 0.702 |
| Multiple correlation coefficient for cross validation ($R^2$) | 0.988 | 0.864 | 0.525 |

$$SP = 1.17 - 0.0127 \cdot Ash(\%) - 5.2 \cdot 10^{-4} \cdot SeedVolume(mm^3) - 7.54 \cdot 10^{-3} \cdot Oil(\%) \quad (50)$$

$$OP = 2.5354 - 0.0171 \cdot Protein(\%) + 8.38 \cdot 10^{-3} \cdot Ash(\%) + 6.515 \cdot 10^{-4} \cdot SeedVolume(mm^3) \quad (51)$$

$$TP = 3.3963 - 0.1102 \cdot Oil(\%) - 0.6539 \cdot BulkDensity(g/cm^3) - 4.43 \cdot 10^{-3} \cdot Starch(\%) \quad (52)$$

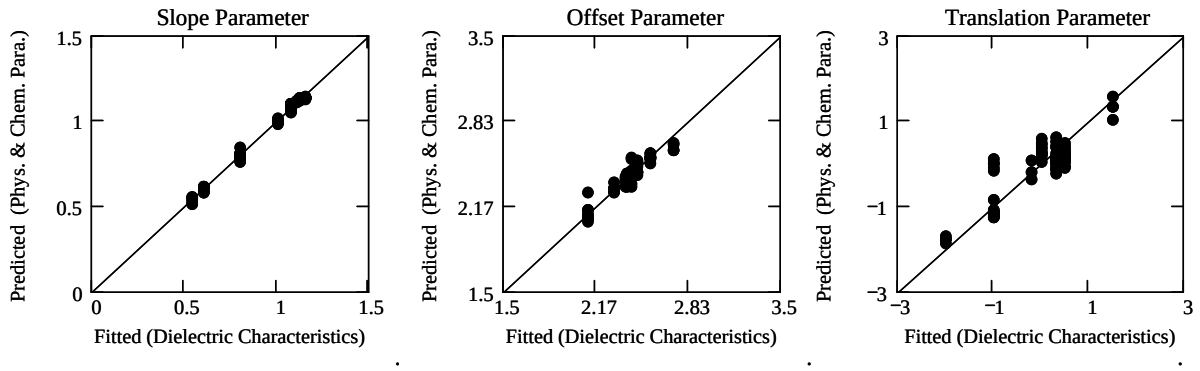


Figure 32. Calibration results for predicting Slope, Offset and Translation parameters from grain physical and chemical properties (each point represents a grain type).

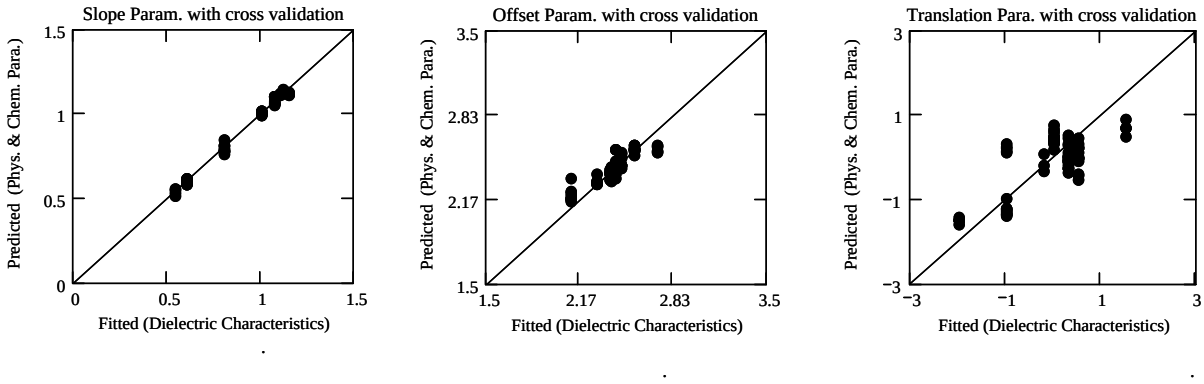


Figure 33. Cross-validation results for predicting slope, offset and translation parameters from grain physical and chemical properties (each point represents a grain type).

Unifying parameters of mustard seed were calculated from mustard physical and chemical properties. The significance of this test is that the physical and chemical properties (ash content: 4.51%, oil content: 27%, Protein: 26.36%, Starch: 35.7%, Seed volume: 3.7 $mm^3$, Bulk density: 0.69 $g/cm^3$) (Paliwal 1998, Canadian Grain Comission 2003, Kansas State University 2003) of mustard were not included among the independent variables (10 grain types) which were chosen to determine the Unifying parameters by Multiple Linear Regression. Table 10 shows that for this grain type, the predicted Slope parameter is correct but the predicted Offset and Translation parameters are not acceptable.

Table 10. Mustard reference and calculated unifying parameter

| | SP | OP | TP |
|---|---|---|---|
| Reference | 0.88 | 2.399 | 0.5 |
| Predicted | 0.9 | 2.125 | -0.189 |
| Difference | 0.02 | -0.274 | -0.689 |

## 7.8. Prediction of temperature correction coefficients from grain physical and chemical properties

Temperature correction coefficients (KTC – moisture-independent, KTC0, KTCS – linear moisture-dependent, KTC01, KTCS1, KTCQ – linear moisture-dependent and quadratic temperature-dependent temperature correction coefficients) were also modeled from grain physical and chemical properties by means of step-up multiple linear regression and were tested by cross-validation. Equations 53-58 show the factors that were selected and the prediction coefficients. The predicted coefficients and the cross-validation results of moisture-independent temperature correction coefficients are presented in Figure 34. Table 11 gives calibration and cross-validation statistics for predictions of temperature correction coefficients from grain chemical and physical parameters for 6 grain types. These results suggest that the moisture independent temperature correction coefficients may be predicted successfully from the grain chemical and physical parameters. Models were also developed to predict the temperature correction coefficients for more complex temperature correction functions (Equations 46 and 47), but the cross-validation results were poor—especially for the KTC0 and KTC01 parameters.

For the moisture-independent temperature correction, the standard deviation of cross-validation errors was 0.007 percent wb moisture per degree Celsius sample temperature difference from 25 ɑC. This suggests that using such predicted moisture independent temperature correction coefficients (in *Equation 45*) (instead of performing temperature tests to optimize the moisture independent temperature correction coefficient) would likely cause an additional moisture ambiguity of about +/- 0.1 percent wb moisture over the temperature range of 15 to 35 °C. For some applications, this may be acceptable and may provide a cost-effective means of developing calibrations quickly and easily for additional grain types.

$$Ktc = 0.0779 - 2.306 \cdot 10^{-3} \cdot Oil(\%) + 0.0266 \cdot Ash(\%) - 0.0693 \cdot Sphericity \qquad (53)$$

*Sphericity* was defined at the ratio of the 3rd axis (smallest) dimension to the major axis dimension.

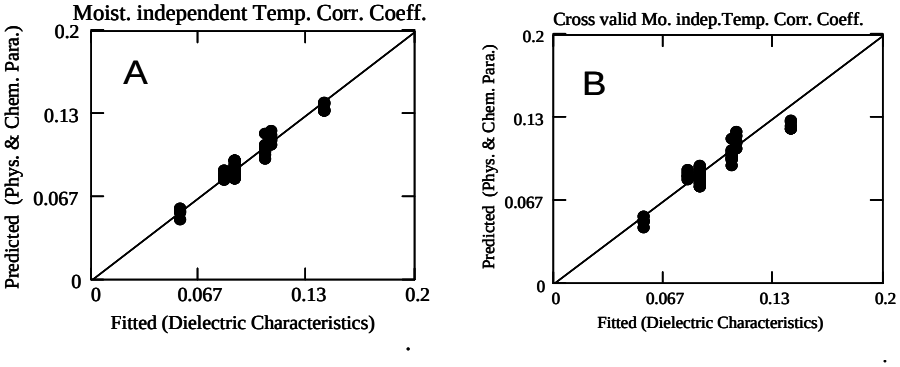


Figure 34. A) Calibration, B) Cross validation results for moisture independent temperature correction coefficients from grain physical and chemical properties
(each point represents a grain type)

Table 11 Statistical results for step-up multiple linear regressions for temperature correction coefficients with three factors

| Statistical Tests | KTC | KTC0 | KTCS | KTC01 | KTCS1 | KTCQ |
|---|---|---|---|---|---|---|
| F-test | 290 | 114 | 670 | 55 | 214 | 334 |
| Standard error of calibration | 0.005 | 0.013 | $3.7*10^{-4}$ | 0.015 | 0.001 | $1.1*10^{-4}$ |
| Multiple correlation coefficient ($R^2$) | 0.95 | 0.885 | 0.978 | 0.786 | 0.934 | 0.957 |
| Multiple correlation coefficient for cross validation ($R^2$) | 0.89 | 0.139 | 0.924 | 0.213 | 0.765 | 0.943 |

$$KTC0 = 0.0634 + 5.36 \cdot 10^{-4} \cdot Seedmass(mg) + 0.1161 \cdot BulkDens.(g/cm^3) - 5.48 \cdot 10^{-4} \cdot Oil(\%) \quad (54)$$

$$KTCS = 3.47 \cdot 10^{-3} - 4.42 \cdot 10^{-3} \cdot Sphericity - 2.92 \cdot 10^{-5} \cdot Seedmass(mg) - 7.39 \cdot 10^{-3} \cdot BulkDens.(g/cm^3) \quad (55)$$

$$KTC01 = -0.1098 + 0.0445 \cdot Ash(\%) + 2.45 \cdot 10^{-3} \cdot Starch(\%) - 0.0402 \cdot Sphericity \quad (56)$$

$$KTCS1 = 5.44 \cdot 10^{-3} + 4.7 \cdot 10^{-3} \cdot Sphericity - 1.49 \cdot 10^{-3} \cdot Ash(\%) - 7.15 \cdot 10^{-5} \cdot Starch(\%) \quad (57)$$

$$KTCQ = 3.1 \cdot 10^{-3} - 2.43 \cdot 10^{-3} \cdot BulkDens(g/cm^3) - 2.45 \cdot 10^{-3} \cdot KernelDens.(g/cm^3) - 2.75 \cdot 10^{-6} \cdot Seedweight(mg) \quad (58)$$

## 7.9. Moisture measurement accuracy using predicted parameters

To test the overall effect of using predicted parameters (based on grain physical and chemical parameters) for moisture measurement, the predicted unifying parameters and temperature coefficient values were substituted into the third generation of UGMA moisture prediction algorithm (Equations 32-35). Moisture prediction accuracy for the set of 5141 samples was compared to the accuracy with the original optimized parameters. With the original parameters, the overall standard deviation of differences (with respect to the air-oven reference method) was 0.308 percent wb moisture. Substituting only the predicted Slope parameters, the overall calibration error increased to 0.3712. Using both the predicted Slope parameters and the predicted temperature correction coefficients (Ktc) again increased the error slightly to 0.4092. When the predicted Offset parameters were substituted for the optimized Offset parameters, the overall calibration error increased dramatically to 0.7737 percent wb moisture.

## 7.10. Drying of apple slices

Changes in sample mass with time during drying were analyzed to characterize the drying process. During the drying of apple slices (approximately 20x20x10 mm) no constant-rate period was observed, only two falling-rate periods. This was consistent with some other reported research (Labuza and Simon 1970, Üretir et al. 1996). Figures 36A and 36B show that the constant rate period was missing and that the falling rate period should be divided into two parts. Moisture content at each point was calculated as the average of three independent air-oven tests of approximately same size apple slices. The standard deviation is also shown on the Figure 36A. Best-fit exponential functions were calculated for the full drying time (0 to 780 minutes) and separately for two periods (0 to about 480 minutes and about 480 to 780 minutes). The correlation coefficient for the exponential fit to the first falling-rate period (0.9996) was a bit better than that for fitting one exponential curve to the completely drying period (0.9994). Durbin Watson statistical test was also performed to test the presence of first-order autocorrelation in the residuals of the regression equation. In the case of Figure 36A the fitted exponential curve to the whole drying period shown a positive autocorrelation at all significance level (Durbin Watson test result was 0.486 n=40). The Durbin Watson test of the fitted exponential of the first falling rate period Figure 36B (0 to about 480 minutes) resulted no autocorrelation at 95% significance level (Durbin Watson test result was 1.84 n=25).

In structured foods, liquid movement inside the tissue is controlled not only by capillary and gravity forces, but also by diffusion, and, therefore, water that is evaporated from the surface is not immediately replenished by movement of liquid from the interior. The lack of the constant-rate drying period for apple slices can be explained by the relatively low pressure of intercellular liquid in cold-stored apples. This can decrease the rate of drying in the constant-rate period and the length of the constant-rate period (Labuza and Simon 1970). In the first falling-rate period, the rate of liquid movement to the surface is less than the rate of evaporation from the surface, and the surface becomes continually depleted of liquid water. Parts of the surface dry up by convective transfer of heat from the drying air, the surface temperature begins to rise, and vapour from inside starts diffusing into the air stream (Rao and Rizvi 1995). Beyond this point, the path for transport of both heat and mass becomes longer and more tortuous as the moisture content continues to decrease.

Because of these disadvantageous effects, the correlation coefficient for the fitted exponential curve for the second falling rate period was lower (as in the first falling period), but it was still above 0.996 (Figure 36B). The Durbin Watson test of the fitted exponential on the second falling rate period Figure 36B (480 to 780 minutes) resulted no autocorrelation at 99% significance level (Durbin Watson test result was 1.16 n=15).

In the second falling-rate period, evaporation occurs below the slice surface and the diffusion of vapor occurs from the place of vaporization to the surface. Diffusion may result because of concentration gradients between the inner part of the sample, where the vapor concentration is high, and the surface, where it is low (Rao and Rizvi 1995). When an apple slice was placed in the 50 °C air-oven, the temperature in the centre of the slice increased rapidly (within approx. 100 min.) to about 40 °C and then slowly increased to the temperature of the drying air (Figure 35.). During this period of slow temperature rise, a change in rate appeared at about 480 min. These observations were also consistent with the different periods of drying that were distinguished from each other on the basis of mass loss kinetics.

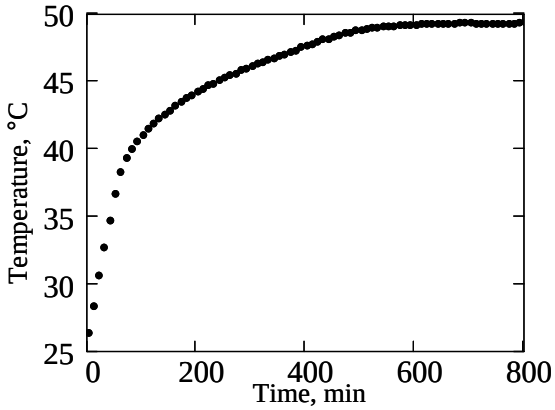


Figure 35. Temperature inside an apple slice during drying

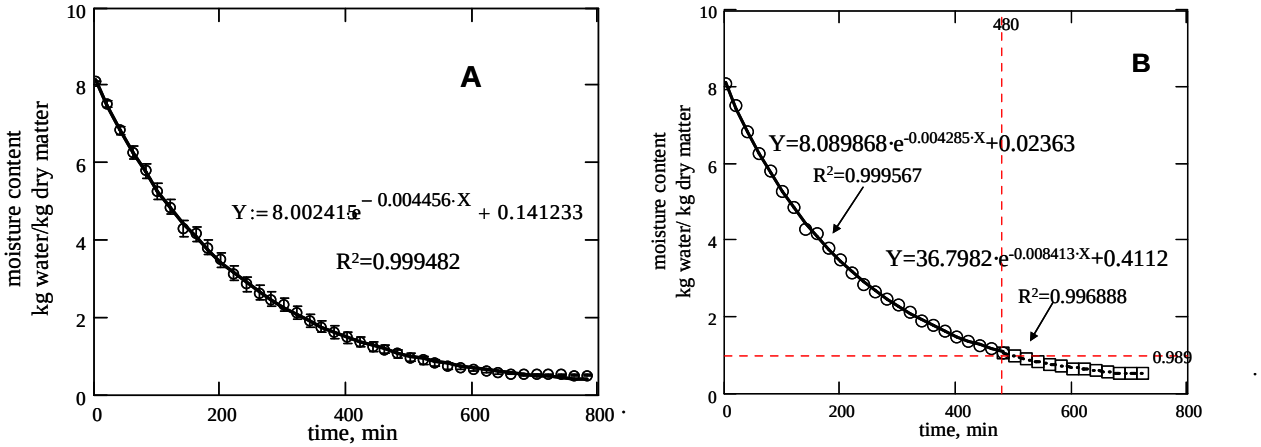


Figure 36. Average moisture content db of three independent air-oven tests (calculated by Equation 23- page 42) versus time. A) Best-fit exponential curve for the full drying time. B) Best-fit exponential curves for two assumed falling-rate periods.

There was another opportunity to observe the two falling rate periods. In this method, the mass loss (average of three independent air-oven tests) of slices (Figure 37) in the whole drying process was approximated with an empirical model (Üretir et al 1996):

$$\frac{dm}{dt} = -k\left(m - m_e\right) \tag{59}$$

Integration of this equation results in:

$$m - m_e = (m_0 - m_e) \cdot e^{-k \cdot t} \tag{60}$$

where $m$ is the mass of the slice at time t, $m_0$ is the initial sample mass, $m_e$ is the mass of slice when the db moisture content of the slice is in equilibrium with that of the drying air, and $(m_0-m_e)$ is constant for a given apple slice. The values of $m_e$ were different for different slices, but the normalized values of $m_e/m_o$ were essentially equal (0.13-0.17) for all slices. Variation of $m_e/m_0$ may be caused by different water/solids ratios among the different apple slices. This result was consistent with the results of Üretir et al (1996). They found $m_e/m_0$ is about 0.13-0.18. Values for $k$ were obtained for the two falling-rate periods with linear regression from the experimental data using the integrated form of Equation 59. The points depicted in Figure 37 were calculated from the average mass of three approximately same size apple slices during drying. Tests with all slices as the average of them showed similar straight lines, and the change in slope appeared for each slice at about 480 min. after beginning drying. This breakpoint was considered the end of the first falling-rate period and the beginning of the second falling-rate period.

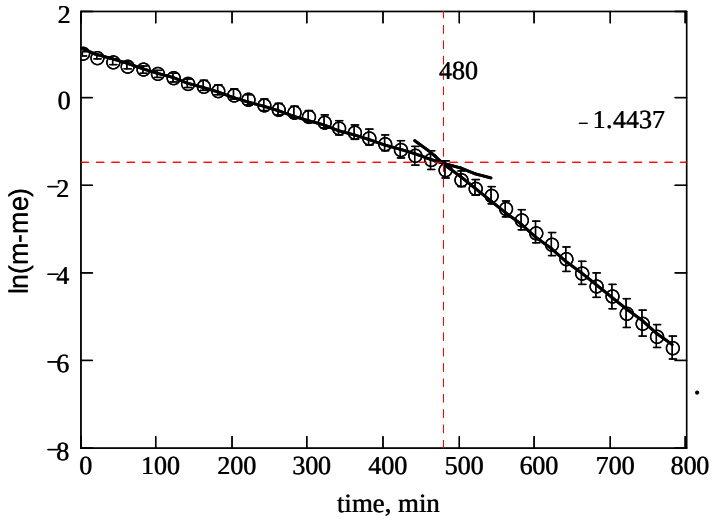


Figure 37. Mass loss of apple slices (20 mm x 20 mm x 10 mm) during drying at 50°C in a Venticell air-oven. $m$ is the mass of the slice at time $t$, and $m_e$ is the mass of the slice with db moisture content in equilibrium with the moisture content of the drying air. (O) calculated values from weighing [each point is an average of three independent air-oven test], (—) best-fit lines from linear regression.

## 7.11. Electrical Impedance measurements of apple slices

The magnitude of the measured impedance continuously increased during drying at lower frequency (<10000 Hz - Figure 38) in slices placed into the oven with inserted electrodes (Method 1 – page 50). After 600 minutes drying and above 10000 Hz the increasing tendency is not obvious from Figure 38. In the slices punctured with electrodes after drying for a given time period (Method

2 – page 50), the magnitude of impedance showed a similar increasing tendency (Figure 39). The minimum point of the phase angle curve shifted slightly to lower frequencies during the first 480 minutes of drying (Figures 38A, 38B, 39A, 39B). During the next 100 minutes of drying, this shift became more pronounced, and after 600 min. drying time the minimum point had shifted so far that this minimum was not observable in the measured frequency range (Figures 38C, 39C). The phase angle spectrum after 700 minutes of drying showed a spectrum typical of a capacitor connected in parallel with a resistor (close to zero degrees at low frequencies, close to -90 degrees at high frequencies) (Figures 38C, 39C).

The impedance spectra measured with 1.8 mm, 4.6 mm, and 6.8 mm electrode distances in three slices with different db moisture contents can be seen in Figure 39**.** These slices were dried for different lengths of time and their db moisture contents were evaluated with Equation 23 from weighing. The slices were punctured with electrodes immediately before the impedance measurements.

In the case of slices of 8.1 kg water/kg dry matter (no drying), the shapes of the phase-angle spectra measured with different electrode distances were the same, indicating homogeneity of the inner structure of slices at these high moisture contents (Figure 39A). For the samples with 1.9 kg water/kg dry matter (300 min. drying), the three phase-angle spectra measured by 1.8 mm, 4.6 mm and 6.8 mm electrode distances were totally different from each other (Figure 39B). The spectra measured with the smallest and the largest electrode distance were characteristic of samples with higher and lower moisture content, respectively, denoting the decrease of water content from the centre to the sides in sample. For the biggest electrode distance (6.8 mm) the pins are closer to the drier part of the apple slice than the other two electrodes (4.6 mm and 1.8 mm). The measured resistance between the two electrodes is smaller than at the outside parts. The phase angle is different for those apple samples where the moisture distribution is different at the inner and outside part. The dried apple slice of 0.52 kg water/kg dry matter (560 min. drying) again had uniform low db moisture content (Figure 39C) based on phase-angle spectra. Unfortunately, we could not compare our result with the literature, because we have not found reference for low frequency electrical impedance measurement during drastical water draw away from fruit or vegetables.

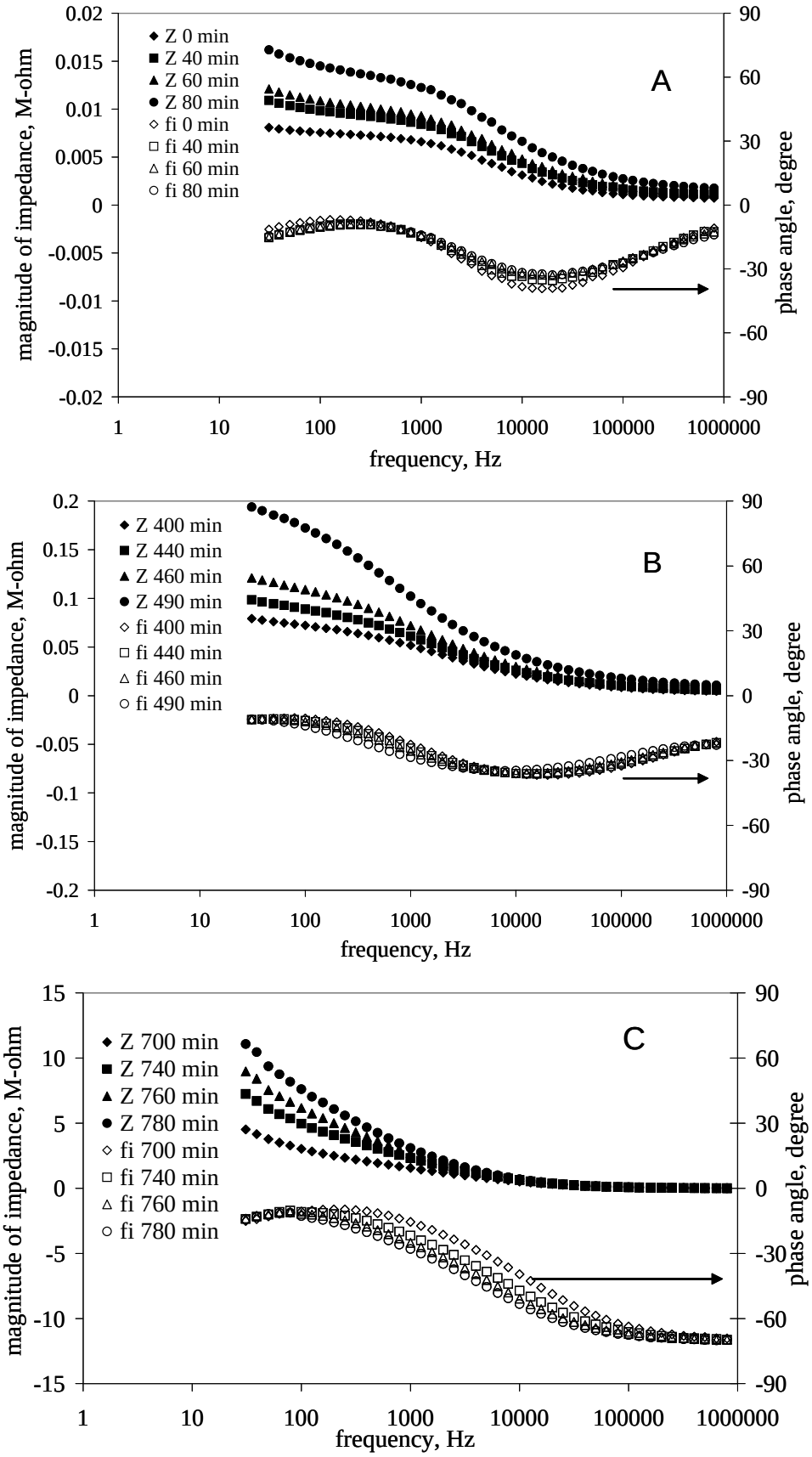


Figure 38. The magnitude, Z, (♦ ■, ▲, ●,) and phase angle,ϕ (◊, □, Δ, ○) of the measured impedance with 1.8 mm electrode spacing in an apple slice (about 20 mm x 20 mm x 10 mm) after different (indicated) drying times (with electrodes inserted—method I) in a 50 °C air-oven.

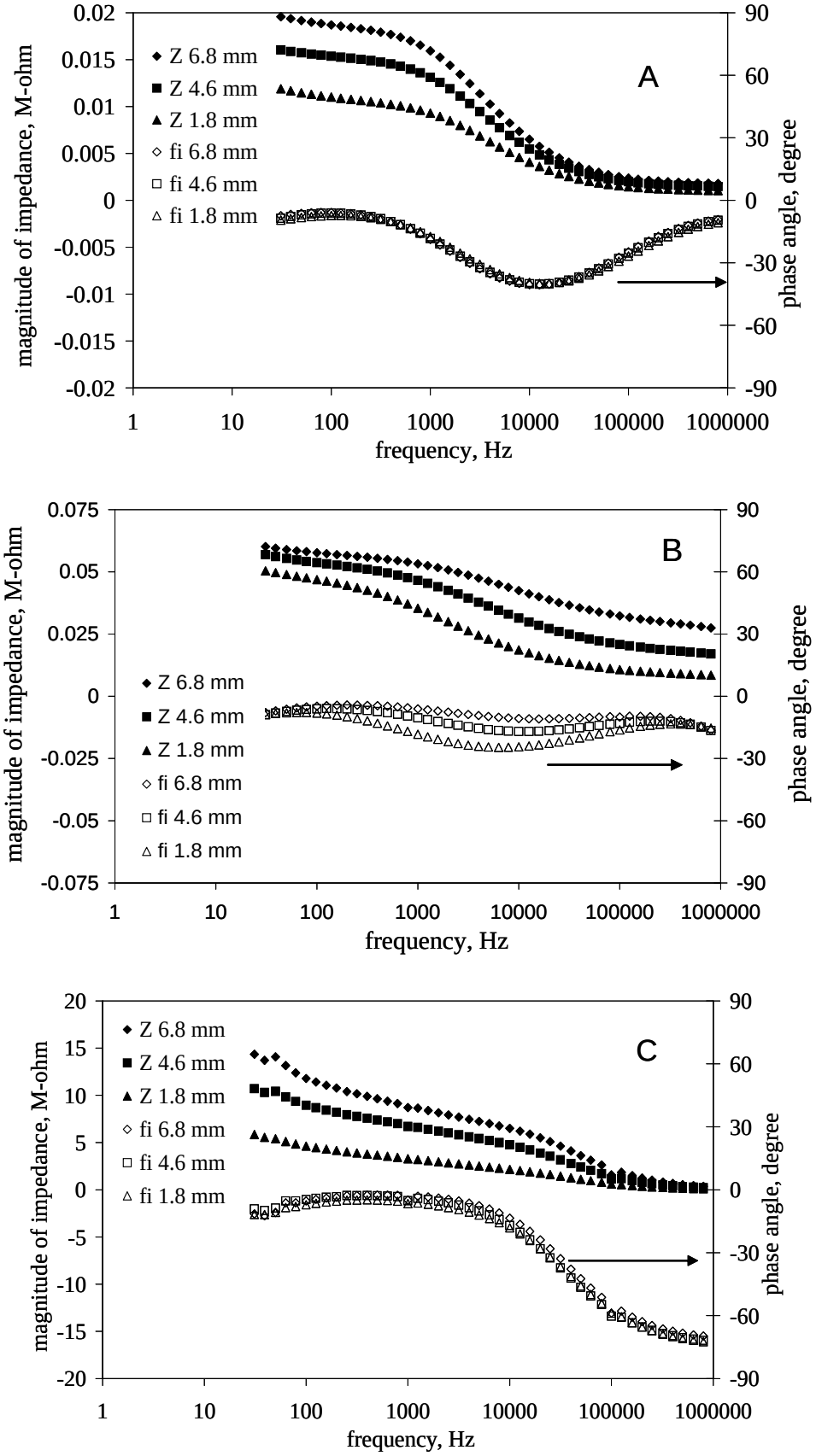


Figure 39. The magnitude, Z, (♦ ■, ▲) and phase angle, ϕ, (◊, □, Δ) of the measured impedance with 1.8 mm, 4.6 mm and 6.8 mm electrode spacing in apple slices after different drying times (method II). A) 0 min., 8.1kg water/kg dry matter. B) 300 min., 1.9kg water/kg dry matter. C) 560 min., 0.52 kg water/kg dry matter.

The method I. measurement (electrode inserted) was repeated many times. Magnitude of impedance and phase angle of seven independent measurements is shown on Figure 41 A and B. unfortunately we could not cut exactly 20x20x10 mm slices out from the whole apple. The error during slicing was about ± 0.5-1.5 mm. When these seven individual measurement was plotted on the same (magnitude of impedance and phase versus time) graph it was observed, that the impedance and phase data in the repeated measurements are close to parallel with each other, but there is a significant difference between measurements in the Time axis (Figure 41A and B). Dielectric and electrical impedance parameters are dependent of the measured material size, density and so on (Nelson 1973, Sembery 2002), but usually can be corrected (Nelson 2004). In the case of dielectric moisture meter, the same volume was used with different density grain sample. Our dielectric data in the unifying algorithm could be corrected by the density (Equation 17). In Figure 5. which is a huge data matrix, it also can be observed that there is a correlation between the sample mass and the dielectric constant. (The shapes of the data clouds are very similar.)

Therefore, it was belived that the differences along the time axis are due to the different masses of the seven apple slices. To test this hypothesis, impedance values (322 kohm ±16 kohm at 100 Hz, 62 kohm ±8 kohm at 100 kHz and 40 kohm ± 3kohm at 800 kHz) were selected in the transient period, where differences between the individual measurements are the most apparent. The phase angles belonging to these impedance values are -27 degree ± 0.8 degree at 100 Hz, -15 degree ± 0.8 degree at 100 kHz and -32 degree ± 0.8 degree at 800 kHz. These impedance and phase angle values versus drying time are shown in Figure 40A and Figure 40B. Figure 40C shows the initial mass of the seven apple slices versus that time when the impedance and phase angle given above were detected. The initial mass increases as the time required to reach the given impedance value increases too. The correlation coefficients between mass and time was $R^2$=0.9422.

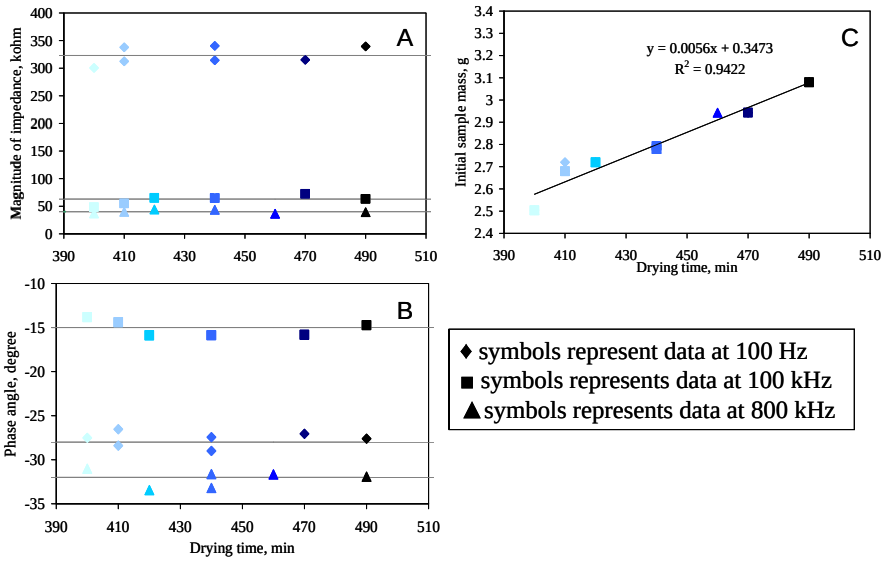


Figure 40. A) Magnitude of impedance, B) phase angle values and C) initial sample mass versus drying time

After that, we found the relationship between the initial mass of the apple slices and the time; a mass correction was introduced. We normalized the initial mass to 3 gram. The ratio of the normalized mass (3 gram) and the initial value was calculated. The Time axis value belonging to each measurement was multiplied by the ratio. After this adjustment, the corrected values for seven measurements were averaged. The averaged impedance and phase angle before the adjustment can be seen on Figure 41 C and D. Big standard deviations can be seen in the impedance spectra especially in the transient period, after 400 minutes. The standard deviations of the phase data are even more significant. The same data after the adjustment can be observed on Figure 42 A and B. The standard deviation of the seven measurements is not so significant after the adjustment.

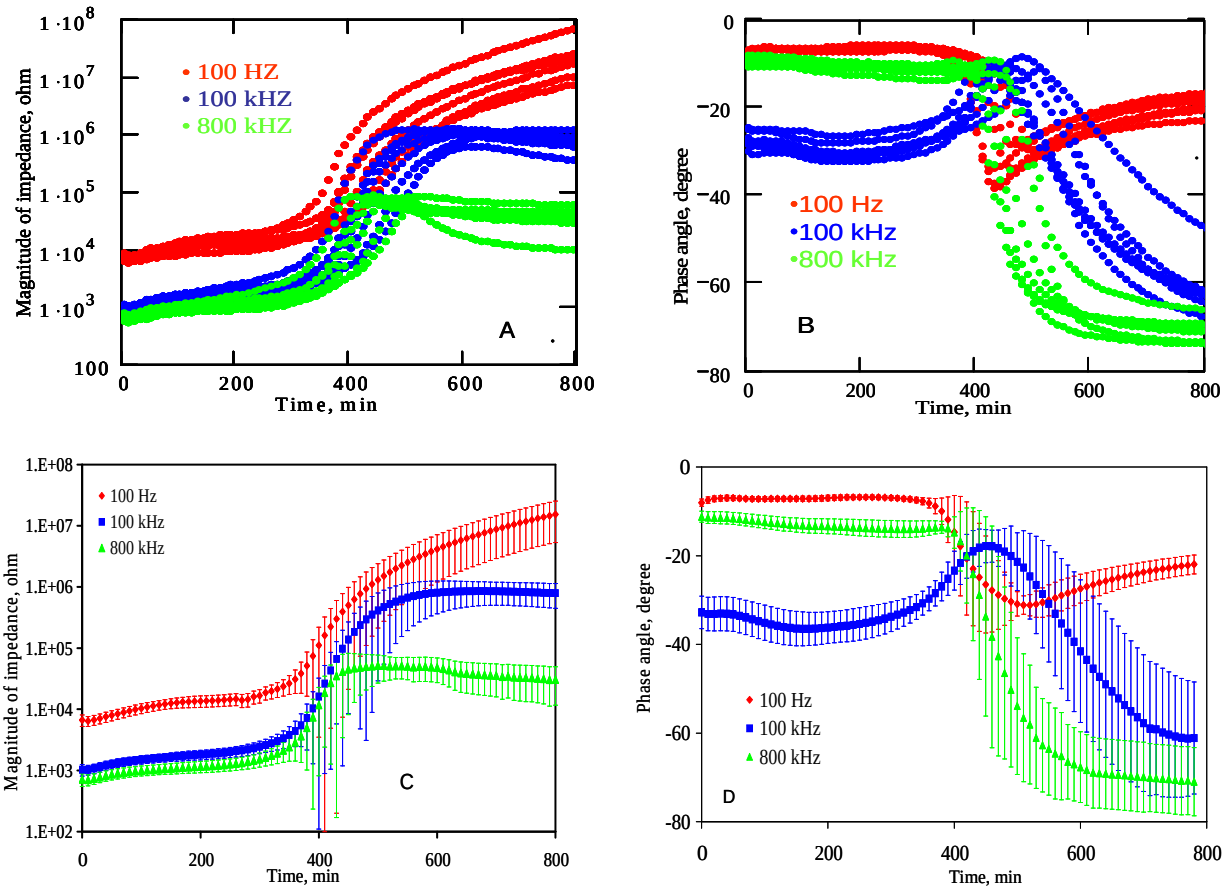


Figure 41. Impedance spectra A) Magnitude of impedance B) Phase angle of the seven repetition measurements in apple slices as a function of drying time at 100 Hz (♦), 100 kHz (□), and 800 kHz (▲) and the average and the standard deviation of the magnitude (C) and the phase angle (D) of impedance for the seven measurements without mass correction.

Points in Figure 42A and 42B are the average of seven independent measurements. The standard deviation of the measurements is also indicated. The magnitude of the impedance at frequencies of 100 Hz, 100 kHz, and 800 kHz had an initial relatively quick increasing period (Figure 42A,) in the slices punctured with electrodes at the beginning of drying (in the first 100 min) and placed into the air-oven. This supposed to cause by the warming up effect of the slice and the electrode (Mészáros et al. 2003). Figure 35. is also indicate this quick temperature increase

(from about 25 °C till 40 °C) in the apple slice during the first 100 minutes. The warming up effect does not appear for the samples measured by method II (Figure 42 C) because these samples were measured at room temperature. This quick increase was followed by a slower one from 80-100 min. until 400 min. drying time. At about 400 min. drying there was a drastic rise (two orders) in the magnitude of the impedance, and after about 480 min. the impedance value at 100 Hz rose again, and the impedance values at 100 kHz remained nearly constant and at 800 kHz it is start to decreasing slowly. The second falling-rate period appeared at about 480 minutes, as can be observed on Figures 36-37. The impedance values at 100 Hz and 800 kHz (100 kHz not shown on Figure 42C because of the perspicuity) for the apple slices punctured with electrodes after drying and removal from the air-oven varied similarly with drying time (Figure 42C). In Figures 42C and 41D, each point (166 sample obtained in six independent measurement) was measured in a different slice that was dried for different time periods. The considerable spreading of the points can be explained by different distortions of slices during the drying and by different db moisture content as a consequence of uneven drying. The transition – the quickly increasing - period for slices punctured with electrodes after removing from oven was observable at about 400 min. drying time, same time than for samples dried together with electrodes.

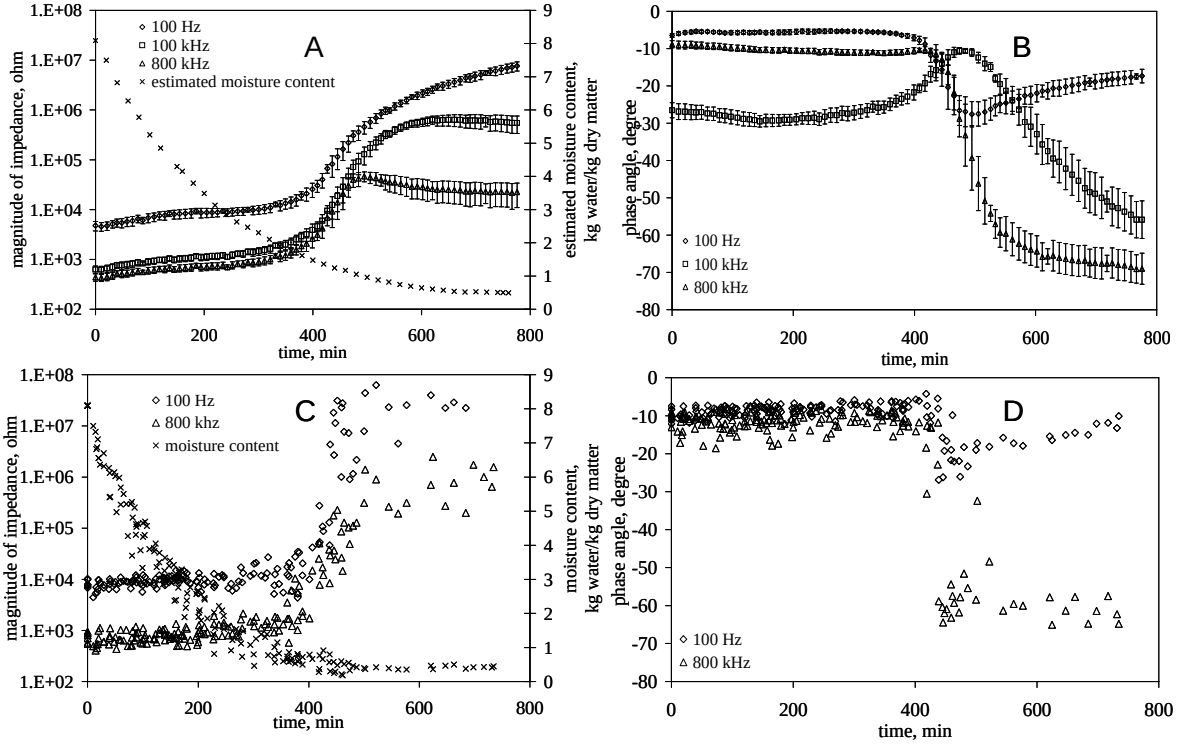


Figure 42. The magnitude (A&C) and the phase angle (B&D) of impedance, and db moisture content in apple slices as a function of drying time at 100 Hz (♦), 100 kHz (□), and 800 kHz (▲). Comments: In Figures 42A and B, the average and the standard deviation of the magnitude (A) and the phase angle (B) of impedance of seven measurements can be seen (electrodes were inserted into the sample at the beginning of drying—method I), measurement was corrected by the mass; and in Figures 42C and D, each point was measured in a different slice (electrodes were inserted into the sample before impedance measurement—method II).

In Figure 42A the estimated db moisture content shows the moisture at the different periods of drying. It is estimated because the impedance measurement was performed in another slice of apple, but the drying procedure for this slice was the same. In apple slices dried with electrodes inserted, the phase angle at 100 Hz was practically constant for the first 400 minutes of drying. Between 400 and 480 minutes drying time, there was a sharp decrease in phase angle (from -10° to -30°), and after that the phase angle increased slowly till-20o (Figure 42B). At 800 kHz similar changes of phase angle took place during the drying period, but the decrease was much more considerable: from – 8° to – 70°. At 100 kHz the phase angle increased slowly in the first period from -30o to -10o and in the second period it started to drastically decrease till -60o. In the slices dried without electrodes and punctured after a given drying time, the phase angles' change as a function of time was the same as in apple samples that were dried together with electrodes (Figure 42D). The db moisture content of the samples shows the same effect as Figure 42A. Two periods of drying can be separated.

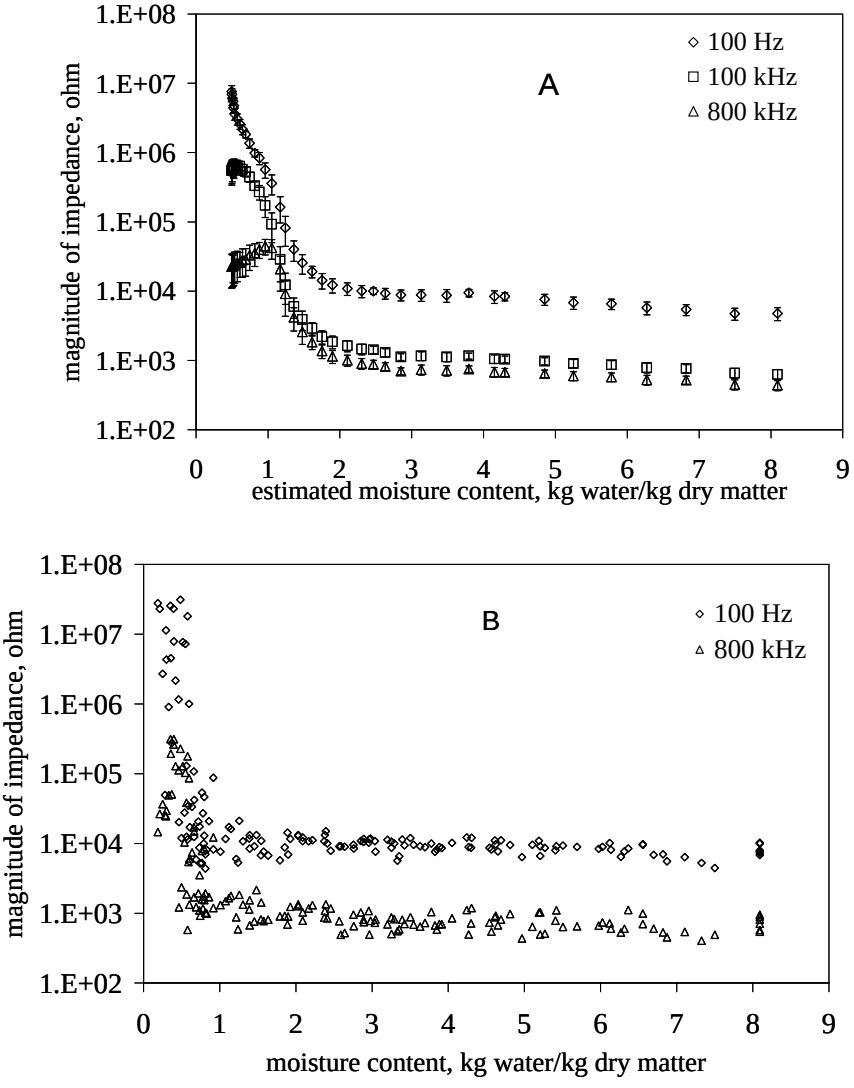


Figure 43. Dry basis moisture content versus magnitude of impedance. A) Method I. B) Method II

Figure 43 A shows the average and the standard deviation of the magnitude of impedance of seven measurements (electrodes were inserted into the sample at the beginning of drying—method I) versus estimated db moisture content, and in Figure 43B, each point was measured in a different slice (electrodes were inserted into the sample before impedance measurement—method II). Figure 43A show relatively slow changes from 8.1 kg water/kg dry matter until 2 kg water/kg dry matter, below 2 kg water/kg dry matter, the magnitude of impedance is increasing sharper until about 1 kg water/kg dry matter content. A breakpoint appears in the magnitude of impedance at 1 kg water/kg dry matter content. Below this point the magnitude of impedance is increasing rapidly at 100 Hz, became practically constant (about 0.6 M-ohm) at 100 kHz and start to decrease slowly at 800 kHz. In Figure 43B the slow increasing of the moisture content can bee seen till about 1 kg water/ kg dry matter at all (100 kHz not shown because of the perspicuity) frequency. Changes between 2 and 1 kg water/dry matter is not as sharp as on Figure 43A. After the breakpoint at about 1 kg water/ kg dry matter the same effects can be observed in the magnitude of impedance as on Figure 43A. In both cases (A and B) the 100 Hz spectra show the highest impedance values and the biggest changes in magnitude (3 orders of magnitude). We supposed that the end of the first falling-rate period and the beginning of the second falling-rate period appeared at about 1 kg water/kg dry matter moisture content at 50 °C in an air-oven. This result is consistent with Sacilik and Elicin (2005) results.

## 7.12. Modeling of impedance spectra

The impedance spectra for the seven times measured apple slices by method I and for the 166 individual apple slices measured by the method II were approximated with the expression (Equation *39 – page 55*) and the parameters were evaluated. Figure 44A and 44B present the measured impedance values and estimated impedance spectrum in a Wessel diagram (positive imaginary values can be seen on these figures). In the initial warming up period (80-100 min. drying time) and in the first falling-rate period (until about 400 min. drying time) there was only one circular arc and a straight line (constant-phase section) (Figure 44A). The evaluated parameters in the case of method I were averaged. The standard deviation of the seven measurements is also indicated. The time axis was mass corrected as in Figure 42 A, B. After 400 min. the chord-length ($R_{inf1}$ *minus* $R_{o1}$) of this first circular arc increased so quickly that the straight line section disappeared, a small part of the first circular arc remained observable in the frequency range of our measurements, and after 480 min., a second circular arc appeared (Figure 44B) at higher frequencies. Model parameters changed the same way as the impedance parameters.

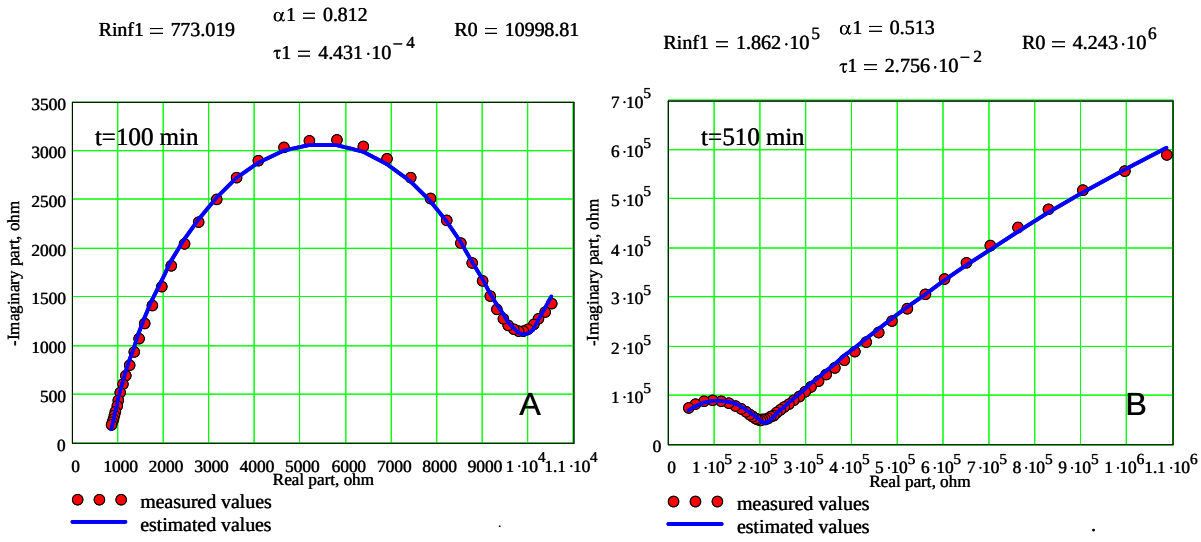


Figure 44. Measured impedance values and fitted model (by Equation 39) for an apple slice A) after 100 minutes drying and B) after 510 minutes drying

The first circular arc represents the impedance of cells separated with membranes (Grimnes and Martinsen 2000, Kuang and Nelson 1998). This biological system is one of the examples of the Maxwell-Wagner effect (Kuang and Nelson 1998) that occurs at the interface of two dielectrics: apoplasmic and symplasmic parts own different dielectric constants. The $R_{o1}$ resistance gives the resistance of the intercellular (apoplasmic) part and $R_{inf1}$ is the parallel resultant of intercellular and intracellular (symplasmic) parts' resistances when the membrane impedance at "infinitely" high frequency can be neglected (Toyoda and Tsenkova 1998).

The second impedance arc probably can be due to the rotation of biological molecules (Grant et al. 1978). In living tissues with high water content, the frequency range characteristic of the rotation of macromolecules is higher than 1 MHz (Grimnes and Martinsen 2000), but in dried (db moisture content lower than 1 kg water/kg dry matter) tissues the rotation frequencies can decrease below 1 MHz because of increasing frictional forces.

"Zero frequency" and "infinite frequency" refer to a frequency ranges that are low enough and high enough, respectively, that the relaxation mechanism in question does not affect impedance characteristics. Resistance $R_{inf1}$ increased continuously and slowly in the first falling-rate period of drying (Figure 45A) in the apple slice contained the electrodes during the whole drying time. This continuous increase can be explained by the continuous transport of water from the inside of cells across the membrane in the first falling-rate period. This concept is supported by electron microscopic images illustrating the shrinking of apple cells (Lengyel et al. 1999). In the first falling-rate period, there were no changes in the shapes of cells; only the size of cells decreased. In the second falling-rate period, the value of $R_{inf1}$ sharply increased, showing the

disappearance of free water from the intracellular part (Figure 45A). On the electron microscopic images in this phase of drying, considerably shrunken cells can be observed.

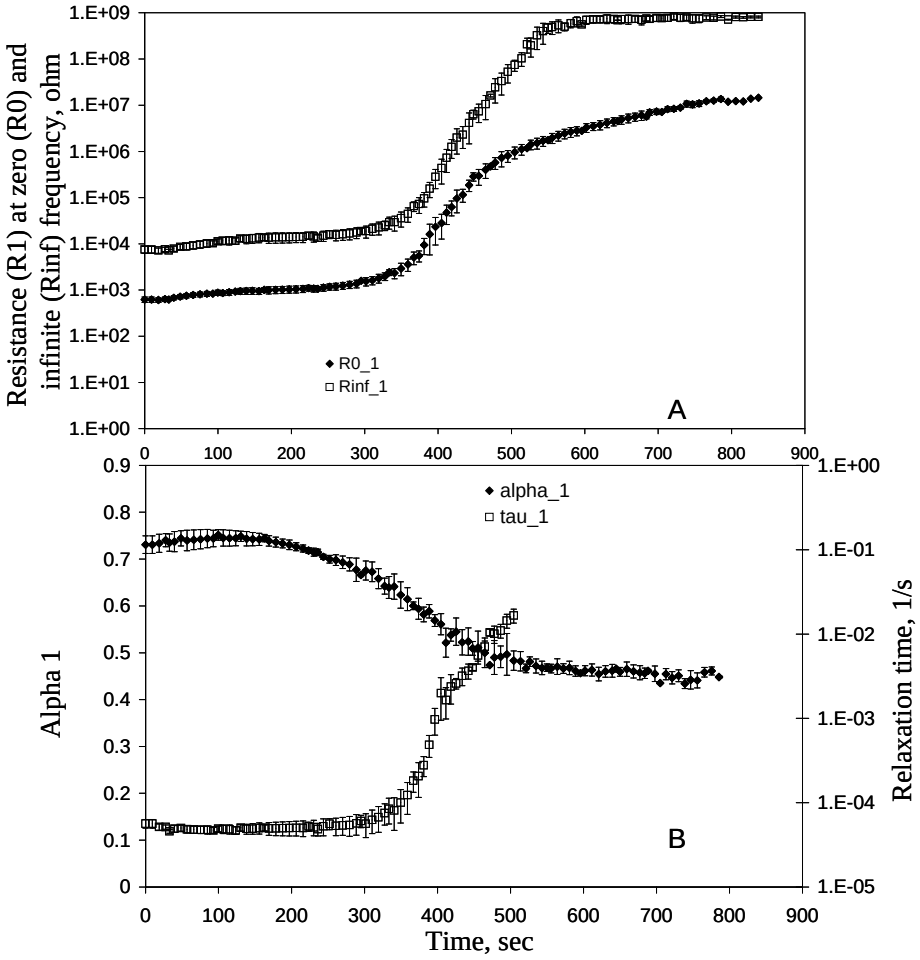


Figure 45 The values of $R_{inf1}$ (A: □), $R_{o1}$ (A: ♦), $\tau_1$ (B:□), and $\alpha_1$ (B: ♦) parameters as a function of drying time for apple slices dried with inserted electrodes. (Electrodes were inserted into the sample at the beginning of drying—method I.)

The $R_{o1}$ resistance also showed a slight increase in the first falling-rate drying period and a significant increase in the second falling-rate period (Figure 45A). The changes in the rates of increase of both $R_{inf1}$ and $R_{o1}$ occur at the practically the same drying time, at about 400 min. This observation can indicate the simultaneity of disappearance of free water from both apoplasmic and symplasmic parts of drying tissue.

The $R_{o1}$ and $R_{inf1}$ values for the samples that were dried without electrodes (and punctured immediately before the impedance measurement) changed as a function of both drying time and db moisture content in the same manner as for the samples dried with electrodes (Figure 46A). The sharp increase in $R_{o1}$ and $R_{inf1}$ values denoted the beginning of the second falling-rate period of drying (at about 1 kg water/kg dry matter).

The parameter $\tau_1$, ($\tau_1 = \frac{1}{2 \cdot \pi \cdot centerFreq.}$) where the centerFreq. is the frequency (interpolated) that is associated with the maximum (most reactance) point on the first arc, in samples dried with and

without electrodes remained almost constant in the first falling-rate period and increased considerably in the second falling-rate period (Figures 45B and 46B). When the free water disappeared from apple slices, the relaxation times increased for different polarizable groups that caused the impedance of first circle arc (Grimnes and Martinsen 2000). The $\tau_1$ parameter can be predicted till about 510 minutes, after this time the model was not able (there is not enough measured data point) to predict (interpolate) the center frequency. The $\tau_1$ parameter change drastically and increase two magnitudes at 1 kg water/kg dry matter in Figure 46B for the samples that were dried without electrodes (and punctured immediately before the impedance measurement). The decrease of the $\alpha_1$ parameter of samples dried in two different ways (Figures 45B and 46B) in the second falling-rate period can be explained by the assumption that the distribution curve of the $\tau_1$ relaxation time became wider as a consequence of a disorderly dried structure. Altough it is possible to give some biological meaning to these model parameters and the drying of apple slice can be followed by these parameters, it would be necessary to compare this relatively simple model with more complex, but commonly used models, which could offer more information about the biological meanings.

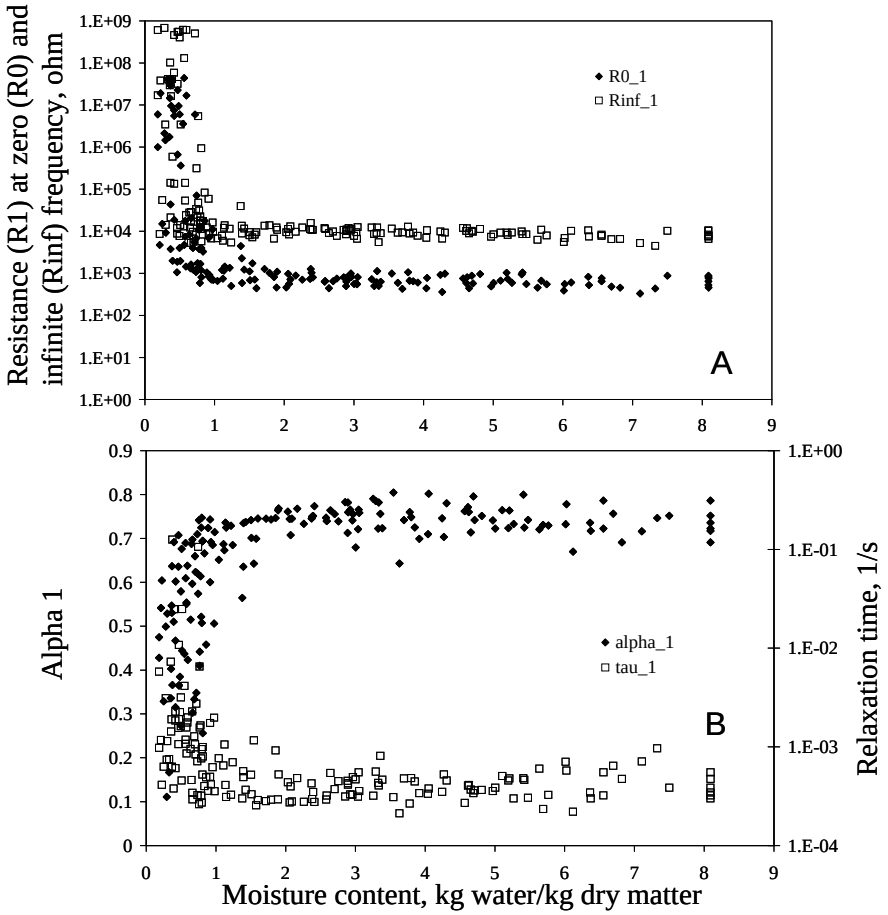


Figure 46. The values of $R_{inf1}$ (A: □), $R_{o1,}$(A: ♦) $\tau_1$ (B:□) and $\alpha_1$ (B: ♦) parameters in the function of db moisture content, each point was evaluated from spectrum measured in different slices (electrodes were inserted into the sample before impedance measurement—method II).

## 7.13. New scientific results

1. In the first generation of Unified Algorithm (4887 dielectric and air-oven tests) the number of grain groups was reduced from 15 to 13. The $5^{th}$ order polynomial was found as the best choice (among $3^{rd}$, $4^{th}$, $5^{th}$, and $6^{th}$ order polynomial equations) for the calibration curve because of practical reasons and by the graphical and numerical statistical analysis. The overall calibration error (standard deviation of differences with respect to reference wb moisture values) with the first generation of unifying parameters for 4887 data points and the $5^{th}$ order polynomial calibration equation was 0.349 percent wb moisture. New methods were developed with the same data set to calculate unifying parameters (SP and OP). This method became the second generation of Unified Algorithm. A fifth-order polynomial calibration curve was fitted, as in the first generation of Unified Algorithm. These new methods reduced the overall calibration error to 0.3066 percent wb moisture.
2. A new algorithm was developed in the third generation of Unified Algorithm, where the original (4887) data set was extended to 5141 dielectric and air-oven tests. In this algorithm, the cubic spline interpolation (instead of the interpolation of the offset and translation parameters as in the second generation of Unified Algorithm) was used to determine unifying parameters and fit new grain types into the calibration. The overall calibration error with this method and these data was 0.308 percent wb moisture. This new approach to developing unifying parameters greatly simplified the process of developing unifying parameters for additional grain types in the future.
3. Temperature correction of dielectric grain moisture measurements (earlier was considered independent regarding the grain moisture content) was found to be dependent upon grain moisture content. A linear moisture-dependent temperature correction provided less moisture error (as concluded from the residual slope and moisture values) in the 0-30 °C temperature range than the moisture-independent function, but the linear moisture- and quadratic temperature-dependent form presented most accurate moisture measurement at temperature extremes (below 0 °C and above 30 °C).
4. Temperature tests at low and high frequencies have demonstrated that the dielectric method can be used successfully for grain moisture measurements of diverse grain types at temperatures well below zero Celsius if the grain wb moisture content is below certain threshold grain-specific values (10-20%). This threshold is appearing where the free water is frozen in the grains. The high-moisture limits were estimated (for moisture measurement below zero Celsius) for several major grain types (soft wheat 17% wb, autumn barley >19% wb, oats 17% wb, sunflower 10% wb, soybean 19% wb, and rapeseed 10% wb).
5. Models were developed to predict unifying parameters and temperature correction coefficients from chemical and physical parameters of grains. The Slope parameters and the moisture-

independent temperature correction coefficients were predicted with sufficient precision. Multiple correlation coefficients with cross validation for the Slope parameter was 0.994 and for Ktc parameter was 0.9.

6. Magnitude and phase angle of electrical impedance can be used to distinguish the periods of drying of apple slices. No constant-rate period and only two falling-rate periods were observed by the traditional weighing method (confirming previous reports in the literature) and with electrical impedance parameters. With both methods, the end of the first falling-rate period and the beginning of the second falling-rate period appeared when the db moisture content was about 1 kg water/kg dry matter in the apple slice.
7. Sample mass correction of apple slices on the drying time could reduce significantly the standard deviation (which was due to the different sample volume) between repeated impedance measurements.
8. Each impedance spectra measured by Method I and II was modeled by one or two distributed (Cole) elements and a Constant-Phase element. The $R_0$, $R_{inf}$, $\alpha$ and $\tau$ parameters were evaluated. (The $R_o$ is the resistance at zero frequency, $R_{inf}$ is the resistance at “infinitely” high frequency, $\tau$ is the relaxation frequency and $\alpha$ parameter describe the distribution of relaxation time ) (page 54-55. equation 39. figure 16) . I found that the $R_o$ and $R_{inf}$, $\alpha$ and $\tau$ values can be used as indicators for the different periods of drying.

## 7.13. Új Tudományos Eredmények

9. A rádió frekvenciás dielektromos gabona nedvesség mérő műszer első generációs egyesített algoritmusában a termény csoportok számát 15-ről 13-ra csökkentettem. A grafikus és numerikus statisztikai elemzések és gyakorlati érvek alapján az ötöd fokú polinomot találtam a legmegfelelőbb (harmad, negyed, ötöd és hatod fokú polinomok közül) kalibrációs görbének. Az első generációs egyesítő paraméterekkel 4887 mérésre az ötöd fokú polinom kalibrációs egyenlettel a kalibráció összes hibája (szórás különbségek a referencia nedvesség tartalomra vonatkozólag) 0.349 % nedves bázisú nedvesség tartalom. Ugyan erre az adathalmazra új módszereket fejlesztettem az egyesítő paraméterek (SP, OP) számolására ez lett a második generációs Egyesített Algoritmus. Az első generációs algoritmusnak megfelelően ötöd fokú kalibrációs görbét illesztettem. Az új módszerekkel a kalibráció összes hibája 0.3066 % nedves bázisú nedvesség tartalomra csökkent.
10. A harmadik generációs Egyesített Algoritmus fejlesztése során a korábbi 4887 adat dielektromos és szárítószekrényes 5141 mérésre bővült. Ebben az algoritmusban a köbös-spline interpolációt (a második generációs algoritmusban alkalmazott Offset és Translation paraméterek folyamatos iteratív meghatározása helyett) alkalmaztam az egyesítő paraméterek meghatározására és az új termény fajták és csoportok kalibrációba illesztésére. A módszer összes kalibrációs hibája 0.308-ra változott, ami az adatok számának növekedésével magyarázható.
11. Megállapítottam, hogy a dielektromos gabona nedvesség mérés hőmérséklet korrekciója függ a termény nedvességtartalmától (korábban nedvesség tartalomtól független hőmérséklet korrekciót alkalmaztak a dielektromos gabona nedvesség mérő műszereknél). A lineáris nedvesség függő hőmérséklet korrekció hibája (dielektromos mérésekből származtatott hőmérséklettel korrigált nedvesség tartalom és a referencia szárítószekrényes nedvesség tartalom különbsége) 0-30 °C tartományban kisebb volt, mint a nedvesség független hőmérséklet korrekció hibája. Az extrém hőmérséklet tartományban (-25-0 °C és 30-50 °C között) a lineáris nedvesség és négyzetes hőmérsékletfüggő hőmérséklet korrekció volt a legoptimálisabb.
12. Megállapítottam, hogy a dielektromos módszer alacsony (1-20 MHz) és nagy frekvencián (149 MHz) egyaránt alkalmazható a termény nedvesség tartalmának mérésére 0 °C alatt, ha a termény nedvesség tartalma egy bizonyos határérték alatt van. Az adott terményben, ha ennél a küszöbértéknél nagyobb a nedvességtartalom, akkor már annyi szabad víz halmozódik fel, amely megfagyva, már befolyásolja a dielektromos mérést. Ez a határérték búzánál 17%,

árpánál >19%, zabnál 17%, napraforgónál 10%, szójánál 19% és repcénél 10% nedves bázisú nedvesség tartalomnál jelentkezik.

13. A terméynek fizikai és kémiai tulajdonságaiból a többváltozós lineáris regresszió segítségével meghatároztam az egyesítő paramétereket és a hőmérséklet korrekciós tényezőket. A Slope paramétert és a nedvesség tartalomtól független hőmérséklet korrekciós tényezőt sikerült elegendő pontossággal meghatározni. A többváltozós korrelációs tényező a kereszt validállás során a Slope paraméterre 0.994 a nedvesség tartalomtól független hőmérséklet korrekciós tényezőre 0.9 adott.
14. Megállapítottam, hogy az impedancia nagysága és fázis szöge alkalmas az almaszeletek száradási szakaszainak megkülönböztetésére. Mind az elektromos impedancia paraméterekkel, mind a hagyományos tömeg mérés módszerével az alma szeletek száradása során állandó száradási szakaszt nem, csak két csökkenő sebességű száradási szakaszt figyeltem meg (megerősítve más kutatók eredményeit). Mindkét módszernél az első szakasz vége és a második szakasz kezdete hozzávetőlegesen 1 kg víz/kg szárazanyag nedvesség tartalomnál jelentkezett az alma szeletben.
15. A különböző alma szeletek száradási idejét egységnyi tömegű alma szeletre korrigáltam, ezáltal a mért impedancia paraméterek szórása csökkent.
16. Az I. és II. Módszerrel mért impedancia spektrumokat elektromos modellel közelítettem (egyenlet 1. ábra 1.). Meghatároztam az $R_0$, $R_{inf}$, $\alpha$ és $\tau$ paramétereket. Megállapítottam, hogy az $R_{01}$, $R_{inf1}$, $\alpha_1$ és $\tau_1$ paraméterek alkalmazhatóak a szárítás szakaszainak jelzésére.

# 8. CONCLUSIONS

The unified calibration database has increased year by year (in 2001 only 2714 tests, 2002-2004 4887 tests, in 2005 already 5141 tests), with new dielectric and air-oven test results and with new calibration data measured by USDA-GIPSA.

The Unified Grain Moisture Algorithm was improved in a few steps (generations) and the unifying parameters were optimized at the Corvinus University of Budapest, Physics and Control Department. In the first, second and third generation of unified algorithm more new grain types were inserted (all together 5141 tests). These methods were optimized and some new techniques were introduced to reduce the calibration error.

In the first generation of unified algorithm, we reduced the number of grain groups from 15 to 13. Confectionary sunflower was grouped with oil-type sunflower seed and durum wheat was grouped with rice based on similar unifying parameters. The order of the fitted calibration equation was examined. It was found that the $5^{th}$ order polynomial calibration curve is better, because of practical and statistical reasons, than the original $4^{th}$ order polynomial.

In the second generation of unified algorithm a new approach was developed for defining the unifying parameters. Instead of selecting a separate target density for density-correcting the samples in each grain group a single target density (approximately the average for all samples tested) was used for density-correcting all grain samples of all groups. The second generation method required iteratively optimizing the offset parameter OP and the translation parameter TP for each grain type and the fifth-order polynomial equation for all grain types together each time a new grain type was added.

In the third generation a new method (cubic-spline interpolation) was introduced. In this method, the $5^{th}$ order calibration curve shape was fixed and the curve of the additional grain types (calculated from the air-oven wb moisture content) was adjusted to match the existing standard curve shape. This process provided a much simpler, more precise, and less iterative way of determining the unifying parameters for the Unified Grain Moisture Algorithm. The possibility of producing accurate calibrations quickly and with minimal cost makes the UGMA an attractive alternative for meeting the needs of domestic and international trade in emerging types of special crops.

The dielectric method at low (1-20 MHz) and high (149 MHz) frequencies can be used successfully for grain moisture measurements for diverse grain types at temperatures well below zero Celsius (till -25°C)—if the grain wb moisture content is below certain grain-dependent threshold (10-20%) values. These high-moisture limits were estimated for several major Hungarian grain types (soft wheat, autumn barley, oats, soybean, sunflower seed and rapeseed). Optimum

temperature correction coefficients were determined for grain samples at different wb moisture levels (5-30%) and different measurement frequencies (2, 20 and 149MHz).

The temperature corrections needed at VHF are generally smaller than at lower frequencies—especially at higher moisture contents (>20% wb). This reduces the moisture measurement errors caused by temperature measurement error (thus making temperature measurement less critical) for VHF moisture tests as compared to moisture measurements at lower frequencies.

A moisture-dependent temperature correction function was found to be much more effective than a simple moisture-independent function for the Unified Grain Moisture Algorithm. Linear moisture- dependent and a linear moisture- and quadratic temperature-dependent temperature correction functions were found to be more effective than a simple moisture-independent function—especially below zero degrees Celsius. It was found that the residual slope values are smaller with the moisture-dependent temperature correction than with the moisture-independent temperature correction.

Models were developed to predict unifying parameters and temperature correction coefficients (for the Unified Grain Moisture Algorithm) from grain chemical and physical parameters. The Slope parameters and the moisture-independent temperature correction coefficients were predicted with sufficient precision to be useful for some applications. The Offset and Translation parameters and the temperature correction coefficients for moisture-dependent temperature correction functions were not modeled successfully.

The capability to model the Slope parameter ($R^2$=0.998) would mean that new grain types could be added to the Unified Grain Moisture Algorithm without the need to test samples over wide moisture ranges. The Offset parameter could be determined relatively easily by measuring a small number of samples over a limited moisture range. The Translation parameter is not critical unless high accuracy at very low wb moisture levels is important for the grain type.

The capability to predict the moisture-independent temperature correction coefficient (Ktc) is similarly important because approximate temperature correction factors could be estimated for new grain types without performing time- and labor-intensive grain temperature tests. For grain types of major economic significance, more precise (better than $R^2$=0.988) estimates of the moisture-independent correction factor or coefficients for the more effective temperature correction functions (like moisture-dependent functions) could be achieved through grain tests.

The phase angle spectra of electrical impedance, measured at 31Hz to 1MHz frequency region in one apple (approximately 20x20x10 mm) sample with different electrode distance, was found suitable to determine the inner state of the sample, or the moisture distribution in the sample. In the case of apple drying, the drying curve was divided into two falling-rate periods that could be

approximated with two exponential functions. The breakpoint between the two falling-rate periods was found at about 1 kg water per kg dry matter. This db moisture content was reached after approximately 480 minutes of drying time for about 20 mm x 20 mm x 10 mm apple slices in a 50 °C air-oven. A correction with the sample mass of the apple slices can reduce the differences of the impedance parameters when the impedance measurement is repeated. During the first falling-rate drying period, the magnitude of impedance showed a relatively slow change while the db moisture content decreased from 8.1 kg water per kg dry matter to 1 kg water per kg dry matter. Below 1 kg water per kg dry matter moisture content, the magnitude of impedance changed sharply until the db moisture content reached 0.49 kg water per kg dry matter content, which could be the equilibrium db moisture content for an approximately 20x20x10 mm apple slice drying in the 50 °C air-oven. The evaluated $R_{o1}$, $R_{inf1}$, $\alpha$ and $\tau_1$ impedance parameters changed very slowly in the first period and drastically in the second period of drying. The rate of the parameter changes could be used for detecting the different periods of drying. A second impedance arc after about 480 minutes drying – probably characterizing the low rotation rate of macromolecules in dried samples – appeared at the beginning of the second falling-rate period.

## 8.1. Further research

Insert new grain classes or (and) grain types to the UGMA calibration and refine the unifying parameters.

More dielectric measurement at different temperatures are needed at low moisture levels (<8% wb) and high moisture (>25% wb) levels to confirm that a linear moisture-dependent and quadratic temperature-dependent correction is the optimum temperature correction function for the Unified Grain Moisture Algorithm and to establish the correction coefficients more precisely. Similar tests are needed to determine correction coefficients for additional grain types. Further temperature tests on low (<8% wb) and high (>25% wb) moisture content samples also needed in the low frequency range to examine whether the moisture-dependent temperature correction is also applicable in this frequency range. Some further temperature tests are needed in low (1-20 MHz) and high (149 MHz) frequency range to predict the moisture threshold limit more precisely below zero degrees Celsius.

Collect more physical and chemical properties for other grain types and over wider moisture ranges to develop more precise models for predicting unifying parameters and temperature correction coefficients from the grain physical and chemical properties.

Further work is needed to develop a non-destructive method to measure the impedance spectra (on-line and off-line) of the apple slices and other fruit and vegetables during drying.

Evaluate other electrical fitted models for the impedance spectra of the drying apple slices to get more information about the physical, biological, and electrical changes in the apple tissue during drying. Compare other electrical fitted models with the Cole-Cole model.

Determine the dielectric constant and loss during the drying of apple slices at low frequencies.

Further electrical impedance measurements are necessary (especially in the second falling-rate period) to develop a function for impedance parameter versus db moisture content of apple slices during drying.

# 9. SUMMARY

Electrical properties of food products have generally been of interest for two reasons. One relates to the possibility of using the electrical properties as a means for determining moisture content or some other quality factors (seed viability, fruit maturity, egg quality, lactose content) (Nelson 1984). The other has to do with the absorption of energy in high-frequency dielectric heating or microwave heating applications useful in the processing of food materials (Brown et al 1947, Szabó 1998, 2003).

Investigations of the dielectric properties of different agricultural products, grains, and foods stretch back more than a half-century (Debye and Hückel 1923, Nelson 1973, Sembery et al. 1999). The huge number of publications in dielectric spectroscopy indicates the great interest regarding dielectric properties. Considering the different kinds of basic material, the wide range of the measurement frequencies, and the effects of influential factors (moisture content, temperature, bulk density, oil content, protein content, etc.) the numbers of the necessary measurements are inexhaustible.

The $P_2O_5$ and Karl Fischer methods provide the most accurate results for moisture content but they are time consuming and require special apparatus, ground grain samples and different chemicals (Iod, $SO_2$, Pyridine). The air-oven method is the most common reference method for grain moisture determinations, but most air-oven methods require hours or days to complete. Clearly, grain producers, handlers, and processors need much more rapid methods to assess moisture content (Funk 2001).

Many different technologies have been tried for rapid grain moisture measurement (Near-infrared method, Conductivity method, Microwave method, Radio-frequency dielectric method). Rapid indirect methods all measure some physical parameters (by electrical or optical sensing) and predict moisture content with calibration equations or charts. During the past fifty years, dielectric grain moisture measurements have developed significantly. During the past fifty years, dielectric grain moisture meters have developed significantly, with many new models introduced and used world-wide (Examples include: Perten (Aquamatic 5100), Dickey-john (GAC 2100), Kett (PB-3010, Waddy PV-100, PT-2300), Seedburo (Model 1200A) and many others). Different type moisture meters have different precision in measuring grain moisture content. In grain trading there are strict rules about rapid moisture measurements in the U.S.A. and in the E.U.

Research collaboration between USDA-GIPSA and USDA-Agricultural Research Service (Athens, GA) over the period of 1995 to 2001 resulted in an improved RF dielectric moisture measuring method that effectively combines many diverse grain types and classes calibration into a single “unified calibration.” The unified calibration method increased year by year, with new

dielectric and air-oven test results and with new calibration data. GIPSA has been supporting continuing research at Corvinus University of Budapest, Faculty of Food Science Physics and Control Department for the purpose of developing methods for optimizing the necessary unifying parameters and developing methods that make the calibration process easier in the future for those grain types or classes which have not yet been fit in the calibration.

Another important question and problem is the temperature correction of dielectric moisture meters. Temperature has a significant effect on the dielectric parameters (Nelson 1984, Sembery 2002, Lawrence 1989). Nowadays most grain dielectric moisture meter manufacturer use a linear temperature correction (percent moisture per degree Celsius) and the equipment can measure in the region of 0-45 °C, but the recommendation of the manufacturers is to use the grain moisture meter close to room temperature because the equipment is the most accurate in that region (Wallis 2006). Since some types of grain are sometimes harvested during cold weather (below 0 °C), the grains may be very cold when harvested. Storage in very cold weather (with or without prior drying) during winter may also cause the grains temperature to be very low (sometimes less than -10, -15 °C) when the grain is removed from storage for sale. In other cases, grains may be harvested at high temperatures (above 30 °C) and taken directly to market. Grain is also very warm at the output of grain dryers. Waiting for grain to equilibrate to near room temperature to obtain accurate moisture measurements causes unacceptable delays in handling. Therefore, it is very desirable to be able to make accurate moisture measurements on grain that is very warm or very cold—even below the freezing point of water.

Electrical properties are able to follow the changes in the moisture content, and they are able to indicate the changes of inner structure of foods and agricultural products (Nelson 1973). One of the most important fruits in Hungary is apple, which contain about 85-89% wet-basis moisture (Mohsenin 1980, Sass and Horn 1974). Changes of this relatively high moisture content during the drying process can be followed by weighing, or, since dielectric parameters are successfully used to predict moisture content in many agricultural materials, it is supposed that electrical impedance parameters are also suitable to follow a drying process. (Vozáry and Horváth 1998).

The aims of this study were to measure the electrical properties of different kinds of agricultural products.

Improving and optimizing a VHF dielectric grain moisture meter and its calibration was also an important task. This involved:

- Developing temperature corrections at low (1-20 MHz) and at high (149 MHz) frequency for some major Hungarian grain type (soft wheat, autumn barley, oats, sunflower, soybean, rapeseed).

- Determining the moisture limits at low and high frequency dielectric measurements, where the free water has frozen in the sample.
- Predicting Unifying Parameters (Slope, Offset, Translation, moisture-independent and moisture-dependent temperature correction) from grain physical and chemical properties.
- Validating models, which used unifying parameters calculated from grain physical and chemical properties.

Another purpose was to measure the electrical impedance of apple slices during drying, determining the periods of apple drying by the electrical impedance parameters, and comparing it with the traditionally weighing method. This included evaluating the parameters of an electrical model fitted on the measured impedance spectra of apple slices during drying.

For measuring the electrical parameters of grains, oilseeds, and apples at different frequencies, LCR meters (HP 4284A and HP 4285A), a HP-4291A RF Material/Impedance Analyzer, and a special VHF (Very High Frequency) prototype were used. The dielectric properties of grains and oilseeds were obtained with capacitive and transmission line test cells and the electrical impedance spectra of apples were evaluated by pin electrodes.

The Unified Grain Moisture Algorithm was improved in several steps (generations) and the unifying parameters were optimized at the Corvinus University of Budapest, Physics and Control Department. In the first, second and third generation of unified algorithm more new grain types were inserted (all together 5141 test). These methods were optimized and some new techniques were introduced to reduce the calibration error for the expanded set of samples and grain types.

In the first generation of Unified algorithm we reduced the number of grain groups from 15 to 13. Confectionary sunflower was grouped with oil-type sunflower seed and durum wheat was grouped with rice based on similar unifying parameters. The order of the fitted calibration equation was examined. It was found that the $5^{th}$ order polynomial calibration curve is better than the original $4^{th}$ order polynomial.

In the second generation of unified algorithm a new approach was developed for defining the unifying parameters. Instead of selecting a separate target density for density-correcting the samples in each grain group a single target density (approximately the average for all samples tested) was used for density-correcting all grain samples of all groups. The second generation method required iteratively optimizing the offset parameter OP and the translation parameter TP for each grain type and the fifth-order polynomial equation for all grain types together each time a new grain type was added.

In the third generation a new method (cubic-spline interpolation) was introduced. This process provided a much simpler, more precise, and less iterative way of determining the unifying parameters for the Unified Moisture Algorithm. The possibility of producing accurate calibrations

quickly and with minimal cost makes the UGMA an attractive alternative for meeting the needs of domestic and international trade in emerging types of specialty crops as well as high-volume grains.

The dielectric method at low (1-20 MHz) and high (149 MHz) frequencies can be used successfully for grain moisture measurements for diverse grain types at temperatures well below zero Celsius—if the grain moisture content is below certain grain-dependent threshold values (10 - 20%). This suggests that there is "free" water that can be frozen in high moisture grain, but not in low-moisture grain.

Optimum temperature correction coefficients were determined for some major Hungarian grain type (soft wheat, autumn barley, oats, sunflower, soybean, and rapeseed) at different wb moisture levels (5-30%) and different measurement frequencies (2, 20, and 149MHz). The temperature corrections needed at VHF were generally smaller than at lower frequencies—especially at higher moisture contents. This reduces the moisture measurement errors caused by temperature measurement error (thus making temperature measurement less critical) for VHF moisture tests as compared to moisture measurements at lower frequencies.

Linear moisture-dependent temperature correction function and linear moisture-dependent and quadratic temperature-dependent correction were found to be more effective than a simple moisture-independent function—especially below zero degrees Celsius. This information should be very helpful for grain moisture meter manufacturers and for moisture meter users who need to determine grain moisture contents at very cold temperatures to be able to market grain more efficiently.

Models were developed to predict unifying parameters and temperature correction coefficients from grain chemical and physical parameters. The Slope parameters and the moisture-independent temperature correction coefficients were predicted with sufficient precision to be useful for some applications. The Offset and Translation parameters and the temperature correction coefficients for moisture-dependent temperature correction functions were not modeled successfully.

The capability to model the Slope parameter well would mean that new grain types could be added to the Unified Grain Moisture Algorithm without having to test samples over wide moisture ranges (5-30% wb). The Offset parameter could be determined relatively easily by measuring a small number of samples over a limited moisture range (10-20% wb). The Translation parameter is not critical unless high accuracy at very low moisture levels is important for the grain type (<8% wb).

The capability to predict the moisture-independent temperature correction coefficient (Ktc) is similarly important because approximate temperature correction factors could be estimated for new grain types without performing time- and labor- intensive grain temperature tests. For grain

types of major economic significance, more precise estimates of the moisture-independent correction factor or coefficients for the more effective (and complex) temperature correction functions could be achieved through grain tests.

Electrical impedance spectra (phase angle), measured in one apple sample with different electrode distance, was found that suitable to determine the inner state of the sample, and the moisture distribution in the sample. In the case of apple drying, the drying curve was divided into two falling-rate periods that could be approximated with two exponential functions. The breakpoint between the two falling-rate periods was found at about 1 kg water per kg dry matter. This db moisture content was reached after approximately 480 minutes of drying time for about 20 mm x 20 mm x 10 mm apple slices in a 50 °C air-oven. A correction with the sample mass of the apple slices was found to reduce the differences of the impedance parameters when the impedance measurement was repeated. During the first falling-rate drying period, the magnitude of impedance showed a relatively slow change while the moisture content decreased from 8.1 kg water per kg dry matter to 1 kg water per kg dry matter. Below 1 kg water per kg dry matter moisture content, the magnitude of impedance changed sharply until the moisture content reached 0.49 kg water per kg dry matter content, the equilibrium moisture content (in the 50 °C air-oven). The evaluated $R_{o1}$, $R_{inf1}$, $\alpha$ and $\tau_1$ impedance parameters changed very slowly in the first period and drastically in the second period of drying. The rate of the parameter changes also could be used for detecting the different periods of drying. A second impedance arc – probably characterizing the low rotation rate of macromolecules in dried samples – appeared at the beginning of the second falling-rate period.

# 9. ÖSSZEFOGLALÁS

Az élelmiszerek dielektromos paraméterei függnek a nedvesség tartalomtól és a kémiai összetételtől (olaj, fehérje, laktóztartalom, stb). A dielektromos paraméterek ismeretében lehet a nagyfrkvenciás vagy mikrohullámú kezelés, szárítás energiaigényét kiszámítani.

Különböző mezőgazdasági termékek, gabonák és élelmiszerek dielektromos tulajdonságának vizsgálata körülbelül fél évszázadra tekint vissza. A dielektromos spektroszkópia területén eddig napvilágot látott tetemes mennyiségű publikáció jelzi, hogy nagy az érdeklődés a dielektromos tulajdonságok iránt. Tekintettel a különböző alapanyagokra, a széles frekvencia tartományra és a befolyásoló tényezők hatására (nedvesség tartalom, hőmérséklet, sűrűség, olaj tartalom, fehérje tartalom, stb.) a szükséges mérések száma gyakorlatilag végtelen. A nedvesség tartalom mértéke szerepet játszik a különböző mezőgazdasági termékek árának, tárolásuk módjának és egyes feldolgozási módszerének meghatározásában.

A gabona nedvességtartalmának meghatározására, a szárítószekrényes módszer a legáltalánosabb referencia módszer. A legtöbb szárítószekrényes módszer elvégzéséhez órákra esetleg napokra van szükség. A pontos analitikai módszerek, mint a $P_2O_5$ és a Karl-Fischer módszer a nedvességtartalom meghatározására viszonylag időigényesek és emellett még különböző kémiai vegyszereket (jód, $SO_2$ és piridin) is igényelnek. Természetesen a gabonatermesztők, kereskedők és feldolgozók sokkal gyorsabb módszert (módszereket) szeretnének alkalmazni a nedvességtartalom megállapítására (Funk 2001).

A nedvességtartalom mérésére léteznek különböző gyors eljárások (a közeli-infravörös, vezetőképesség, mikrohullámú mérés vagy a rádiófrekvenciás (RF) dielektromos módszer). A gyors indirekt mérések mindegyike valamilyen fizikai (elektromos vagy optikai érzékelés) paramétert mér és ezekből a paraméterekből számítható a nedvesség tartalom kalibrációs egyenletek, diagrammok segítségével (Funk 2001).

Az USDA-GIPSA és az USDA-Agricultural Research Service (Athens, GA) között kötött kutatási együttműködés keretében 1995 és 2000 között kifejlesztettek egy RF dielektromos módszert, amely hatékonyan egyesíti különböző terményekre vonatkozó kalibrációs eljárásokat, egy úgynevezett Egyesített Gabona Nedvesség Algoritmusba. A módszerben a dielektromos permittivitást mérik, és egy többlépcsős kalibrációs eljárás segítségével határozzák meg a nedvességtartalmat. Egy gabona csoportba (pl. búza) különböző gabona fajtákat (őszi, tavaszi, keményszemű vörös őszi, puhaszemű fehér tavaszi búza, stb) helyeznek. Az egyesítő kalibrációs módszer évről évre gyarapodott új dielektromos és szárítószekrényes mérésekkel és kalibrációs adatokkal. A GIPSA műszerekkel és ösztöndíjjal támogatta az egyesítettkalibrációs eljárás fejlesztését a Budapesti Corvinus Egyetem Élelmiszertudományi Karán.

Fontos kérdés és probléma, a hőmérséklet korrekció a dielektromos nedvességtartalom mérőknél, mivel hőmérséklet jelentős hatással van a dielektromos paraméterekre. Jelenleg a dielektromos gabona nedvességtartalom mérőt gyártó cégek lineáris hőmérséklet kalibrációt (%nedvességtartalom/ Celsius fokonként) alkalmaznak, és a műszerek a 0-45 °C tartományban képesek mérni. A gyártók javaslata azonban az, hogy a gabonákat inkább szobahőmérsékleten mérjük, mert a műszer abban a tartományban a legpontosabb.

Mivel néhány terményt néha hideg időben takarítanak be (0 °C fok alatt), illetve a gabona tárolása télen szintén okozhatja, hogy a szemek hőmérséklete alacsony (előfordulhat, hogy kisebb, mint –10, -15 °C fok), amikor eladásra kerül sor. Más esetekben a gabonát nagyon meleg időben aratják (30 °C fok felett) így a gabonaszemek melegen kerülnek a piacra. A gabona szárítása során a magok szintén felmelegedhetnek. Arra várni, hogy a termények szobahőmérsékletűek legyenek, hogy pontos nedvességtartalom mérést végezhessünk rajtuk, elfogadhatatlan időveszteség a kereskedelemben. Ezért nagyon fontos, hogy a termény nedvességtartalmának mérését nagyon hideg (fagypont alatt), vagy meleg szemeknél (30 °C felett) is pontosan elvégezhessük.

Az elektromos tulajdonságok alkalmasak a nedvességtartalom változásának követésére, és alkalmasak arra is hogy jelezzék a belső szerkezeti változásokat az élelmiszer vagy mezőgazdasági termékekben (Nelson 1973).

Az egyik legjelentősebb gyümölcs Magyarországon az alma, amely körülbelül 85-89% nedvességet (nedves bázis) tartalmaz (Mohsenin 1980, Sass és Horn 1974). Egyre elterjedtebb módszer az alma tartósítására a szárítás. Magyarországon új és ízletes termékek a szárított alma chips-ek. A nagy nedvességtartalomnak a változását követhetjük a hagyományos tömegméréssel, illetve feltételezzük, hogy az elektromos impedancia paraméterek is alkalmasak a szárítás követésére (Vozáry és Horváth 1998), azonban szisztematikus impedancia mérést az alma szeletek száradása során még nem végeztek.

A célunk az volt, hogy a különböző mezőgazdasági termények elektromos tulajdonságait mérjük. Fejlesszünk és optimalizáljunk egy nagy frekvencián (149 MHz) működő dielektromos gabona nedvességtartalom mérő műszert és a műszer kalibrációját. Alacsony (1-20 MHz) illetve nagy frekvencián (149MHz) hőmérséklet korrekciós eljárásokat dolgozzunk ki. Meghatározzuk néhány jelentősebb gabonafajtánál és olajos magnál (búza, zab, árpa, repce, napraforgó, szója) alacsony és nagy frekvencián azt a nedvességtartalom küszöbértéket, ahol fagypont alatt a dielektromos módszer már nem alkalmas a nedvességtartalom mérésére. Meghatározzuk a matematikai az összefüggéseket az egyesítő paraméterek, illetve a gabonák és olajmagvak fizikai és kémiai paraméterei között. További célunknak tekintettük, hogy megmérjük a száradó almaszelet impedanciáját. Meghatározzuk az impedancia paraméterek változását a nedvességtartalom

függvényében. A mért spektrumokat elektromos model áramkörökkel közelítsük. A modell paraméterek értékeit meghatározzuk a szárítás során.

A gabonák, olajmagvak és almák elektromos tulajdonságainak méréséhez különböző LCR mérő műszereket (HP-4284A, HP-4285A), HP-4291A RF Material/Impedance Analyzer és egy speciális VHF (Very High Frequency - Nagyon Magas Frekvencia, 30MHz – 300MHz) prototípust alkalmaztam. A gabonák és olajmagvak dielektromos tulajdonságait alacsony frekvencián (1-20 MHz) egy kapacitív, magas frekvencián (149 MHz) egy transzmissziós vonalú tesztcellával, az alma szeleteknél, pedig az elektromos impedancia spektrumokat tű elektródákkal mértem különböző elektróda távolságokkal. Az impedancia spektrumok meghatározásakor két különböző módszert alkalmaztam. Az első módszernél (módszer I) az almaszeletek (hozzávetőlegesen 20x20x10 mm) együtt száradtak az elektródákkal, így az impedancia spektrumokat ugyan abban a szeletben bizonyos (10 perc) időközönként folyamatosan tudtam rögzíteni. A második módszernél (módszer II) több hozzávetőlegesen egyforma (20x20x10 mm) almaszelet száradt egyidejűleg a szárítószekrényben és az impedancia mérés a szeletek tömegének mérése után szobahőmérsékleten történt. Az almaszeleteket 50 oC-on Venticell szárítószekrényben szárítottam (hozzávetőlegesen 800 percig)

Több különböző módszert fejlesztettünk a kalibráció optimalizállására. Ezeket különböző generációkba csoportosítottam. Az első generációs egyesítő algoritmust, amelyet Funk (2001) fejlesztett ki optimalizáltam, azzal a céllal, hogy a kalibráció a legkevesebb termény csoportot tartalmazza, illetve a kalibrációs hiba a legkisebb legyen. Az évek során a USDA-GIPSA-nál újabb több ezer mérést végeztek különböző régebbi és újabb termény csoportokon. Ezeket az adatokat (összesen 5141 dieletromos, szárítószekrényes, tömeg és hőmérsékletmérés) szintén beillesztettem a kalibrációba. Egy második illetve egy harmadik generációs algoritmust fejlesztettem az „egyesítő” paraméterek meghatározására a Unified Grain Moisture Algorithm-hoz (Egyesített Gabona Nedvesség Algoritmushoz). Az eredeti első generációs algoritmus 2714 db mérést tartalmazott és a kalibráció összes szórása 0.29 volt. A második generációs algoritmus 4887 db mérést tartalmazott és a kalibráció összes szórása 0.3066. A harmadik generációs algoritmus 5147 db mérést tartalmazott és a kalibráció összes szórása 0.308. Az Egyesített Gabona Nedvesség Algoritmus előnye a pontossága és alkalmazása jelentősen csökkenti a gabona nevességmérő műszer fejlesztésére és karbantartására fordított időt és a költségeket.

A dielektromos módszer alacsony (1-20 MHz) illetve magas (149 MHz) frekvencián sikeresen alkalmazható nedvesség tartalom meghatározására különféle terményeknél jóval nulla Celsius fok alatt (ha a termény nedvességtartalma nem haladja meg, egy terményenként változó nedvesség határértéket, hozzávetőlegesen 10-20%). Ez a jelenség a szabad víz kifagyásának az

eredménye, amely jelen van a nagy nedvességtartalmú terményekben, de nincs jelen az alacsony nevesség tartományban.

Az optimális hőmérséklet korrekciós tényezőket meghatároztam különböző terményekre (búza, árpa, zab, szója, napraforgó és repce) különböző nedvességtartalomnál (5-30%) és különböző frekvencia tartományban (2, 20 és 149MHz).

VHF, Nagyon Magas Frekvencián a hőmérséklet korrekciós tényezők általában kisebbek, mint az alacsony frekvenciákon –különösen magasabb nedvességtartalomnál, így a nagyon magas frekvencia tartományban kisebb a nedvességtartalom mérésének hibája, amely a hőmérséklet mérés hibájából eredne (ily módon a hőmérséklet mérése kevésbé jelentős tényező) összehasonlítva az alacsony frekvenciás nedvességtartalom mérésével.

Lineáris és a másodfokú nedvességtartalomtól függő hőmérséklet korrekciót jóval hatékonyabbnak találtam (különösen nulla Celsius fok alatt), mint az egyszerű, nedvességtartalomtól független hőmérséklet korrekciót. Ez az információ hasznos lehet a dielektromos gabona nedvességtartalom mérőket gyártóknak, és azoknak a felhasználóknak, akiknek a gabona nedvességtartalmát nagyon hideg hőmérsékleten kell mérniük.

A termények fizikai és kémiai jellemzőiből meghatároztam az egyesítő paramétereket és a hőmérséklet korrekciós tényezőket. A Slope paraméter és a nedvességtartalomtól független hőmérséklet korrekciós tényezőt elfogadható pontossággal tudtam meghatározni. Az Offset és az Translation paramétereket, valamint a nedvességtartalomtól függő hőmérséklet korrekciós tényezőket nem sikerült megfelelő hatékonysággal meghatározni.

Az a lehetőség, hogy a meredekség paramétert kiszámoljuk a termények fizikai vagy kémiai tulajdonságaiból, azt eredményezi, hogy az új terményeknél, az Egyesített Gabona Algoritmusba illesztésnél nem kell a teljes nedvesség tartományban dielektromos és szárítószekrényes méréseket végezni. Az eltoló paramétert viszonylag egyszerűen meg lehet határozni néhány mérésből, szűkebb nedvesség tartományban (10-20%). Az áthelyező paraméter sem jelentős, hacsak nem akarunk nagyobb pontosságot az alacsony nedvesség tartományban (<8%).

Szintén jelentős eredmény, hogy a nedvességtartalomtól független hőmérséklet korrekciós tényezőt a termények fizikai és kémiai paramétereiből határozzuk meg, mivel így a hőmérséklet korrekciós tényezőket új termények esetén meg tudjuk becsülni anélkül, hogy idő és óriási munkaigényes hőmérséklet teszteket végeznénk. A kereskedelemben gyakori terményeknél azonban egy jóval pontosabb nedvességtartalomtól független hőmérséklet korrekcióra, vagy a jóval hatékonyabb (és összetettebb) hőmérséklet korrekciós függvényekre lehet szükség.

Egy almaszeleten különböző elektróda távolságokkal mért impedancia fázisszög értéke alkalmas arra, hogy megkülönböztessük a külső szárazabb és a belső nedvesebb alma szövetet, és így szemléltessük az inhomogén nedvesség eloszlást a száradó mintában. Az alma szárítása során a

száradási görbe két csökkenő száradási sebességű szakaszra osztható, amelyekre exponenciális függvényeket illesztettünk. A két csökkenő száradási sebességű szakasz között 1 kg víz/kg szárazanyag nedvességtartalomnál egy töréspont figyelhető meg.

A különböző méretű almaszeletek impedancia spektrumain az almaszeletek tömegével végzett korrekció csökkentette a szórást. Az első csökkenő szárítási sebességű szakaszban az impedancia nagysága egy viszonylag lassú emelkedést mutatott mialatt az alma szelet nedvességtartalma 8.1 kg víz/kg száraz anyagról 1 kg víz/kg száraz anyagra csökkent. Hirtelen növekedést figyelhettünk meg 1 kg víz/kg szárazanyag nedvességtartalomnál, amíg a nedvességtartalom el nem érte a 0.49 kg víz/kg száraz anyag értéket, ami hozzávetőlegesen az egyensúlyi nedvességtartalomnak felel meg az alma 50 °C fokos szárítása során.

Két különböző módszerrel (módszer I és II) mért impedancia spektrumokat elektromos modellel közelítettem és meghatároztam a modell paramétereit. A két különböző módszerrel kapott eredmények egymásnak megfeleltek. A számolt $R_{o1}$, $R_{inf1}$ ,$\alpha$ és $\tau_1$ impedancia paraméterek szintén lassan változtak ($R_{o1}$, $R_{inf1}$ és $\tau_1$ növekedett, az $\alpha$ csökkent)az első szakaszban és drasztikusan a szárítás második szakaszában. A számított paraméterek segítségével szintén meghatározhatjuk a szárítás különböző szakaszait. A második impedancia körív, ami valószínűleg a makromolekulák gyenge rotációjának mértékét jelzi a száradó mintában, megjelenése jelezte a szárítás második csökkenő száradási sebességű szakaszának kezdetét.

# 10. APPENDIX

## 10.1. References


Algie J. E. (1969): The measurement of regain of wool by electrical capacity-type moisture meters. Part IV: The effect of packing density on the dielectric constant of cones of yarn. *Textile Res. J.*, 39. 213-216. p.

Asher W. C. (1964): Electrical potentials related to reproduction and vigor in slash pine. *Forest Sci.*, 10(1)116-124. p.

Analoge Devices Inc. (2002): AD8302 RF/IF Gain and Phase Detector Available at: http://www.analog.com/UploadedFiles/Data_Sheets/797075782AD8302_a.pdf, Accessed: September 2006

Association of Official Analytical Chemists [1990.]: In Official Methods of Analysis. 15th Edition. Arlington, Virginia

Atungulu G., Nishiyama Y., and Koide S. (2004): Electrode configuration and polarity effects on physiochemical properties of electric field treated apples post harvest. *Biosystem Engineering*, 87(3)313-323. p.

Bakker-Arkema F.W., Lerew L.E., Deboer S.F. and Roth, M.G. (1974): Grain dryer simulation, Research Report 224, Agricultural Experiment Station, Michigan State University, East Lansing, Michigan.

Beke J. (1997): Terményszárítás. Agroinform, Budapest

Bertin R. and Blazquez M. (1986): Modelling and optimization of a drier. *Drying Technol*, 4(1)45-66. p.

Bourvellec C. and Renard C.M.G.C. (2005): Non-covalent interaction between procyanidins and apple cell wall material. Part II: Quantification and impact of cell wall drying. Accepted by Biochimica et Biophysica Acta. Available at: www.sciencedirect.com

Boyce D.S. (1966): Heat and moisture transfer in ventilated grain. *J. Agric. Eng. Res.*,11. 255-265. p.

Brooker D.B., Bakker-Arkema, F.W. and Hall C.W. (1992): Drying and Storage of Grains and Oilseeds. New York, NY: The AVI Publishing Company.

Brown G. H., Cyril N. H. and Rudolp A. B. (1947): Theory and application of radio-frequency heating. New York: D. Van Nostrand Company, Inc.

Burden W. J. (1998): Working Instructions for Air Oven Methods. In *WI No: AO1-10* USDA-GIPSA-TSD, Kansas City, Missouri

Burr H. S. (1950): An electrometric study of cotton seeds. *J. Exp. Zool.*, 113(1)201-210. p.

Busker L. H. (1968): Microwave moisture measurement. *Instruments and Control Sys.,* 41. 89-92. p.

Cagampang G. B. and A. W. Kirleis (1984): Relationship of sorghum grain hardness to selected physical and chemical measurements of grain quality. *Cereal Chemistry* 61(2): 100-105. p.

Canadian Grain Comission (2003): Crop quality data, highlights, and reports. Available at: http://www.grainscanada.gc.ca/Quality/crop_qual-e.htm Accessed: February 2004.

Caugh R. K., Stuchly S.S. and Rzepecka M.A. (1973): Dielectric properties of wheat at microwave frequencies. *Transaction of the ASAE,* 16(5)906-909. p.

Czaba I. and Neményi M. (1997): Investigation of simultaneaous heat and mass transfer within the individual maize kernels during drying time. *Hungarian Agric. Engineer,* 10. 58–60. p.

Cole K. S. (1928): Electrical impedance of suspensions of Arabica eggs. *J Gen Physiol*, 12, 37-54 p.

Cole K. S. (1940): Permeability and impermeability of cell membranes for ions. *Cold Spring Harbor Sympos. Quant. Biol.*, 8, 110-122 p.

Corcoran P. T., Nelson S.O., Stetson L. E. and Schlaphoff C. W. (1970): Determining dielectric properties of grain and seed in the audio frequency range. *Transactions of the ASAE,* 13(3)348-351. p.

Cox M. A., Zhang M. I. N., Willison J. H. M. (1993): Apple bruise assessment through electrical impedance measurements. *J. Hort. Sci..,* 68(3)393-398. p.

Debye P., Hückel E. (1923): Zur Theorie der Elektrolyte. I. Gefrierpunktserniedrigung und verwandte Erscheinungen *Z. Phys.*, 24. 185. p.

Delate, K., K. V. Dee, and H. Friedrich. (2002): Evaluation of Corn, Soybean and Barley Varieties for Certified Organic Production-Crawfordsville Trial, Available at: http://extension.agron.iastate.edu/organicag/researchreports/crawf02.pdf Accessed: 2005 February

Dickey-john GAC 2100 Grain Analysis Computer. Available at www.dickey-john.com Accessed: 2006.08.20

Doug E. (2004): Nutrition content of Amaranth, Buckwheat, Millet, Oats and Quinoa. Available at: http://waltonfeed.net/self/ntr2.html Accessed: January 2004.

Duke J. A. (2003): Handbook of Energy Crops. Available at: http://www.hort.purdue.edu/newcrop/duke_energy/Helianthus_annuus.html Accessed: February 2004

Earle R. L. and Earle M. D. (1983): Unit operation in food processing. New Zeland: NZIFST Inc.

EC Commission Regulation Nr. 824/2000. Intervention for the grain quality control and quality insurance Available at: http://www.legaltext.ee/text/en/U50369.htm Accessed: September 2006

Felföldi J., László P., Barabássy and S., Farkas J. (1993): Dielectric method for detection of irradiation treatment of potatoes. *Rad. Phys. Chem.,* 41. 471-480. p.

Feng H. and Tang J. (1998): Microwave finish drying of diced apples in spouted bed. *J. FoodSci.* Vol 63(4) 679-683 p.

Feng H., Tang J., Cavalieri R. P. (2002): Dielectric Properties of Dehydrated Apples as Affected by Moisture and Temperature. *Transaction of the ASAE*, Vol. 45(1)129-135. p.

Fortes M. and Okos M.R. (1980): Changes in physical properties of corn during drying, *Trans. ASAE* 23(4)1004-1010. p.

França A. S. and Fortes M. (1994): Numerical simulation of intermittent and continuous deep-bed drying of biological materials. *Drying Technology*, 12(7)1537-1560. p.

Fricke H. (1932): Theory of electrolytic polarization. *Phil Mag,* 14, 310-318 p.

Funebo T. and Ohlsson T. (1998): Microwave-assisted air dehydration of apple and mushroom. *Journal of Food Engineering*, 63(3)349-359. p.

Funk D. B. (2001): An investigation of the nature of the radio-frequency dielectric response in cereal grains and oilseeds with engineering implications for grain moisture meters, Ph.D. diss. Kansas City, Missouri: University of Missouri-Kansas City

Funk D. B. (2000): Uniformity in Dielectric Grain Moisture Measurement, In Uniformity by 2000--Highlights of an International Workshop on Maize and Soybean Quality, edited by Lowell D. Hill (Scherer Communications, Champaign, Ill., 1990) 69-91. p.

Funk D. B., Gillay Z. and Meszaros P. (2005): A Unified Moisture Algorithm for Improved RF Dielectric Grain Moisture Measurements. 6th International Conference on Electromagnetic Wave Interaction with Water and Moist Substances. Weimar, Germany, 2005, "edited by K. Kupfer", MFPA an der Bauhaus-Universitat Weimar p. 495-502

Gillay B. and Funk D. B. (2002): Temperature effects in corn moisture measurements, Paper no. 02-PH-074, European Ag Engineering Conference, Budapest, Hungary

Gillay B. and Funk D. B. (2002): Efficacy of the Landau-Lishitz, Loyenga mixture equation for density-correcting dielectric measurements of yellow-dent corn subjected to vibration and pressure, ASAE Paper No026038 St. Joseph, MI 49085.

Gillay B. and Funk D. B. (2003): Mathematical modeling of the low-frequency range changes in dielectric constant measurements due to settling and pressure. ASAE Paper No: 033135. St. Joseph, MI 49085.

Gillay B. (2005): Szemes termények nedvességtartalmának meghatározása, Országos Mezőgazdasági Szakfolyóirat – IX. évfolyam available at: “www.agronaplo.hu” accessible: 2006.01.09

Gillay B. and Funk D. (2005): Effects of Moisture Distribution on Measurement of Moisture Content of Dried Corn. , *Progress in Agricultural Engineering Sciences* Vol 1 77-93 p.

Gillay Z. and Funk D. B. (2003): Sensitivity analysis for VHF dielectric grain moisture measurements. ASAE Paper No. 033136 . Joseph, MI 49085.

Gillay Z. and Funk D. B. (2005): Analysis of frequency sensitivity of the Unified Grain Moisture Algorithm. ASAE Paper No. 053047 . Joseph, MI 49085.

Ginzburg A. Sz. (1978): Élelmiszerek szárításelméletének és technikájának alapjai. Mezőgazdasági Kiadó, Budapest, 1976

Grant E. H., Sheppard R. J. South G. P. (1978): *Dielectric Behaviour of Biological Molecules in Solutions*, Clarendon Press, Oxford, 4.

Grimnes S., Martinsen O.G. (2000): Impedance and Bioelectricity Basics. London: Academic Press, 87. p.

Győri, Z. and Mile I. (1998): A búza minősége és minősítése, Mezőgazdasági Szaktudás Kiadó, Budapest

Haas G. J., Bennett D., Herman E. B. and collette D. (1975): Microbial Stability of intermediate moisture foods. *Food Product Development*, 9. 68-94 p.

Hamond J. E., Brandenburg N. R. and Booster D. E. (1961): Seed cleaning by electrostatic separation. *Agricultural Engineering*, 42(1)22-25 p.

Harker F. R. and Maindonald J. H. (1994): Ripening of Nectarine Fruit. *Plant Physiol.*, 106-165. p.

Harsányi G., Nyéki J., Soltész M., Gonda I. and Szabó Z. (2005): Az almatermesztés jövője az Észak-alföldi Régióban, *Agrártudományi közlemények*, 2005/17 Különszám 35-38. p available at: http://www.date.hu/acta-agraria/2005-17/index.pdf accessible: 2006.02.09.

Hart J. R. and Golumbic C. (1966): The use of electronic moisture meters for determining the moisture content of seeds. *Proc. Int. Seed Testing Assoc.*, 31(2)201-212. p.

Hasted J. B. (1973): Dielectric Properties of Absorbed Water in Aqueous Dielectrics. London: Chapman and Hall, 234-255. p.

Hilhorst M. A., Groenwold J. and Groot de J. F. (1992): Water Content Measurements in Soil and Rockwool Substrates: Dielectric Sensores For Automatic in Situ Measurements. *Acta Horticulture*, 304. 209-217. p.

Holaday C. E. (1964): An electronic method for the measurement of heat damage in artificially dried corn. *Cereal chem.*, 41. 533-542. p.

Honda M. (1989): *The Impedance Measurement Handbook – Guide to Measurement Technology and Techniques*. Hewlett-Packard LTD. Yokogawa. 4.2-4.4 p.

Hungarian Air-Oven Standard MSZ ISO 6367/3-1983: Élelmezési, takarmányozási, ipari magvak és hántolt termények vizsgálata. Nedvességtartalom meghatározása

Hunt W. H. and Pixton S.W. (1972): Moisture--Its Significance, Behavior, and Measurement,. in Storage of Cereal Grains and Their Products, edited by C.M. Christenson (American Association of Cereal Chemists, Minneapolis, Minn.), 1-55. p.

Hurburgh Jr. C.R., Bern C.J., and Grama S.N. (1981): Improvements in the accuracy of corn moisture measurement in Iowa. ASAE Paper No. 81-3515, ASAE. St. Joseph, MI 49085.

Hurburgh Jr.C.R., Hazen T.E., and Bern C.J. (1985): Corn moisture measurement accuracy. *Transactions of ASAE*, 28(2)634-640. p.

Hurburgh, Jr., C.R., Bern C.J., and Sitzman C.D. (1980): Performance of electronic moisture meters in corn. ASAE Paper No. 80-3057. St. Joseph, MI 49085.

Iglesias H. A. and Chirfe J. (1982): Handbook of Food Isotherms. New York, NY: Academic Press,

ICC - Standard Nr. 109/1 Determination of the Moisture Content of Cereals and Cereal Products (Basic Reference Method),. edited by J. L. Multon (International Association for Cereal Chemistry, Vienna, Austria, 1976).

International Grain Program. (1988): *Grain Manufacturing Processes Handbook.* Manhattan Kansas. Kansas State University.

ISO, International Standard ISO 712 (1998):-- Cereal and cereal products – Determination of moisture content – Routine reference method,. (International Standards Organization, Geneva, Switzerland).

ISO, International Standard ISO 760 (1978):--Determination of Water -- Karl Fischer Method (General Method),. (International Standards Organization, Geneva, Switzerland).

ISO, International Standard ISO 7700:1 (1984):-- Check of the calibration of moisture meters -- Part 1: Moisture meters for cereals, (International Standards Organization, Geneva, Switzerland).

ISO, International Standard ISO 7700:2 (1987):-- Check of the calibration of moisture meters -- Part 2: Moisture meters for oilseeds, (International Standards Organization, Geneva, Switzerland).

Jayarman K. S. and DasGupta D. K. (1992): Dehydration of fruits and vegetables - recent developments in principles and techniques. *Drying Technology*, 10. 1-50. p.

Jones R. N., Bussey H. E., Little W.E. and Metzker R. F. (1978): Electrical characteristics of corn, wheat and soya in the 1-200 MHz range NBSIR 78-897, National Bureu of Standards, U. S. Dept. Commerce.

Kaffka, K. J., Norris K. H., Perédi J. and Balogh A. (1982): Attempts to determine oil, protein, water and fiber content in sunflower seeds by the NIR technique. *Acta Alimentaria*, 11, 254 - 269.

Kaffka K. J. and Seregély Zs. (2000): Wavelength range optimisation using the PQS (Polar Qualification System). Davies, A.M.C. & Giangiacomo, R., Eds. NIR Spectroscopy: Proceedings of the 9th International Conference. NIR Publications, Chichester (U.K.) 26l-267. p.

Kajdi F. (2003): A "minőség" szerepe a búza termesztésében. Available at: http://kredit.sth.sze.hu/nemall/magyar/bminos.htm Accessed: January 2004.

Kansas State University (2003): Crops and Soils Library. Available at: http://www.oznet.ksu.edu/library/crpsl2 Accessed: May 2004

Karathanos V. T., Kostaropoulos, A. E. and Saravacos G. D. (1995): Air-drying of osmotically dehydrated fruits. *Drying Technol.*, 13(5-7)1503-1521. p.

Kett moisture meters: PB-3011, Waddy PV, PT-2300 Available at www.kett.co accessed 2006.08.20

Klein R. (2003-2004): Nebraska Corn Quality Report. Available at: http://www.nebraskacorn.org Accessed: February 2004.

Kocabiyik H., Akta T. and Kay. B. (2004): Porosity Rate of some kernel crops. *Journal of Agronomy* 3 (2): 76-80, ISSN 1680-8207

Kraszewski A. W., Trabelsi S, and Nelson S. O. (1998): Comparison of Density-independent Expressions for Moisture Content Determination in Wheat at Microwave Frequencies. *J. Agric. Engng Res.*, 71. 227-237. p.

Kraszewski A. W. (1996): Microwave Aquametry: Introduction to the Workshop. In Microwave Aquametry--Electromagnetic Wave Interaction with Water-Containing Materials, edited by Andrzej W. Kraszewski (IEEE Press, New York), 3-34. p.

Kraszewski A. W. and Nelson S. O. (1992) Wheat Moisture Content and Bulk Density Determination by Microwave Parameters Measurement. *Canadian Agricultural Engineering*, 34(4) 327-335. p.

Kuang W., Nelson S. O. (1998): Low-frequency dielectric properties of biological tissues: A review with some new insights. *Transaction of the ASAE,* 41(1)173-184. p.

Kutrubes D. L. (2000): Use of a Ground-Coupled Monostatic antenna for Determining Deterioration of Concrete Structures. Proceedings of the Symposium for the Applications of Geophysics for Engineering and Environmental Problems (SAGEEP), 21-24 February, 2000, Washington, D.C., 851-5. p.

Labuza I. P. (1984): Moisture Sorption: Practical Aspects of Isotherm Measurement and Use. American Association of Cereal Chemists, St. Paul, MN.

Labuza T. P. and Simon I. B. (1970): Surface tension effects during dehydration. *Food Techn.*, 24(6)712-715. p.

László P., Vozáry E., Zana J. Zsivánovits G. and Sass, P. (1997): Electrical properties of apple cultivars during ripening and storage. *Acta Horticulture,* 485. 239-247. p.

Lásztity R. (1998): Gabona fehérjék. Mezőgazdasági kiadó, Budapest

Lawrence K. C., Funk D. B., and Windham W. R. (1999): "Parallel-Plate Moisture Sensor for Yellow-Dent Field Corn," *Trans. ASAE*. 42 (5), 1353-1357

Lawrence K. C., Nelson S. O. and Kraszewski A. W. (1989): Temperature dependence of the dielectric properties of wheat. *Transaction of the ASAE,* 33(2)535-540. p.

Lawrence K. C., Nelson S. O., Kraszewski A. W. (1990): Temperature Dependent Model for the Dielectric Constant of Soft Red Winter Wheat. *Transaction of the ASAE*, Vol. 34(5) 2091-2093. p.

Lawrence K. C., Nelson S. O. and Kraszewski A. W. (1991): Temperature-dependent model for the dielectric constant of soft red winter wheat. *Transaction of the ASAE*, 34(5) 2091-2093. p.

Lawrence K. C., Nelson S. O. and Bartley P. G. (1998): Flow-Through Coaxial Sample Holder Design for dielectric Properties Measurements from 1 to 350 MHz. IEEE Transactions on Instrumentation and Measurements 47(2), 354-361 p.

Lee K. H., Zhang N., Kluitenberg G., Kuhn W. B. And Das S. (2004): A dielectric permittivity sensor for simultaneous measurement of multiple soil properties. ASAE paper No. 041045, ASAE, St. Joseph, Mich. 49085

Lee W. J., Shelton D. R. and Pedersen J. F. (2003): 159 Relationship of sorghum grain size to physicochemical properties. Available at: http://www.aaccnet.org/meetings/99mtg/ abstracts/acabb60.htm Accessed: September 2004.

Lenart A. and Lewicki P. P. (1988): Osmotic preconcentration of carrot tissue followed by convection drying. *In Preconcentration and Dying of Food Materials,* ed. S. Bruin, 307-308. p. Elsevier Science, Amsterdam.

Lengyel A (1997): Gyümölcsök szárítási paramétereinek meghatározása különös tekintettel a szárítmányok minőségére. Kandidátusi értekezés, Nyíregyháza

Lengyel, A., Sikolya, L., Szabó, B. (1999): Szövettani változások a gyümölcsök szárításánál *3rd Hungarian Drying Symposium*, Nyíregyháza, 48-53. p.

Lupien, J. R. (2004): Sorghum and millets in human nutrition. Available at: http://www.fao.org/documents/show_cdr.asp?url_file=/DOCREP/T0818e/T0818E0b.htm Accessed: June 2004

MacDonald J. R. (1987): *Impedance Spectroscopy,* New York: John Wiley and Sons, 17. p

Maertens K., Reyns P., Baerdemaeker J. D. (2004): On-line measurement of grain quality with NIR technology. *Transaction of the ASAE* ISSN 0001-2351 47(4): 1135-1140 p.

Martinsen O. G., Grimnes S. and Schwann H. P. (2002): Interface phenomena and dielectric properties of biological tissue. *Encyclopedia of Surface and Colloid Science* 2643-2652 p.

Mathsoft. 2000. Mathcad Users Guide with Reference Manual, Ver. 2001. Cambridge, Mass.: Mathsoft, Inc.

Matthes R. K. and Boyd A. H. (1969): Electrical properties of seed associated with viability and vigor. *Transactions of the ASAE,* 12(6)778-781. p.

Matthews J. (1963): The design of an electrical capacitance-type moisture meter for agricultural use. *J. Agr. Eng. Res.,* 1. 17-30. p.

Mészáros P., Vozáry E., Funk D. B., (2003): Elektromos impedancia paraméterek változása gyümölcsszárítás folyamán 5. Szárítási szimpozium, Szeged

Milani, A. P., R. A. Bucklin, A. A. Teixeira, and H. V. Kebeli. 2000. Soybean Compressibility And Bulk Density. *Transactions of the ASAE* VOL. 43(6): 1789-1793

Mini-Circuits (1999): Directional Couplers Available at: http://www.minicircuits.com/appnote/coup7-2.pdf Acessed: September 2006

Mohsenin N. N. (1989): *Physical properties of food and agricultural materials*, Gordon and Breach Science Publishers, New York

Molitorisz J. (1966): Engineering applications of electro-physiological properties of plants. *Agr. Sci. Rev.,* 4(3)8-11. p.

Moller A. (1971): Measurement and control of moisture in cereals. *Milling,* 153(8)24-28. p.

Muir, W .E., S. Cenkowski, and Q. Chang. (2004): Physical characteristic of grain bulks. Available at: http://res2.agr.ca/winnipeg/storage/pubs/presbios/chap07rf.pdf Accessed 2005 April.

Nelson S. O. and Whitney W. K. 1960. Radio-frequency electric fields for stored grain insect control. *Transactions of the ASAE,* 3(2):133-137. p.

Nelson S. O. (1973): Electrical properties of agricultural products (a critical review), *Transactions of the ASAE,* 16(2.)1-21. p.

Nelson, S. O. 1978. Moisture-Dependent Kernel and Bulk Density Relationships for Wheat and Corn. ASAE Paper No. 78-3059 St. Joseph, Mich.: ASAE.

Nelson S. O. (1984): Moisture, frequency, and density dependence of the dielectric constant of shelled, yellow-dent field corn. *Transaction of the ASAE,* 25(5)1573-1578. p.

Nelson S. O. (1985a): A mathematical model for estimating the dielectric constant of hard red winter wheat. *Transaction of the ASAE,* 28(1)234-238. p.

Nelson S. O. (1985b): A model for the estimating the dielectric constant of soybeans. *Transaction of the ASAE,* 28(6)2047-2050. p.

Nelson S. O. (1986a): Mathematical models for the dielectric constants of spring barley and oats. *Transaction of the ASAE,* 29(2)607-610. p.

Nelson S. O. (1986b): Models for estimating the dielectric constant of winter barley. *International Agrophysics,* 2(3)189-200. p.

Nelson S. O. (1992): Correlating Dielectric Properties of Solids and Particulate Samples Through Mixture Relationships *Transaction of the ASAE,* 35(2) 625-629. p.

Nelson, S. O., 2002. Dimensional and density data for seeds of cereal grain and other crops. *Trans.ASAE*. VOL. 45(1): 165-170

Nelson S. O. (2003): Agricultural application for dielectric spectroscopy, ASAE Paper No. 033139 . Joseph, MI 49085.

Nelson S. O. (2004): Dielectric properties and density relationships for granular materials ASAE Paper No. 04086 . Joseph, MI 49085.

Neményi M. (2003): Szemestermények mesterséges szárítása. Budapest: Mezőgazda Kiadó

Neményi M, Czaba I, Kovács A, Jáni T (2000): Investigation of simultaneous heat and mass transfer within the maize kernels during drying. *Computers and Electronics in Agriculture*, 26: 123-135 p.

Norris K. H. (1956): Measurement of quality in foods and agricultural commodities by physical methods. Proc. First Symp. Food Phys. 113-124. p.

Nowak D., Lewicki P. P. (2004): Infrared drying of apple slices, Innovative Food Science and Engineering Technologies, available online at www.sciencedirect.com accessible: 2006.02.09

OIML (International Organization of Legal Metrology) (1984): Moisture Meters for Cereal Grains and Oilseeds. International Recommendation R59

Özilgen M., Güvenc G., Makaraci I. M. and Tümer Z. (1995): Colour change and weight loss of apple slices during drying. *Lebensm. Unters. Forsch.,* 201. 40-45. p.

Üretir G., Özilgen M. and Katnas S. (1996): Effects of Velocity and temperature of Air on the Drying Rate Constant of Apple Cubes. *J. Food Eng.,* 30. 339-350. p.

Paliwal J., Visen N. S. and Jayas D. S. (1998) Determination of physical properties of different grain types using machine vision. ASAE Paper No. 98-3060. St. Joseph, Mich.: ASAE.

Paulsen M.R., Hill L.D. and Dixon B.L. (1983): Moisture meter-to-oven comparisons for Illinois corn. *Transactions of ASAE*, 26(2)576-583. p.

Perten Aquamatic 5100 dielectric moisture meter. Available at www.perten.com accessed 2006.08.20

Pething R., Kell D. B. (1987): The passive electrical properties of biological systems: their significance in physiology, biophysics and biotechnology. *Phys. Med. Biol.,* 33. 933. p.

Petrie A., Bulman J. S. and Osborn J. F. (2002): Further statistics in dentistry part 6: multiple linear regression. *British Dental Journal,* Vol. 193(12) 675-682 p. available at: www.nature.com accessed: January 2007

Pullman J. O., Hollenbeck W. J. and Gibson G. W. (1965): The measurement of the moisture content of cut tobacco by means of microwave absorption—Part 2. *Tobacco Sci.*, 9. 173-178. p.

Rahman M.D. S. and Lamb J. (1991): Air drying behavior of fresh and osmotically dehydrated pineapple. *J. Food Eng.*, 14. 163-171. p.

Rao M. A. and Rizvi S. S. H. (1995): Engineering Properties of Foods, New York: Marcel Dekker, Inc. 276. p.

Rajewsky B., Schwan H. P. (1948): The dielectric constant and conductivity of blood at ultrahigh frequencies. *Naturwissenschaften* 35, 315

Repo T. and Zhang M. I. N. (1993): Modeling woody plant tissues using distributed electrical cicuit, *J. Exp. Bot.*, 44. 977. p.

Sacilik K. and Elicin A. K. (2005): The thin layer drying characteristics of organic apple slices, *Journal of Food Engineering*, available online at www.sciencedirect.com accessible 2006.02.09

Santalla, E. M. and R. H. Mascheroni. (2003): Physical Properties of High Oleic Sunflower Seeds. Available at: http://fst.sagepub.com/cgi/content/refs/9/6/435 Accessed: February 2004.

Saravacos G.D., and Charm S.E. (1962): A study of the mechanism of fruit and vegetable dehydration. Food Technology, 15. 78-80. p.

Sass P. and Horn E. (1974): Az alma súlyveszteségének és méretcsökkenésének alakulása változatlan és szabályozott légterű tárolás során. A Kertészeti Egyetem Közleményei. Vol 38. 107-114 p.

Satterlee, L.D.and P.R. Duarte. Oklahoma Wheat Quality Survey 2000-2002. Available at: http://www.fapc.okstate.edu/crops/ Accessed: January 2004.

Seedburo Model 1200 A moisture meter Available at www.seedburrow.com Accessed: 2006.08.20

Schwan H. P. (1954): Electrical properties of muscle tissues at low frequencies. *ZS. F. Naturforsch* 9B, 245

Schwan H. P., Schwarz G., Maczuk J. and Pauly H. (1962): On the low-frequency dielectric dispersion of colloidal particles in electrolyte solution. Phys. Chem 66, 2626 p.

Schwan H. P. (1964): Electric characteristics of tissues, a survey. *Biophysik*, 1. 198-208. p.

Schwan H. P. (1966): Alternating current electrode polarization. *Biophysik*, 3. 181-201. p.

Schwan H. P. (1959): Alternating current spectroscopy of biological substances. *Proc. IRE*, 47(11)1841-1855. p.

Schwan H. P. (1993): Mechanism responsible for electrical properties of tissues and cell suspensions. *Med. Prog. Technol*. 19. 163-165 p.

Schwan, P.H. and Ferris D.C. (1968): Four-Electrode Null Techniques for Impedance Measurement with High Resolution. *Rev. of Sci. Instr.* 1968/4 481-485 p.

Scott M., Paul R. and Kaler K. V. I. S. (2000): Theory of Frequency-Dependent Polarization of General Planar Electrodes with Zeta Potentials of Arbitrary Magnitude in Ionic Media 1. Theoretical Foundations and General Results *J. Colloid Interface Sci.,* 230. 377-387. p.

Sembery P. (2002): Mezőgazdasági termények dielektromos jellemzői, Budapest: Akadémiai Kiadó

Sembery P. (1994): Dielectric Properties of Agricultural Materials. *Hungarian Agricultural Engineering*, Gödöllő (7). 14-16. p.

Sembery P., Géczi G., Kovács M. and Douba M. (1999): High frequency and microwave dielectric properties of basic food material, *Hungarian Agricultural Engineering*, Gödöllő (12). 15-19 p.

Sembery P., Völgyi F. (1989): Moisture measurement of maize at microwave frequency. Bulletin of University of Agricultural Sciences. Gödöllő 157-164. p.

Sembery P., Géczi G. and Váczy G. (2001): Measurement Methods of Dielectric Properties of Mustard Seeds at Microwave Frequency *Hungarian Agricultural Research*, HU ISSN 1216-4526, Vol. 10, No.3, p.16-18

Seregély ZS. (2000): Investigating the NIR characteristics of winter and spring barley and mait. Davies, AM.C. & Giangiacomo, R., Eds. NIR Spectroscopy: Proceedings of the 9th International Conference, NIR Publications, Chichester (D.K.) p. 543-546

Sharp J. R. (1982): A review of low temperature drying simulation models. *J. Agric. Eng. Res.,* 27. 169-190. p.

Simal S., Deya E., Frau M. and Rosselo C. (1997): Simple modeling of air drying curves of fresh and osmotically pre-dehydrated apple cubes. *Journal of Food Engineering*, 33. 139-150. p.

Stencl J. (1999): Water activity of skimmed milk powder in the temperature range of 20-45 °C. *Acta Vet. Brno,* 68. 209-215. p.

Stetson L. E. and Nelson S. O. (1972a): Audiofrequency dielectric properties of grain and seed. *Transactions of the ASAE,* 15(1)180-184. p.

Stetson L. E. and Nelson S. O. (1972b): Effectiveness of hot air, 39-MHz dielectric and 2450 MHz microwave heating for hard seed reduction in alfalfa. *Transactions of the ASAE,* 15(3)530-535. p.

Stoy R. D., Foster K. R., Schwan H. P. (1982): Dielectric properties of mammalian tissues from 0.1 to 100 MHz: a summary of recent data *Phys. Med. Biol.* 1982, 27, 501-513

Szabó G., Rajkó R., Hodúr C. (1998): Combined Energy Transfer by Microwave-Convective Drying of Agriculture Materials. *Hung. Agric. Eng*. Vol. 11. 23-25 p.

Szabó G., Ludányi L., Rajkó R., Forgacs E. (2003): Recent Developments of Combined Microwave-assisted Hot-Air Vibrfluidised Bed Dryer with Homogenius Distribution of

Electromagnetic Field. 4th International Conference for Conveying and Handling of Particulate Solids. 2. 13.31-13.36 p.

Torreggiani D. (1993): Osmotic dehydration in fruit and vegetable processing. *Food Res. Int.*,26.59-68. p.

Toyoda, K. Tsenkova, R. (1998): Measurement of freezing process of agricultural products by impedance spectroscopy Control Applications in Post-harvest and Processing Technology, *IInd workshop on Control Applications in Post-harvest and Processing Technology* Budapest, Hungary, p. 139.

Trabelsi S. and Nelson S. O. (1998): Density-Independent Functions for On-Line Microwave Moisture Meters: A General Discussion. *Meas. Sci. Technol.*, 9. 570-578. p.

Trabelsi S., Kraszewski A. W. and Nelson S. O. (1998): Nondestructive Microwave Characterization for Determining the Bulk Density and Moisture Content of Shelled Corn. *Meas. Sci. Technol.*, 9. 1548-1556. p.

Trabelsi S., Kraszewski A. W. and Nelson S. O. (1999): A Unified Calibration Method for Moisture Sensing in Particulate Materials. Presented at the Third Workshop on Electromagnetic Wave Interaction with Water and Moist Substances, Athens, Georgia

Troller, J. A., and J. H. B. Christian. (1978): Water Activity and Food. New York, NY: Academic Press,

U. S. Department of Agriculture –GIPSA (2005): 2005 Annual report to congress Federal Grain Inspection Service. Available at: http://archive.gipsa.usda.gov/pubs/05ar.pdf Accessed: September 2006

U. S. Department of Agriculture -GIPSA. (1999): *Moisture Handbook*, Washington, D.C. Available at: http://www.usda.gov/gipsa/reference-library/handbooks/moisture/moisture.htm, Accessed: May 2004.

U. S. Department of Agriculure, (1963): Comparison of various moisture meters with the oven method in determining moisture content of grain. AMS-511, 11 p., Agricultural Marketing Service, Standardization and Testing Branch, Grain Division

U.S. Grains Council (1986): Grain Quality and U.S. Standards, Importer Manual. Chapter 4, available at: http://www.grains.org/galleries/importer_manual/ accessible: 2006.02.09

U.S. Grains Council. Value-Enhanced Grains Report (2001-2002): Available at: http://www.vegrains.org/documents/2002veg_report/testing/ctallsamples.html Accessed: February 2004

Yao Z. and Le Maguer M. (1994): Finite element modeling of osmotic dehydration processes. *Food Res. Int.*, 27. 21 l-212. p.

Vagenas G. K. and Marinos-Kouris D. (1991): The design and optimization of an industrial dryer for sultana raisins. *Drying Technol.,* 9(2)439-461. p.

Velic D., Planinic M., Tomas S. and Bilic M. (2004): Influence of airflow velocity on kinetics of convection apple drying. *Journal of Food Engineering,* 64(1)97-102. p.

Venkatesh M. S., Raghavan G. S. V. (2005): An overview of dielectric properties measuring techniques. *Canadian Biosystem Engineering* (47) 7.15-7.29 p.

Vozáry E., Niemirow B. K., László P. and Sass P. (1996): Electrical Impedance of Apple Tissues during Ripening. *Progr. Biophys. Mol. Biol*., 65 suppl.1, 213. p.

Vozáry E. and Horváth E. (1998): Changes of impedance parameters of apple slices during drying. Control Applications in Post-Harvest and Processing Technology. Vol 2. 123 p.

Vozáry E., László P. and Zsivánovits G. (1999): Impedance Parameter Characterizing Apple Bruise. *Ann. N.Y. Acad. Sci*., 873. 421-429. p.

Wallis B. (2006): Moisture Determination Guidelines for Model 919/3.5" and 393/3.5" Moisture Meters Available at: www.grainscanada.gc.ca/PUBS/Moisture/moisture-e.htm accessed: September 2006

Wanaanen K. M., Litchfield J. B. and Okos M. R. (1993): Classification of drying models for porous solids. *Drying Technology*, 11. 1-40. p.

Wang J. and Chao Y. (2002): Drying characteristics of irradiated apple slices. *Journal of Food Engineering,* 52(1)83-88. p.

Wang S. and Tang J. (2004): Temperature dependent dielectric properties of tropical foods and insects. ASAE Paper No. 046192 . Joseph, MI 49085.

Wilhelm L. R., Suter D. A., and Brusewitz G. H. (2004): Drying and Dehydration. Food & Process Engineering Technology, St. Joseph, Michigan: ASAE. Chapter 10. 259-284. p.

Williams P, Norris K (1987): Near-infrared technology in the agriculture and food industries. (American Association of Cereal Chemists Inc.: Minnesota)

Wittkopf J. J. and Macdonald M. D. (1949): Dielectric properties of Douglas fir at high frequencies. Bull. No. 28 Eng. Exp. Sta., Oregon State System of Higher Education, Oregon State Coll., Corvalis, Ore., 23 p.

Zeleny L. (1960): Moisture measurement in the grain industry. *Cereal Sci. Today,* 5(5)130-136. p.

Zeleny L. (1954): Methods for grain moisture measurements. *Agricultural engineering,* 35(4)252-256. p.

Zhang M. I. N., Willison J. H. M. (1991): Electrical impedance analysis in plant tissue: a double shell model. *J. Exp. Bot.,* 42. 1465-1475. p.

## 10.2. Appendix 1. Tested grain types by USDA-GIPSA technical staff

| GRAINS TESTED BY USDA-GIPSA TECHNICAL STAFF | | | | | | | |
|---|---|---|---|---|---|---|---|
| Grain typename | Grain name | 1998 Crop | 1999 Crop | 2000 Crop | 2001 Crop | 2002 Crop | Totals |
| Soybean | Soy | 99 | 137 | 135 | 123 | 148 | 642 |
| Sorghum | Sorghum | 11 | 44 | 54 | 42 | 42 | 193 |
| Sunflower | Oil type | 66 | 137 | 77 | 74 | 69 | 423 |
| | Confectionary | | 49 | | | | 49 |
| Corn | Corn | 115 | 217 | 143 | 179 | 214 | 868 |
| | Waxy corn | | 44 | | | | 44 |
| | Popcorn | | | | | 14 | 14 |
| Oats | Oats | 25 | 19 | 13 | 47 | 21 | 125 |
| Wheat | Hard white wheat | 33 | 68 | 65 | 7 | 26 | 199 |
| | Soft white wheat | 28 | 53 | 46 | 15 | 34 | 176 |
| | Soft red winter wheat | 15 | 55 | 56 | 68 | 70 | 264 |
| | Hard red winter | | | | 48 | 61 | 109 |
| | Hard red spring | 40 | 47 | 55 | 79 | 58 | 279 |
| Barley | Two row barley | 10 | 29 | 32 | 31 | 34 | 136 |
| | Six row barley | 29 | 25 | 39 | 32 | 47 | 172 |
| Rice &Durum | Short grain rough rice | | 25 | | 60 | | 85 |
| | Long grain rough rice | 38 | 33 | 44 | 86 | 43 | 244 |
| | Durum wheat | 4 | 50 | 24 | 50 | 49 | 177 |
| | Medium grain rough rice | 48 | 50 | 37 | 56 | 49 | 240 |
| Peas | Austrian winter peas | | | | 14 | 12 | 26 |
| | Smooth green dry peas | | 42 | | | | 42 |
| | Wrinked dry peas | | | | 4 | 9 | 13 |
| Mustard | Brown mustard seed | | | | | 27 | 27 |
| | Yellow mustard seed | | | | | 6 | 6 |
| Edible beans | Dark red kidney bean | | 12 | | 6 | | 18 |
| | Large lima beans | | | | 1 | | 1 |
| | Light red kidney bean | | 11 | | | | 11 |
| | Split peas | | | | | 16 | 16 |
| | Garbonzo bean | | | | 15 | | 15 |
| | Small red beans | | | | 13 | 17 | 30 |
| | Dark light red kidney bean | | | | 4 | | 4 |
| | Pink beans | 11 | | | 7 | 23 | 41 |
| | Yellow eyed bean | | | | | 5 | 5 |
| Triticale | Triticale | | | | | 12 | 12 |
| Canola | Canola | 16 | | | | | 16 |
| Safflower | Safflower | | 12 | | | | 12 |
| Flaxseed | Flaxseed | | 28 | | | | 28 |
| High-oil corn | High oil corn | 17 | 16 | | | | 33 |
| Edible bean 2 | Great northern beans | 10 | | | | | 10 |
| | Pinto beans | 20 | | | | | 20 |
| Processed rice | Medium grain brown | | | | 30 | 22 | 52 |
| | Long/medium second head milled rice | | | | 16 | 16 | 32 |
| | Brewers milled rice | | | | 6 | | 6 |
| | Short grain second head milled rice | | | | 13 | | 13 |
| | Short grain milled rice | | | | 15 | 12 | 27 |

| | | | | | | | |
|---|---|---|---|---|---|---|---|
| | Second head milled rice parboiled | | | | | 10 | 10 |
| | Short grain brown rice | | | | 9 | 8 | 17 |
| | Brewers milled rice parboiled | | | | | 10 | 10 |
| | Medium/short second head milled rice | | | | | 16 | 16 |
| | Medium grain milled rice parboiled | | | | | 14 | 14 |
| | Medium grain milled | | | | 29 | 34 | 63 |
| Long Grain Processed Rice | Long grain milled rice | 10 | 20 | | | | 30 |
| | Long grain brown rice | 10 | 16 | | | | 26 |
| Total Samples | | 655 | 1239 | 820 | 1179 | 1248 | 5141 |
| Total Classes | | 21 | 25 | 14 | 31 | 34 | 53 |

## 10.3. Appendix 2. The Hungarian air-oven method for grain moisture measurement

### 10.3.1 Grains (wheat, barley, rye, rice, oats) and corn

The sample is used after grinding or conditioning and drying for the moisture content determination

Required particle size:

Maximum particle size: 1.7 mm

Fraction above 1.0 mm is at most 10% (m/m) of the sample

Fraction below 0.5 mm is at least 50% (m/m) of the sample

#### 10.3.1.1 Grinding

First of all a small amount of sample has to be grind which will be waste, then from grain about 5g, from corn about 30g has to grind. If the sample wb moisture content before grinding is bigger than 15% or smaller than 9% the sample has to conditioning.

If the sample moisture content is bigger than 15% wb:

5-6g has to weigh and put into the 130-133 °C air-oven and the sample has to dry 7-10 minutes, then without insulating of the sample from the air it has to leave for 2 hours in a room temperature place. In the case of corn, the method is similar, but sample weight has to be about 100g, the air oven temperature has to be 60-80 °C.

If the sample moisture content is smaller than 9% wb:

5-6g or 100g has to weigh and leave without insulating from the air in a room temperature place until the sample moisture content reach 9% wb.

After grinding from the grain sample 5g, from corn sample 8g has to put immediately into laboratory dish.

10.3.1.2 Drying

The laboratory dishes with the samples and with the top (without covering) of the dishes have to place into the 130-133 °C air-oven. Grain has to dry for 2 hours, corn has to dry for 4 hours.

After drying, the laboratory dishes have to cover immediately and have to put in an exicator fo3 30 minutes to cool down. Finally, the samples weights have to measure. Measuring of the weights have to be done ±1 mg precision.

10.3.1.3 Calculation of the sample moisture content

- without sample conditioning

$$w_a = (m_o - m_1) \cdot \frac{100}{m_o}$$

where:
$w_a$ is the moisture content of the sample, (m/m)%
$m_o$ is the sample weight before drying, g
$m_1$ is the sample weight after drying, g

- with sample conditioning

$$w_a\left[(m_o - m_1) \cdot \frac{m_3}{m_0} + m_2 - m_3\right] \cdot \frac{100}{m_2} = 100\left(1 - \frac{m_1 \cdot m_3}{m_0 \cdot m_2}\right)$$

or

$$w_a = \frac{((m_2 - m_3) + (\frac{m_0 - m_1}{m_0})) \cdot m_3}{m_2} \cdot 100$$

$m_0$ is the sample weight after grinding before drying, g
$m_1$ is the sample weight after drying, g
$m_2$ is the sample weight before pre-drying, rewetting
$m_3$ is the sample weight after pre-drying, rewetting

Two or three parallel measurement has to prepare. The final sample moisture content will be the mean of the two or three parallel measurement and rounding 0.05.

10.3.1.4 Repeatability:

In the same laboratory, from the same sample, with the same equipments the differences between two measurements won't be bigger than: in the case of grain samples 0.15%(m/m), in the case of corn 0.2%(m/m). If the differences bigger the process has to repeat.

10.3.1.5. Reproducibility:

In different laboratories, from the same samples the standard deviation won't be bigger than: in the case of grain samples ±0.3 %(m/m), in the case of corn ±0.5%(m/m)

### 10.3.2 Oilseeds, other seeds.

10.3.2.1 Samples measured without grinding

Small and middle size oilseeds and other seeds (sorghum, coriander, millet, caraway, buckwheat, et.) except peanut and soybean are dried without grinding. The measured sample volume of these seeds has to be between 5-10g.

10.3.2.2 Samples measured with grinding

Beans, peas, lentils, lupin, wild pea, soybean and peanut have to grind before drying. The required particle size is maximum 2mm.

10.3.2.3 Drying

Oilseeds have to dry on 103 ± 2 °C for 4 hours. Other seeds have to dry on 130-133 °C for 2 hours.

10.3.2.4 Repeatability:

In the same laboratory, from the same sample, with the same equipments the differences between two measurements won't be bigger than 0.2 %(m/m). If the differences bigger the process has to repeat.

10.3.2.5 Reproducibility:

In different laboratories, from the same samples the standard deviation won't be bigger than ±0.5%(m/m)

## 10.4. Appendix 3. Moisture content determination at low frequency (1-20 MHz) with a sunflower sample by HP4285A

DENSITY CORRECTED DIELECTRIC CONSTANT PREDICTION ALGORITHM FOR SUNFLOWER

David B. Funk December 12, 2001

$KCC := READPRN("SFSKs030303.txt")$

The following prediction function accepts as parameters: real part of relative dielectric constant ($\varepsilon r$), temperature (T), sample density in gm/liter (D), measurement frequency (F), polynomial calibration coefficients (KCC) (with embedded average cell weight ($\rho$)), volume of the test cell (VTC), and temperature correction coefficient (KTC) and returns predicted moisture content with temperature correction.

These are the coefficients computed for 10 measurement frequencies.

$KCC =$

| | 0 | 1 | 2 | 3 | 4 | 5 |
|---|---|---|---|---|---|---|
| 0 | 5.5365 | 5.9277 | 6.0867 | 4.6021 | -0.2794 | -4.5419 |
| 1 | 0.544 | 0.4772 | 0.4266 | 1.1397 | 3.9644 | 6.966 |
| 2 | $1.5962 \cdot 10^{-3}$ | 0.017 | 0.0338 | -0.0265 | -0.4341 | -1.0174 |
| 3 | $-5.5208 \cdot 10^{-5}$ | $-4.1737 \cdot 10^{-4}$ | $-9.7473 \cdot 10^{-4}$ | $1.1447 \cdot 10^{-3}$ | 0.0242 | 0.0712 |
| 4 | $1.8272 \cdot 10^{-7}$ | $2.2298 \cdot 10^{-6}$ | $6.8096 \cdot 10^{-6}$ | $-1.8304 \cdot 10^{-5}$ | $-4.4148 \cdot 10^{-4}$ | $-1.6602 \cdot 10^{-3}$ |
| 5 | $1 \cdot 10^{5}$ | $2 \cdot 10^{5}$ | $3 \cdot 10^{5}$ | $5 \cdot 10^{5}$ | $1 \cdot 10^{6}$ | $2 \cdot 10^{6}$ |

FN := READPRN("sunfl3p5PE.prn" ) measured at 2003.09.16 by Péter Mészáros

FN =

| | 0 | 1 | 2 | 3 | 4 | 5 |
|---|---|---|---|---|---|---|
| 0 | 0 | 1 | 1 | 2 | 2 | 3 |
| 1 | 0 | 1.443 | 1.443 | 1.442 | 1.442 | 1.441 |
| 2 | 0 | 0 | 0 | 0 | 0 | 0 |
| 3 | 0 | 0 | 0 | 0 | 0 | 0 |
| 4 | $7.94 \cdot 10^4$ | 2.211 | 0.095 | 2.217 | 0.095 | 2.219 |
| 5 | $8.91 \cdot 10^4$ | 2.205 | 0.094 | 2.211 | 0.094 | 2.213 |
| 6 | $1 \cdot 10^5$ | 2.199 | 0.093 | 2.205 | 0.093 | 2.206 |
| 7 | $1.122 \cdot 10^5$ | 2.192 | 0.092 | 2.198 | 0.093 | 2.2 |

$$\begin{aligned}
&\text{MPred}(\varepsilon r, T, D, F, KCC, VTC, KTC, FF) := \\
&\quad I \leftarrow \text{cols}(KCC) - 2 \\
&\quad J \leftarrow \text{rows}(KCC) - 2 \\
&\quad KT \leftarrow KCC^{T} \\
&\quad KT \leftarrow \text{submatrix}(KT, 0, I, 0, J + 1) \\
&\quad K0V \leftarrow \text{lspline}\left(KT^{\langle J+1 \rangle}, KT^{\langle 0 \rangle}\right) \\
&\quad K1V \leftarrow \text{lspline}\left(KT^{\langle J+1 \rangle}, KT^{\langle 1 \rangle}\right) \\
&\quad K2V \leftarrow \text{lspline}\left(KT^{\langle J+1 \rangle}, KT^{\langle 2 \rangle}\right) \\
&\quad K3V \leftarrow \text{lspline}\left(KT^{\langle J+1 \rangle}, KT^{\langle 3 \rangle}\right) \\
&\quad K4V \leftarrow \text{lspline}\left(KT^{\langle J+1 \rangle}, KT^{\langle 4 \rangle}\right) \\
&\quad \rho \leftarrow \frac{KCC_{0, I+1}}{VTC} \\
&\quad K0I \leftarrow \text{interp}\left(K0V, KT^{\langle J+1 \rangle}, KT^{\langle 0 \rangle}, F\right) \\
&\quad K1I \leftarrow \text{interp}\left(K1V, KT^{\langle J+1 \rangle}, KT^{\langle 1 \rangle}, F\right) \\
&\quad K2I \leftarrow \text{interp}\left(K2V, KT^{\langle J+1 \rangle}, KT^{\langle 2 \rangle}, F\right) \\
&\quad K3I \leftarrow \text{interp}\left(K3V, KT^{\langle J+1 \rangle}, KT^{\langle 3 \rangle}, F\right) \\
&\quad K4I \leftarrow \text{interp}\left(K4V, KT^{\langle J+1 \rangle}, KT^{\langle 4 \rangle}, F\right) \\
&\quad \varepsilon dc \leftarrow \left[\left[(\varepsilon r \cdot FF)^{\frac{1}{3}} - 1\right] \cdot \frac{\rho}{D} + 1\right]^3 \\
&\quad M1 \leftarrow K0I + K1I \cdot \varepsilon dc + K2I \cdot \varepsilon dc^2 + K3I \cdot \varepsilon dc^3 + K4I \cdot \varepsilon dc^4 \\
&\quad M2 \leftarrow M1 - KTC \cdot (T - 25) \\
&\quad M2
\end{aligned}$$

Volume of Test Cell

$VTC := \frac{341.52}{997}$ Weight of water to fill test cell divided by approximate density of water at 24.2 C.

$D := submatrix(FN, 0, rows(FN) - 1, 1, cols(FN) - 1)$

$rows(D) = 56$

$FR := submatrix(FN, 4, 55, 0, 0)$ High frequency list

$SW := 158.82$ Specify sample weight here!

$j := 0.. \frac{cols(D)}{2} - 1$

$FF \equiv \frac{4.4}{3.9}$ Adjust "fudge factor"

$i := 0.. rows(D) - 5$

$DEN := \frac{SW}{VTC}$ Calculate density for the sample

$T_j := \frac{1.215 - D_{1,2\cdot j}}{.0042} + 25$ Calculate temperature for each measurement

$\frac{KCC_{0,10}}{VTC} = 374.894$ Average sample weight from GIPSA work.

$\rho bar := \frac{KCC_{0,10}}{VTC}$ Calculated average density

Pick off real and imaginary parts of dielectric constants for
HP-4285A data.

$\varepsilon r_{j,i} := D_{i+4,2\cdot j}$ $\varepsilon i_{j,i} := D_{i+4,2\cdot j+1}$ $rows(\varepsilon r) = 217$

$M_{j,i} := MPred(\varepsilon r_{j,i}, T_j, DEN, FR_i, KCC, VTC, KTC, FF)$ Calculate predicted moisture values with density and temperature correction.

Frequency indices

$FR_8 = 2 \times 10^5$ $FR_{28} = 2 \times 10^6$ $FR_{48} = 2 \times 10^7$ $FR_{42} = 1 \times 10^7$

KTC ≡ 0

Specify Temperature Correction Coefficient

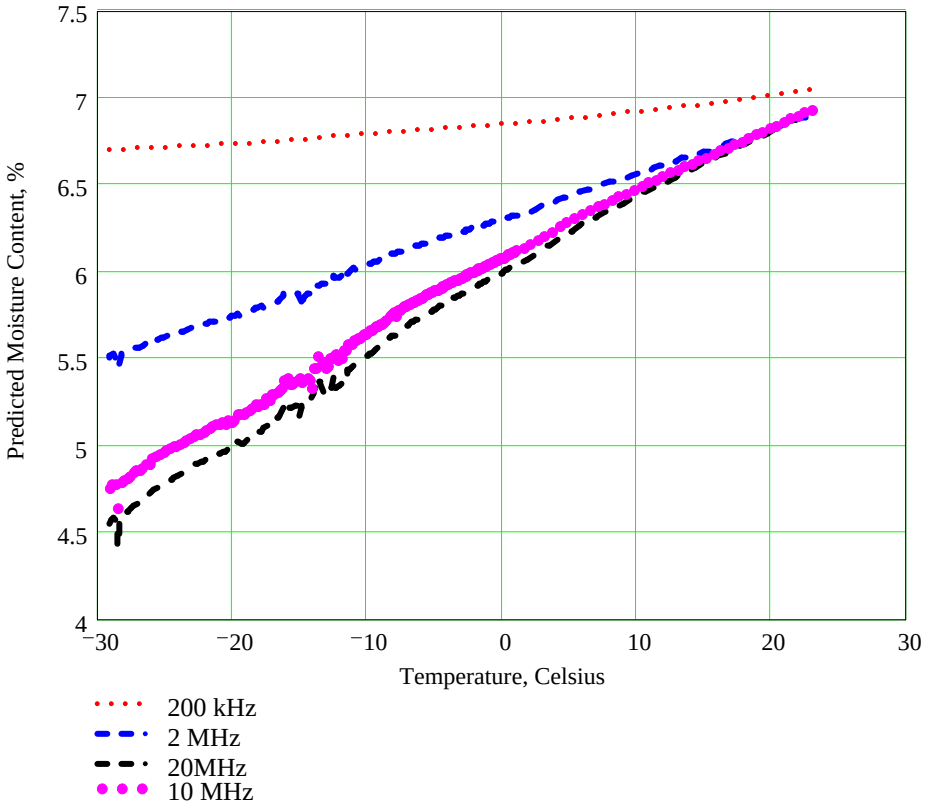


AOM := 6.62

Specify Air-Oven Moisture content

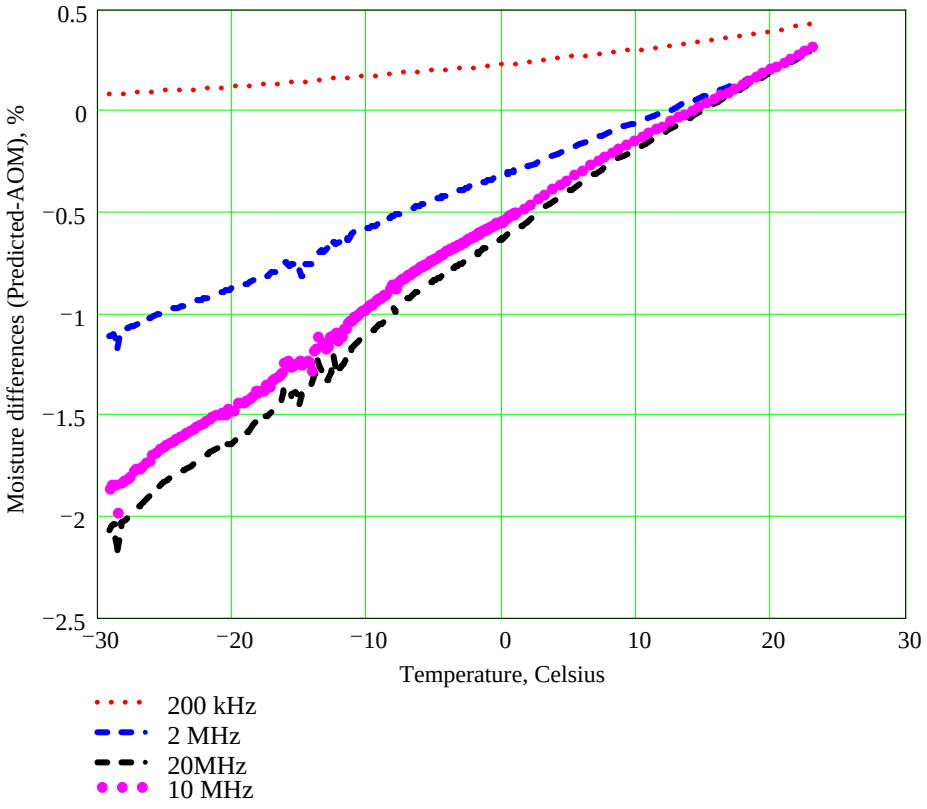

KTC ≡ 0.042 Specify Temperature Correction Coefficient

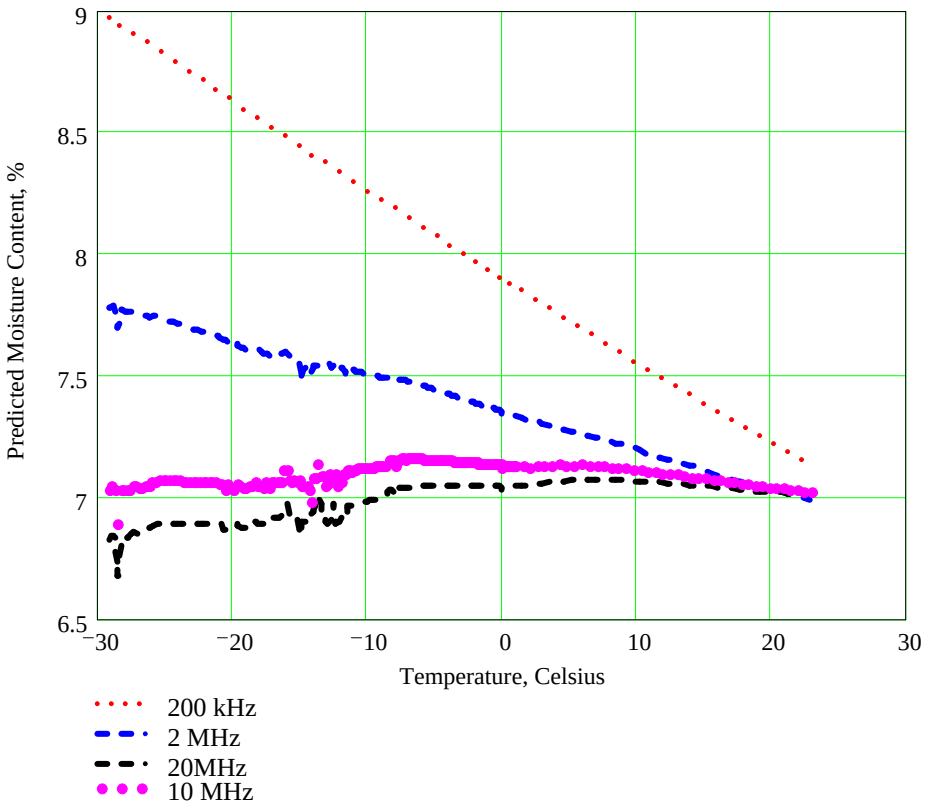


AOM := 6.62 Specify Air-Oven Moisture content

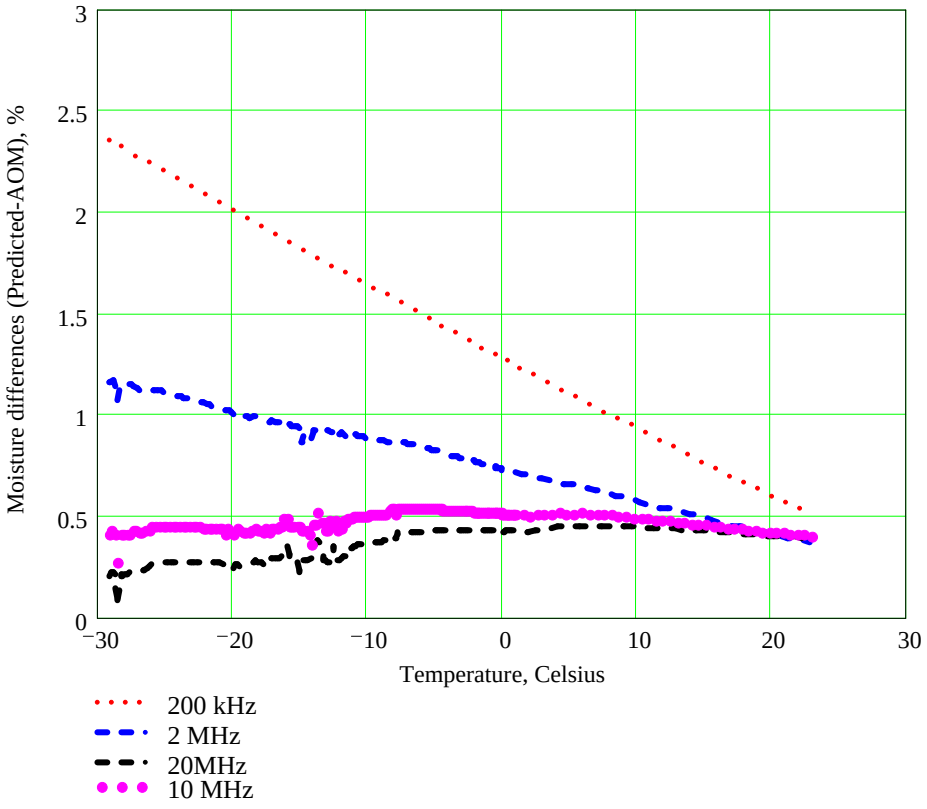

## 10.5. Appendix 4. Residual slope after temperature correction for Barley, Oats, Rapeseed and Wheat

Slope of the corrected moisture predictions versus temperature. Bold numbers indicate tests that included only the low (0-22 °C) temperature range.

| | Residual (uncorrected) slope of the predicted moisture curve (from 0 to + 40 °C) | | | | |
|---|---|---|---|---|---|
| Grain type | Moisture content wb | No temperature correction | Constant temperature correction (Equation 41.) | Linear moisture-dependent temperature correction (Equation 42.) | Linear moisture-dependent temperature correction plus a quadratic temperature term (Equation 43.) |
| Barley | 11.5 | 0.131 | 0.018 | 0.0075 | 0.013 |
| | 11.7 | 0.125 | 0.012 | 0.0018 | 0.0029 |
| | **16.7** | **0.117** | **0.0041** | **0.0056** | **-0.011** |
| | 18.3 | 0.088 | -0.025 | -0.021 | 0.0014 |
| | 19.6 | 0.095 | -0.019 | -0.012 | -0.00009 |
| Oats | **10.1** | **0.141** | **-0.0017** | **0.014** | **-0.0078** |
| | 16.6 | 0.153 | 0.0095 | 0.0039 | 0.019 |
| | 18 | 0.139 | -0.0036 | -0.011 | 0.0097 |
| | 21 | 0.158 | 0.015 | -0.005 | 0.041 |
| | 22.1 | 0.187 | 0.044 | 0.033 | 0.061 |
| | 24 | 0.162 | 0.019 | -0.0012 | 0.053 |
| Rapeseed | **9.3** | **0.138** | **0.057** | **0.035** | **0.019** |
| | 12.7 | 0.106 | 0.025 | 0.02 | 0.0039 |
| | 13.3 | 0.093 | 0.012 | 0.011 | 0.011 |
| | 14.5 | 0.06 | -0.021 | -0.014 | -0.0045 |
| | 14.7 | 0.045 | -0.036 | -0.033 | -0.019 |
| | 14.9 | 0.051 | -0.03 | -0.018 | -0.01 |
| Wheat | **7.3** | **0.139** | **0.051** | **-0.007** | **-0.0021** |
| | **10.1** | **0.127** | **0.039** | **-0.0054** | **-0.0021** |
| | **10.8** | **0.119** | **0.031** | **-0.0081** | **-0.0054** |
| | **16.3** | **0.118** | **0.03** | **0.018** | **0.005** |
| | **19.9** | **0.081** | **-0.0067** | **-0.0061** | **-0.0058** |
| | 20 | 0.057 | -0.031 | -0.03 | 0.0095 |
| | 21.8 | 0.04 | -0.048 | -0.045 | 0.012 |
| | 26 | 0.036 | -0.052 | -0.031 | 0.0037 |
| | **28.5** | **0.044** | **-0.044** | **-0.014** | **-0.033** |

## 10.6. Appendix 5. Physical and chemical properties of grains

| Grain type | Protein, % | Oil/Fat, % | Ash, % | Starch, % | Moist. Content % | Bulk Density (g/cm$^3$) | Seed mass (mg) | Seed volume (mm$^3$) | Kernel Density (g/cm$^3$) | Major axis (mm) | 2nd Axis (mm) | 3rd Axis (mm) | Sphericity |
|---|---|---|---|---|---|---|---|---|---|---|---|---|---|
| soy | 42.00 | 22.00 | 4.90 | 18.00 | 13.40 | 0.71 | 170.00 | 135.60 | 1.25 | 7.60 | 6.60 | 5.70 | 0.75 |
| soy | 41.00 | 23.00 | 5.00 | 24.00 | 10.00 | 0.72 | 164.00 | 134.10 | 1.25 | 7.30 | 6.60 | 5.70 | 0.78 |
| soy | 30.00 | 21.00 | 4.90 | 34.00 | 11.00 | 0.70 | 155.00 | 121.35 | 1.24 | 7.50 | 6.60 | 5.50 | 0.73 |
| soy | 40.00 | 18.00 | 5.00 | 30.00 | 8.00 | 0.71 | 156.00 | 119.21 | 1.25 | 7.40 | 6.50 | 5.50 | 0.74 |
| soy | 43.00 | 23.00 | 4.95 | 21.00 | 8.30 | 0.76 | 173.00 | 133.54 | 1.25 | 7.30 | 6.65 | 5.83 | 0.80 |
| soy | 41.00 | 22.00 | 4.90 | 23.00 | 10.00 | 0.74 | 142.35 | 114.95 | 1.24 | 6.98 | 6.28 | 5.50 | 0.79 |
| soy | 39.00 | 23.00 | 4.90 | 22.00 | 10.50 | 0.74 | 157.00 | 133.00 | 1.29 | 6.89 | 6.48 | 5.76 | 0.84 |
| soy | 43.00 | 21.00 | 4.90 | 24.00 | 8.00 | 0.76 | 142.00 | 120.21 | 1.24 | 7.39 | 6.50 | 5.57 | 0.75 |
| soy | 40.00 | 25.00 | 4.90 | 21.00 | 9.00 | 0.77 | 157.00 | 120.68 | 1.29 | 7.20 | 5.88 | 4.67 | 0.65 |
| sorghum | 8.10 | 3.05 | 1.30 | 72.00 | 14.20 | 0.78 | 31.20 | 24.70 | 1.34 | 4.50 | 4.10 | 3.40 | 0.76 |

| | | | | | | | | | | | | | |
|---|---|---|---|---|---|---|---|---|---|---|---|---|---|
| sorghum | 9.50 | 3.00 | 1.40 | 72.00 | 13.20 | 0.73 | 27.00 | 25.00 | 1.30 | 4.20 | 3.70 | 3.10 | 0.74 |
| sorghum | 8.20 | 3.00 | 1.20 | 73.00 | 13.30 | 0.73 | 30.00 | 25.00 | 1.36 | 4.00 | 3.35 | 2.80 | 0.70 |
| sorghum | 8.10 | 3.10 | 1.80 | 72.70 | 15.20 | 0.68 | 43.00 | 26.20 | 1.03 | 4.20 | 3.70 | 3.10 | 0.74 |
| sunflower | 17.00 | 44.00 | 3.90 | 25.00 | 12.00 | 0.39 | 59.50 | 58.20 | 1.02 | 10.70 | 5.20 | 3.40 | 0.32 |
| sunflower | 17.00 | 44.50 | 3.60 | 20.00 | 15.00 | 0.34 | 70.00 | 69.50 | 1.03 | 21.56 | 10.60 | 4.96 | 0.23 |
| sunflower | 21.00 | 47.30 | 4.00 | 20.00 | 9.00 | 0.32 | 69.00 | 63.50 | 1.03 | 13.00 | 8.10 | 4.96 | 0.38 |
| sunflower | 21.00 | 46.10 | 3.80 | 22.00 | 7.60 | 0.35 | 66.00 | 64.00 | 1.03 | 11.53 | 5.01 | 3.13 | 0.27 |
| corn | 8.40 | 2.70 | 1.14 | 79.20 | 10.00 | 0.81 | 334.00 | 254.00 | 1.27 | 12.60 | 8.30 | 4.50 | 0.36 |
| corn | 11.20 | 3.00 | 1.30 | 67.90 | 16.00 | 0.74 | 326.00 | 256.00 | 1.28 | 12.59 | 8.01 | 4.34 | 0.34 |
| corn | 12.30 | 2.50 | 1.20 | 72.30 | 12.00 | 0.70 | 325.00 | 245.00 | 1.31 | 11.20 | 7.60 | 4.50 | 0.40 |
| corn | 9.00 | 2.40 | 1.30 | 79.10 | 9.00 | 0.70 | 345.00 | 236.00 | 1.31 | 11.20 | 7.60 | 4.50 | 0.40 |
| corn | 8.70 | 2.50 | 1.30 | 75.10 | 13.00 | 0.70 | 330.00 | 275.00 | 1.29 | 11.20 | 7.60 | 4.50 | 0.40 |
| corn | 10.00 | 2.80 | 1.40 | 78.20 | 8.60 | 0.73 | 334.00 | 248.00 | 1.29 | 12.60 | 7.60 | 4.50 | 0.36 |
| corn | 11.00 | 3.90 | 1.30 | 75.00 | 8.10 | 0.73 | 324.00 | 250.00 | 1.33 | 12.32 | 7.95 | 4.62 | 0.38 |
| corn | 9.90 | 4.10 | 1.30 | 79.21 | 7.20 | 0.73 | 326.00 | 250.00 | 1.32 | 10.25 | 8.21 | 4.35 | 0.42 |
| corn | 9.60 | 3.00 | 1.40 | 73.50 | 13.50 | 0.74 | 335.00 | 243.00 | 1.34 | 11.20 | 7.74 | 4.30 | 0.38 |
| corn | 9.70 | 3.00 | 1.30 | 78.00 | 8.20 | 0.73 | 328.00 | 248.00 | 1.34 | 11.02 | 7.58 | 4.60 | 0.42 |
| corn | 9.90 | 3.00 | 1.30 | 78.50 | 9.00 | 0.73 | 328.00 | 250.00 | 1.38 | 7.40 | 5.50 | 4.30 | 0.58 |
| oats | 13.25 | 6.40 | 3.30 | 60.00 | 15.23 | 0.42 | 34.80 | 26.80 | 1.30 | 10.90 | 2.80 | 2.10 | 0.19 |
| oats | 13.42 | 6.10 | 3.50 | 62.00 | 14.50 | 0.45 | 28.10 | 21.40 | 1.31 | 10.20 | 2.80 | 2.20 | 0.22 |
| oats | 12.10 | 5.10 | 3.40 | 65.00 | 15.00 | 0.50 | 34.60 | 24.00 | 1.31 | 10.50 | 2.80 | 2.10 | 0.20 |
| oats | 16.89 | 6.90 | 3.30 | 63.00 | 9.94 | 0.52 | 33.50 | 24.00 | 1.31 | 10.50 | 2.80 | 2.10 | 0.20 |
| oats | 11.30 | 5.80 | 3.20 | 55.50 | 22.00 | 0.53 | 24.00 | 24.00 | 1.31 | 10.50 | 2.80 | 2.10 | 0.20 |
| wheat | 8.50 | 1.20 | 1.70 | 74.50 | 13.80 | 0.73 | 39.70 | 28.60 | 1.39 | 6.40 | 3.40 | 2.90 | 0.45 |
| wheat | 13.00 | 1.11 | 1.70 | 71.20 | 13.00 | 0.73 | 38.70 | 28.60 | 1.35 | 6.30 | 3.30 | 2.90 | 0.46 |
| wheat | 12.20 | 1.20 | 1.70 | 71.90 | 13.00 | 0.73 | 40.00 | 26.20 | 1.35 | 6.30 | 3.30 | 2.90 | 0.46 |
| wheat | 8.20 | 2.00 | 1.70 | 76.20 | 11.50 | 0.74 | 38.90 | 25.80 | 1.35 | 6.30 | 3.30 | 2.90 | 0.46 |
| wheat | 8.20 | 1.20 | 1.80 | 78.00 | 11.79 | 0.69 | 38.40 | 24.00 | 1.35 | 6.30 | 3.30 | 2.90 | 0.46 |
| wheat | 12.36 | 1.10 | 1.70 | 76.00 | 9.19 | 0.79 | 34.00 | 24.00 | 1.35 | 6.30 | 3.30 | 2.90 | 0.46 |
| wheat | 13.00 | 1.00 | 1.70 | 74.00 | 9.53 | 0.71 | 34.00 | 24.00 | 1.35 | 6.25 | 3.25 | 3.21 | 0.51 |
| wheat | 9.60 | 1.00 | 1.70 | 76.00 | 11.80 | 0.76 | 34.00 | 26.40 | 1.35 | 5.80 | 3.20 | 2.90 | 0.50 |
| wheat | 10.20 | 1.50 | 1.70 | 73.00 | 14.00 | 0.69 | 34.00 | 24.00 | 1.26 | 6.25 | 3.20 | 3.25 | 0.52 |
| wheat | 11.75 | 1.52 | 1.61 | 63.00 | 21.50 | 0.73 | 35.20 | 24.00 | 1.39 | 6.50 | 3.26 | 3.36 | 0.52 |
| wheat | 8.20 | 1.00 | 1.83 | 72.38 | 12.10 | 0.76 | 29.20 | 21.00 | 1.39 | 6.50 | 2.90 | 2.60 | 0.40 |
| wheat | 11.00 | 1.50 | 1.70 | 73.21 | 13.00 | 0.73 | 29.50 | 23.00 | 1.31 | 6.35 | 3.55 | 2.90 | 0.46 |
| wheat | 11.10 | 1.24 | 1.50 | 63.20 | 23.00 | 0.72 | 29.84 | 24.00 | 1.35 | 6.35 | 3.60 | 2.65 | 0.42 |
| wheat | 13.80 | 1.12 | 1.65 | 64.20 | 19.50 | 0.72 | 28.80 | 24.00 | 1.32 | 6.45 | 3.55 | 2.54 | 0.39 |
| wheat | 9.10 | 1.10 | 1.84 | 70.20 | 16.90 | 0.72 | 27.70 | 20.20 | 1.37 | 5.90 | 2.80 | 2.60 | 0.44 |
| wheat | 8.65 | 1.00 | 1.85 | 70.20 | 18.20 | 0.77 | 26.00 | 18.50 | 1.41 | 5.80 | 2.60 | 2.40 | 0.41 |
| wheat | 8.20 | 1.29 | 1.71 | 70.20 | 19.20 | 0.77 | 34.80 | 24.00 | 1.35 | 6.42 | 3.54 | 3.14 | 0.49 |
| wheat | 10.00 | 1.40 | 1.70 | 74.20 | 12.50 | 0.71 | 35.25 | 23.56 | 1.32 | 6.25 | 3.10 | 3.25 | 0.52 |
| wheat | 10.75 | 1.21 | 1.69 | 73.00 | 13.50 | 0.71 | 35.60 | 24.00 | 1.35 | 6.35 | 3.54 | 3.02 | 0.48 |
| wheat | 8.90 | 1.26 | 1.95 | 70.00 | 18.00 | 0.71 | 35.80 | 24.00 | 1.35 | 6.47 | 3.58 | 2.90 | 0.45 |
| wheat | 11.50 | 1.54 | 1.44 | 63.00 | 22.50 | 0.71 | 35.40 | 24.00 | 1.36 | 6.40 | 3.59 | 2.90 | 0.45 |
| barley | 17.50 | 3.01 | 2.60 | 70.00 | 8.00 | 0.62 | 44.30 | 35.00 | 1.20 | 9.00 | 3.41 | 2.60 | 0.46 |
| barley | 16.00 | 3.10 | 2.50 | 68.90 | 10.00 | 0.62 | 38.50 | 36.00 | 1.25 | 8.78 | 3.35 | 2.51 | 0.36 |
| barley | 17.50 | 3.40 | 2.60 | 65.00 | 12.00 | 0.60 | 40.50 | 31.00 | 1.32 | 8.90 | 3.10 | 2.40 | 0.27 |
| barley | 15.80 | 3.10 | 2.50 | 73.70 | 7.00 | 0.63 | 43.10 | 37.00 | 1.16 | 8.90 | 3.28 | 2.50 | 0.29 |
| barley | 13.20 | 3.40 | 2.30 | 73.10 | 8.00 | 0.63 | 41.50 | 36.00 | 1.14 | 8.90 | 3.28 | 2.50 | 0.27 |
| rice | 8.40 | 1.98 | 1.60 | 81.00 | 7.40 | 0.64 | 24.90 | 18.00 | 1.38 | 7.80 | 2.90 | 2.00 | 0.26 |
| rice | 8.40 | 1.78 | 1.60 | 83.00 | 6.70 | 0.69 | 33.00 | 17.00 | 1.39 | 8.90 | 2.30 | 2.40 | 0.27 |
| rice | 7.94 | 2.92 | 1.50 | 78.24 | 10.00 | 0.74 | 35.00 | 24.00 | 1.42 | 7.20 | 2.80 | 2.50 | 0.35 |
| rice | 8.18 | 1.20 | 1.40 | 76.80 | 13.00 | 0.75 | 33.00 | 26.00 | 1.45 | 6.80 | 2.70 | 2.60 | 0.38 |
| rice | 8.10 | 1.20 | 1.40 | 81.60 | 8.00 | 0.74 | 29.00 | 25.00 | 1.37 | 7.30 | 2.80 | 2.60 | 0.36 |
| flaxseed | 21.00 | 42.00 | 3.90 | 25.00 | 6.00 | 0.72 | 4.00 | 3.50 | 1.15 | 5.62 | 2.85 | 1.14 | 0.20 |
| flaxseed | 23.00 | 42.00 | 3.80 | 26.00 | 6.00 | 0.64 | 4.70 | 3.60 | 1.12 | 5.56 | 3.10 | 1.24 | 0.22 |
| flaxseed | 24.00 | 41.00 | 3.90 | 25.00 | 6.00 | 0.68 | 4.30 | 3.50 | 1.17 | 5.60 | 2.90 | 1.20 | 0.21 |
| rapeseed | 25.00 | 41.20 | 6.30 | 14.00 | 13.00 | 0.69 | 3.70 | 3.00 | 1.12 | 1.60 | 1.60 | 1.50 | 0.94 |
| rapeseed | 31.00 | 41.30 | 6.40 | 16.00 | 6.80 | 0.64 | 3.84 | 2.80 | 1.15 | 1.50 | 1.50 | 1.50 | 1.00 |
| rapeseed | 32.00 | 40.29 | 6.30 | 15.50 | 7.60 | 0.68 | 3.87 | 2.85 | 1.14 | 1.65 | 1.64 | 1.54 | 0.93 |
| rapeseed | 21.00 | 43.20 | 6.29 | 14.50 | 15.00 | 0.69 | 3.55 | 3.15 | 1.09 | 1.60 | 1.58 | 1.50 | 0.94 |
| rapeseed | 20.60 | 43.30 | 6.30 | 15.00 | 15.20 | 0.71 | 3.62 | 3.20 | 1.10 | 1.62 | 1.63 | 1.48 | 0.91 |

# 11. ACKNOWLEDGEMENTS

I express my deepest thanks to my supervisors **Dr. Eszter Vozáry and Dr. David B. Funk** for the characterization of the principal aims of my work and for their valuable advising and skilful guidance, constructive criticism and inspiration.

I greatly acknowledge to **Prof. András Fekete and Dr. József Felföldi** for providing possibility to work at the Physics and Control Department.

I owe **Steven N. Tanner (Director of United States Department of Agriculture—Grain Inspection, Packers and Stockyards Administration)** my thanks for supporting this thesis in part by a grant and equipment loans and donations.

I am grateful to **my parents** and **my love** for their support and encouragement.

I would like to deliver my special thanks to all **my colleagues, especially for the dielectric moisture team (Zoltán Gillay and Bíborka Gillay) and staff members.**

Department of Physics and Control, Corvinus University of Budapest, are gratefully thanked for creating a supportive and pleasant working environment.

**Dr. Stuart O. Nelson and Dr. Kurt C. Lawrence,** USDA-ARS, Athens, GA, developed and calibrated the original test cell used to collect the dielectric data and loaned a second identical test cell to Corvinus University of Budapest to permit comparison tests.

The USDA-GIPSA-TSD-ISE Moisture Group supervised by **Dr. James Rampton** conducted the instrument tests to acquire all of the VHF dielectric data needed to develop the Unified Moisture Algorithm and the unifying parameters. Special thanks are due **Mr. Steven Burton** and **Ms. Lucille Clark** who did the bulk of the instrument tests and to **Ms. Patricia Jackson** who oversaw and organized the day-to-day operations and data organization in the laboratory. **Ms. Brenda Evans and Mr. Glenn Terrill**, USDA-GIPSA-TSD-ARTS performed the reference moisture analyses for all of the grain samples. **Mr. Larry Freese**, Mathematical Statistician, USDA-GIPSA-TSD-ISE developed SAS programs to facilitate the compilation and processing of data from thousands of separate data files.

**DICKEY-john Corporation** donated the parallel-plate test cell that was used for some of the experiments.